Endothelial cell eNOS regulates sodium excretion and glomerular filtration rate in the kidney as determined in endothelial cell-specific eNOS KO and KI mice

Inaugural dissertation

for the attainment of the title of doctor
in the Faculty of Mathematics and Natural Sciences

at the Heinrich Heine University Düsseldorf

presented by

Anthea Lo Bue, MSc

from Palermo, Italy

Düsseldorf, June 2025

from the Myocardial Infarction Research Laboratory, Department of Cardiology, Pneumology and Angiology, Heinrich Heine University Düsseldorf

Published by permission of the

Faculty of Mathematics and Natural Sciences at

Heinrich Heine University Düsseldorf

Supervisor: Univ.-Prof. Dr. Dr. rer. nat. Miriam M. Cortese-Krott

Co-supervisor: Univ.-Prof. Dr. rer. nat. Holger Gohlke

Date of the oral examination: 13 February 2026

I declare under oath that I have produced my thesis independently and without any undue assistance by third parties under consideration of the “Principles for the Safeguarding of Good Scientific Practice at Heinrich Heine University Düsseldorf.

This dissertation was neither in the same nor in a similar form in another examination procedure submitted. I also declare that I have not yet received or attempted to acquire any further degree.

Anthea Lo Bue

To my family,
without whom
I would not be
who I am today

Summary

Background and hypothesis: The kidney is one of the major regulators of blood pressure by water and sodium handling, and by the renin-angiotensin-aldosterone system (RAAS). The NO/sGC signalling plays a crucial role in medullary blood flow and natriuresis regulation, but the cells in which the regulation occurs are still unknown.

Aim of the study: Understand the role of eNOS in ECs and RBCs in renal function using EC and RBC-specific eNOS knockout (KO) and knockin (KI) mice. The three main goals were to (1) verify that $eNOS^{inv/inv}$ = CondKO construct was efficient for reactivating eNOS expression in global eNOS KI mice as proof of concept, (2) characterize eNOS expression in targeted and non-targeted cells of EC eNOS KO/WT, EC eNOS KI/CondKO, RBC eNOS KO/WT, and RBC eNOS KI/CondKO mice, and (3) investigate the role of EC and RBC eNOS in kidney function.

Material and methods: The founders $eNOS^{flox/flox}$ and $eNOS^{inv/inv}$ mice were generated by gene targeting recombination and crossed with mice expressing Cre recombinase in all cells, or specifically in ECs or RBCs to generate global eNOS KO/WT and global eNOS KI/KO ($eNOS^{fl/fl}$/$eNOS^{inv/inv}$) mice, EC eNOS KO/WT and EC eNOS KI/CondKO mice, and RBC eNOS KO/WT and RBC eNOS KI/CondKO mice. The system specificity was assessed via DNA recombination, eNOS expression, vascular endothelial function, blood pressure, and NO metabolites. Kidney function was investigated before/after angiotensin II (Ang II) treatment by measuring basal sodium and urine excretion, or after salt and volume challenge, and glomerular filtration rate (GFR).

Results: CondKO mice ($eNOS^{inv/inv}$) lacked eNOS, were hypertensive, and had impaired vascular endothelial function. EC and RBC eNOS KO mice lacked eNOS respectively in ECs or RBCs, while EC and RBC eNOS KI mice expressed eNOS specifically in ECs or RBCs. Both EC and RBC eNOS KO mice were hypertensive, while this phenotype was rescued in EC and RBC eNOS KI mice. After salt and volume challenge, EC eNOS KO mice showed decreased sodium and urine excretion at baseline as compared to wild type (WT) mice. Moreover, EC eNOS KI mice showed preserved sodium excretion after Ang II as compared to CondKO mice. RBC eNOS KO and KI mice had the same sodium and urine excretion with/without Ang II as compared to respective WT and CondKO controls. CondKO mice had lower GFR as compared to WT mice with/without Ang II. EC eNOS KO mice showed the same GFR as compared to WT mice with/without Ang II, but reactivation of eNOS in ECs rescued the GFR in EC eNOS KI mice after Ang II infusion. RBC eNOS KO and KI mice showed no changes in GFR as compared to WT and CondKO littermates with/without AngII.

Conclusion: EC and RBC eNOS independently regulate blood pressure; eNOS in ECs, but not in RBCs, modulates sodium and urine excretion and regulates GFR.

Table of contents

List of all figures

List of all tables

Abbreviations

ACE	Angiotensin converting enzyme
ACh	Acetylcholine
ADH	Antidiuretic hormone
Ang II	Angiotensin II
ANP	Atrial natriuretic peptide
AT_1	Angiotensin II receptor type I
AT_2	angiotensin II receptor type II
β-MHC	β-myosin heavy chain
BNP	Brain natriuretic peptide
Bp	Base pairs
cGMP	Cyclic guanosine monophosphate
CondKO	Conditional eNOS knock out or $eNOS^{inv/inv}$
CreER	Cre recombinase bound to a mutated hormone-binding domains of the estrogen receptor
DBP	Diastolic blood pressure
$DelCre^{pos}$	Deleter Cre^{pos}
ECs	Endothelial cells
EDHF	Endothelium-derived hyperpolarizing factor
EDR	Endothelium-dependent relaxation
EDTA	Ethylenediaminetetraacetic acid
ENaC	Amiloride-sensitive epithelial sodium channel
eNOS	Endothelial nitric oxide synthase
ES	Embryonic stem
GFR	Glomerular filtration rate
GTP	Guanosine triphosphate

HEPES	Hydroxyethylpiperazine ethanesulfonic acid
HR	Heart rate
iNOS	Inducible nitric oxide synthase
KI	Knock in
KO	Knock out
LANUV	Landesamt für Natur, Umwelt und Verbraucherschutz Nordrhein-Westfalen
L-NAME	L-N^G-Nitro arginine methyl ester
L-NMMA	N-monomethyl-L-arginine
MAP	Mean arterial pressure
NCC	Sodium-chloride cotransporter
NKCC2	Sodium-potassium-2-chloride cotransporter type 2
nNOS	Neuronal nitric oxide synthase
NO	Nitric oxide
NO/cGMP	Nitric oxide/cyclic guanosine monophosphate
NO-Heme	Nitrosyl heme
NONate	Spermine diazeniumdiolate
NOS	Nitric oxide synthase
PBS	Phosphate-buffered saline
PCR	Polymerase chain reaction
PE	Phenylephrine
PGI_2	Prostacyclin
PKG	Protein kinase G
RAAS	Renin angiotensin aldosterone system
RBCs	Red blood cells
RBF	Renal blood flow
RCN	Relative copies number

ROS	reactive oxygen species
RT	retrotranscription
RXNO	nitrosated products
SBP	Systolic blood pressure
SD	Standard deviation
SDS	Sodium dodecyl sulfate
sGC	Soluble guanylate cyclase
SNP	Sodium nitroprusside
TAL	Thick ascending limb
TAM	Tamoxifen
TEMED	Tetramethylethylenediamine
WT	Wilde type

1. Introduction

Hypertension is the major risk factor for premature cardiovascular diseases like coronary heart disease, ischemic and haemorrhagic stroke, and it is the major cause of premature deaths worldwide (World Health Organization, 2023). The prevention and control of hypertension is therefore crucial to reduce the risk of mortality due to cardiovascular diseases (Sudharsanan et al., 2021). The risk factors, which are correlated to hypertension, include physiological factors like age and genetics, clinical conditions like obesity or incorrect behaviours like high-salt diet, consumption of tobacco and alcohol, and physical inactivity (World Health Organization, 2023).

Physiologically, two primary factors directly affect the variation in blood pressure: the volume of intravascular fluids in the body and the different ability of the vessels to vasodilate. These two factors are in turn regulated by multiple pathways such as the nitric oxide/cyclic guanosine monophosphate (NO/cGMP) signalling cascade, the renin-angiotensin-aldosterone system (RAAS), and the sympathetic system, which make the pathophysiology of hypertension very complex (J. Ma et al., 2023).

1.1. Role of the kidney in hypertension

The kidney has a central role in the long-term blood pressure regulation via the renal-body fluid system, and in the short-term blood pressure regulation by the RAAS (Triebel et al., 2024). Several homeostatic mechanisms maintain the equilibrium between renal output and intake of water and salt in order to keep the extracellular fluid volume and arterial blood pressure constant. When the extracellular fluid volume increases, a cascade of physiological events starts. First, the increased blood volume causes a consequent increase in the mean circulatory filling pressure. This increased pressure enhances the venous return of blood to the heart, leading to an increase in the cardiac output. As a result, arterial pressure also increases due to the autoregulatory mechanism of blood flow in the tissues, which then causes an increase in total peripheral resistance.

In this regard, salt intake assumes an important role since salt is not excreted as easily as water, and when it is accumulated in the body, it leads to an increase in extracellular fluid volume to restore the osmolality with a consequent increase in arterial pressure (Guyton et al., 1972). The kidney contributes to regulating blood pressure through the RAAS. Renin is an enzyme produced in the juxtaglomerular cells expressed mainly in the walls of the afferent arterioles of the glomerulus in response to a decrease in blood pressure. Renin catalyses the reaction of formation of angiotensin I from angiotensinogen, and it is then

converted by the angiotensin converting enzyme (ACE) to angiotensin II (Ang II) in the lungs and released in the circulation. Ang II causes an increase in arterial pressure by two mechanisms: by a direct vasoconstriction effect in the periphery arterioles, which leads to an increase in the peripheral resistance, and by decreasing the excretion of salt and water (Hall et al., 2020). Ang II increases the reabsorption of salt indirectly by stimulating aldosterone secretion and decreasing the blood flow in the efferent arterioles, and directly by stimulating ion channels including the Na^+/K^+ ATPase pump, the Na^+/H^+ exchanger and the sodium-bicarbonate co-transporter in most renal tubular segments (Liu et al., 1988, 1989; He et al., 2010; Hanna et al., 2022).

1.2. Endothelial dysfunction

The endothelium is a monolayer of endothelial cells (ECs) located between the bloodstream and the vascular smooth muscle cells. It plays an important role in the regulation of vascular tone and, more in general in vascular homeostasis (Gallo et al., 2021; Ambrosino et al., 2022). In physiological conditions and in response to chemical and mechanical signals, the ECs produce biomolecules, which work together to maintain a proper structure and function of the vasculature. Specifically, nitric oxide (NO), endothelium-derived hyperpolarizing factor (EDHF), and prostacyclin (PGI_2) have vasodilator and antiproliferative effects, endothelin-1 and Ang II have vasoconstrictor and proliferative effects, while reactive oxygen species (ROS) can have both vasodilator and vasoconstrictor effects (F. C. d. Silva et al., 2022). In this way, the endothelium regulates vasodilation, proliferation and migration of smooth muscle cells, adhesion and aggregation of platelets, and thrombogenesis. The impairment of the balance among these functions leads to an endothelial dysfunction (Davignon et al., 2004), which is usually referred to as an abnormal production of those biomolecules, and in particular of NO. A decreased bioavailability of NO can be due to the deficiency in NO production in the endothelium or by the reaction of NO with $O_2^{\bullet-}$ and subsequently production of $ONOO^-$, which reacts quickly with biological molecules, acting as a potent oxidant and nitrating agent (Cyr et al., 2020).

The pathogenesis of many diseases such as hypertension, atherosclerosis, inflammatory diseases, coronary artery diseases, and chronic kidney failures, is linked to endothelial dysfunction (Landmesser et al., 2004; Brandes, 2014; Seliger et al., 2016). However, intervention with the right therapy (e.g., antihypertensive) or lifestyle modifications (e.g., smoking cessation or physical exercise) may ameliorate endothelial dysfunction and decrease the risk (Hambrecht et al., 2000; I. V. G. Silva et al., 2019).

1.3. Role of eNOS in vascular function

The family of the nitric oxide synthase (NOS) enzyme converts L-arginine into L-citrulline, and NO. Three NOS isoforms exist, which are codified by three independent genes: *Nos1* (Human gene ID: 4842; MGI: 97360), *Nos2* (Human gene ID: 4843; MGI: 97361), and *Nos3* (Human gene ID: 4846; MGI: 97362). The names of the isoforms are based on the tissues in which they were first discovered; NOS1 or neuronal NOS (nNOS) was isolated from neurons, NOS2 or inducible NOS (iNOS) was isolated from monocytes, and NOS3 or endothelial NOS (eNOS) was isolated from ECs. In the vascular endothelium, eNOS plays a key role in the regulation of the vascular tone, systemic vascular resistance, and blood pressure (Lundberg et al., 2022). NO produced by eNOS diffuses to vascular smooth muscle cells, activating soluble guanylate cyclase (sGC), which converts guanosine triphosphate (GTP) into cyclic guanosine monophosphate (cGMP); cGMP activates the protein kinase G (PKG), which phosphorylates myosin light chains, leading to a decreased Ca^{2+} sensitivity of the myosin and vasodilation. Thus, basal NO production by the endothelium helps maintain low vascular resistance in the systemic circulation. In fact, inhibition of NO synthesis using L-NMMA (N-monomethyl-L-arginine) in healthy humans resulted in a significant increase in systemic vascular resistance (Stamler et al., 1994; O'Gallagher et al., 2020), demonstrating the importance of NO in maintaining normal vascular tone. By modulating vascular resistance, NO also regulates blood pressure. The importance of eNOS in blood pressure regulation is highlighted by studies showing that global eNOS knock out (KO) in mice results in a hypertensive phenotype (Shesely et al., 1996; Godecke et al., 1998; Leo et al., 2021).

NO also contributes to the circulating NO pool and can be converted into metabolites, which mediate NO bioactivity in the blood (Pawloski et al., 2001; Rassaf et al., 2002; Wood et al., 2013). Additionally, NO inhibits platelets aggregation and adhesion, preventing fibrous plaques formation in the late step of atherosclerosis (Alheid et al., 1987). Moreover, NO also inhibits leukocyte adhesion to ECs of the vessel walls, which is considered an early event that happens in atherosclerosis development (Kubes et al., 1991). Therefore, NO is a crucial factor in both vascular homeostasis and in the development of atherosclerosis.

1.4. Expression of eNOS in subcellular compartments of the cardiovascular system and kidney

eNOS is mainly expressed in the ECs of the vascular wall, but it was also found to be present in other cells including red blood cells (RBCs), cardiomyocytes, renal epithelial cells, cardiac fibroblasts, and different subpopulations of leukocytes (LoBue et al., 2023).

By using co-immunoprecipitation, it was shown that in mouse cardiomyocytes, eNOS is mainly found in caveolae in association with caveolin-3 (Feron et al., 1996). Here, eNOS modulates cardiomyocyte contractility as shown in isolated cardiomyocytes from cardiomyocyte-specific eNOS overexpressing mice (Massion et al., 2004). Moreover, human cardiomyocytes were shown to express eNOS in heart tissue as measured in heart biopsies of patients with cardiac failure (Heymes et al., 1999). In mouse cardiac fibroblasts, eNOS expression was detected by Western blotting analysis and NOS activity by citrulline assay, and it was proposed that eNOS from cardiac fibroblasts had a protective role against the development of cardiac fibrosis (R. S. Smith, Jr. et al., 2005; Kazakov et al., 2013).

Although the expression of eNOS in the kidney is mostly in ECs of afferent and efferent glomerular arterioles, glomerular capillaries and medullary vasa recta (Bachmann et al., 1995), its expression was found also in epithelial cells of the inner medullary collecting duct and in the thick ascending limb (TAL) of the loop of Henle (Wu et al., 1999; Plato et al., 2000; Baines et al., 2002) where it plays a role in sodium handling and therefore in the long-term blood pressure regulation (S. Chen et al., 2002). Factors such as Ang II, endothelin-1, and renal perfusion pressure can affect NOS isoforms expression. Continuous subcutaneous infusion of Ang II has been shown to increase eNOS expression in the kidney without altering nNOS expression in the macula densa (Tojo et al., 2000). Additionally, an increase in renal perfusion pressure after a high-salt diet led to increased eNOS expression, whereas a low-salt diet had the opposite effect (Sato et al., 2004). Similarly, endothelin-1 increased the eNOS expression in the TAL after a high salt diet (Herrera et al., 2005).

By immunohistochemical analysis it was shown that eNOS is expressed in the human vascular endothelium of pulmonary arteries, veins and bronchial vessels, as well as in the airway and in the bronchiolar and alveolar epithelial cells (Shaul et al., 1994; Giaid et al., 1995), with a central role in the regulation of the vascular tone (Steudel et al., 1999).

eNOS is also expressed in human and rat bone cells, particularly in osteoblasts lineage such as osteocytes (Fox et al., 1998) as well as in stromal cells and osteoclast, suggesting a role in mediating the effect of shear stress and mechanical stress in the bone and regulating the osteoclast function (Helfrich et al., 1997).

1.5. Role of eNOS in the kidney

NO in the kidney is a key regulator of vasculature tone and renal blood flow (RBF) in normotensive and hypertensive conditions (Thieme et al., 2017; Mergia et al., 2018). Research involving pharmacological inhibition or global eNOS KO mice has shown that

eNOS is primarily responsible for modulating RBF and the renal response to changes in pressure (Thieme et al., 2017). In addition, the deletion of sGC has been linked to decreased RBF and increased blood pressure, showing the importance of NO signalling in maintaining vascular homeostasis (Mergia et al., 2018). Studies using microdialysis have demonstrated that NO production is significantly higher in the renal medulla than in the renal cortex (Zou et al., 1997). Accordingly, intravenous administration of the NOS inhibitor L-N^G-Nitro arginine methyl ester (L-NAME) in rats showed a decrease in medullary RBF without affecting cortical RBF, indicating that NO is particularly crucial for medullary perfusion (Mattson et al., 1994; Nakanishi et al., 1995).

RBF is strictly maintained stable by a phenomenon defined as “autoregulation”, which is fundamental to preserve the glomerular structure and thus avoid renal damage. The autoregulation is mediated by two mechanisms, the myogenic response and the tubuloglomerular feedback. The myogenic response involves constriction of preglomerular vessels in response to increased transmural pressure, which leads to an increase in vascular resistance and a decrease in perfusion (Edwards et al., 2022). The tubuloglomerular feedback is activated by changes in NaCl delivery to the macula densa, causing contraction of the afferent arteriole when NaCl concentrations rise, thereby decreasing both RBF and glomerular filtration rate (GFR) (Edwards & Kurtcuoglu, 2022) (Fig. 1). The regulation of tubuloglomerular feedback and the myogenic response involves a complex interplay of vasoconstrictors, such as Ang II and endothelins, and vasodilators such as NO and adenosine. Specifically, NO maintains a lower basal vascular resistance in the kidney through its vasodilatory effect, which counterbalances the effect of vasoconstrictor molecules (Sandner et al., 1999).

The GFR is determined by the relationship between the resistance of the afferent and efferent arterioles of the glomerulus. NO acts as a potent vasodilator preferentially on the afferent arteriole, leading to an increase in the hydrostatic pressure inside the glomerulus, which directly affects the GFR, causing its increase. Efferent arterioles require a higher concentration of NO for a significant modulatory effect (Ichihara et al., 1998). It is very well known that Ang II also has an important effect on the afferent and efferent arterioles, depending on its levels. In fact, Ang II preferentially constricts the efferent arteriole, leading to an increase in GFR. However, at a high level, Ang II constricts both afferent and efferent arterioles, thus reducing GFR (Denton et al., 2000; Carlstrom, 2021).

NO also plays a central role in regulating the pressure-natriuresis response (Majid et al., 1993) by inhibiting tubular sodium transport (Majid et al., 1994). In the nephron, both eNOS and nNOS are constitutively expressed with different localizations; nNOS is highly

expressed in the macula densa, but also in the proximal tubule and in the collecting duct, while eNOS is expressed in the proximal tubule and in the TAL of the loop of Henle. NO produced by both nNOS and eNOS contributes to sodium handling regulation (Carlstrom, 2021). This occurs by the effect of NO on the activity of tubular sodium transporters. Specifically, NO causes a decrease in Na-H exchange activity and Na^+/K^+ATPase activity (Liang et al., 1999). Evidence from studies involving eNOS KO mice suggests that eNOS-derived NO decreases NaCl absorption in the TAL of the loop of Henle (Plato et al., 1999; Plato et al., 2000). eNOS KO mice exhibited increased blood pressure in response to high salt intake and increased salt sensitivity, indicating that eNOS is an important regulator of salt sensitivity and protects against salt-induced hypertension (J. Li et al., 2009). Moreover, nephron-wide eNOS disruption in mice led to hypertension and impaired sodium excretion after high salt intake, likely by modulation of the sodium-chloride cotransporter (NCC) and the sodium-potassium-2chloride cotransporter type 2 (NKCC2) (Gao et al., 2018). Furthermore, by treating isolated cortical collecting ducts from rats with NO-donors like spermine diazeniumdiolate (NONOate) or nitroglycerin, it was shown that NO inhibits the amiloride-sensitive epithelial sodium channel (EnaC) (Stoos et al., 1995), as well as the antidiuretic hormone (ADH)-stimulated water and sodium reabsorption in the collecting duct (Garcia et al., 1996). Therefore, by acting on different channels of the nephron, NO induces an increase in water and sodium excretion (Fig. 1).

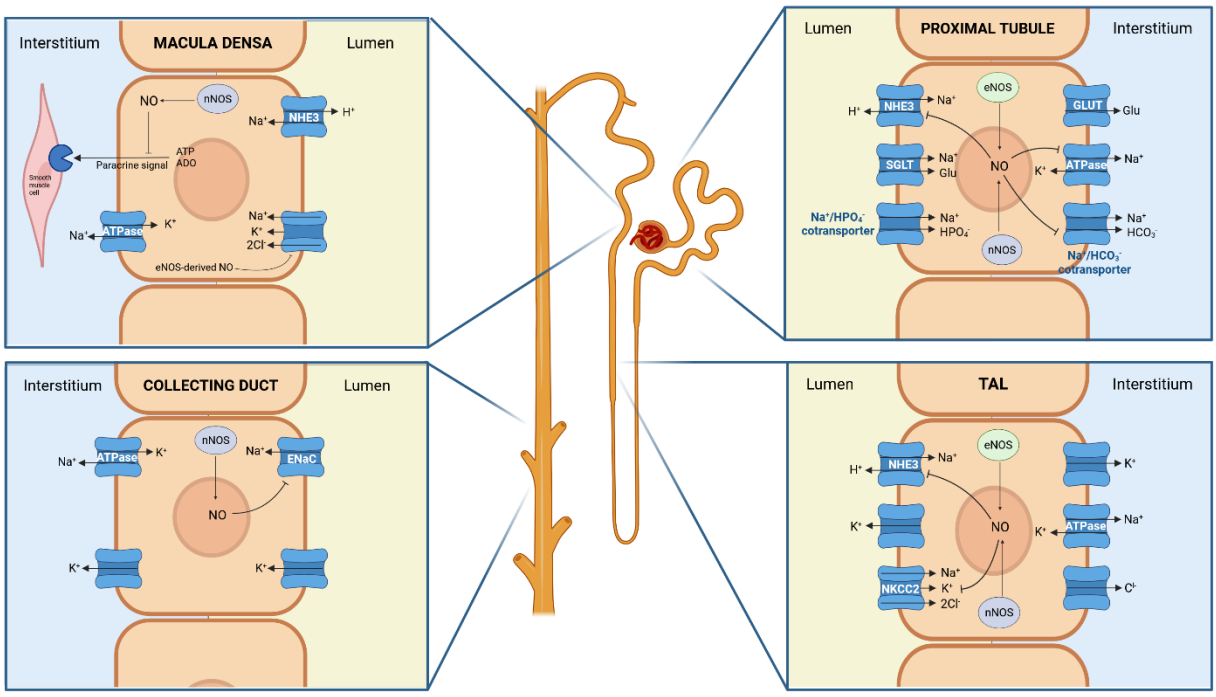

Figure 1 – Effect of NO on sodium transporters in the nephron.

NO produced by NOS plays a central role in sodium handling by inhibiting tubular sodium transport along the nephron. Specifically, NO produced by eNOS and nNOS in the proximal tubule inhibits the apical Na-H exchanger and the basolateral Na-K ATPase; NO produced by eNOS and nNOS in the TAL inhibits the apical Na-H exchanger and the apical NKCC2; NO produced by nNOS in the collecting duct inhibits the apical ENaC. The inhibition of the tubular sodium transport causes a decrease in sodium reabsorption and consequent increase in natriuresis. Figure redrawn and adapted from (Carlstrom, 2021).

Of interest, eNOS-derived NO signalling is also linked to oxygenation within the renal medulla. Inhibition of NOS can lead to decreased RBF and oxygen delivery, and consequently increased renal oxygen consumption (Edwards & Kurtcuoglu, 2022). The medullary circulation is typically more resistant to the vasoconstrictory effect of Ang II, compared to the cortical circulation. In 2002, the research group led by Cowley proposed that NO mediates a tubulovascular crosstalk in the renal medulla (Dickhout et al., 2002). They showed that treatment of the descending vasa recta from rats with Ang II exerted a vasoconstrictory effect by its action on the perycites, as shown by an increase in intracellular Ca^{2+} concentration. Importantly, only when the descending vasa recta were surrounded by the outer medullary vascular bundles, the medullary TAL, they observed a concomitant increase of intracellular NO concentration in the pericytes, which buffered the vasoconstrictor effect of Ang II (Dickhout et al., 2002).

The effects of NO donors and NOS inhibitors in the regulation of RBF, GFR, and sodium and water handling have been deeply investigated. Specifically, NO donors increase RBF and GFR by vasodilating renal vasculature and enhance sodium and water excretion by suppressing key transporters in the nephron; contrary, NOS inhibitors reduce RBF and GFR and enhance sodium and water reabsorption. However, the source of NO, which contributes specifically to the regulation of renal function, is still not fully understood. Both nNOS and eNOS are constitutively expressed in the kidney, with different localizations in the nephron. This suggests a reciprocal involvement in the mechanisms that regulate kidney function.

Our group and others showed that RBC also carry eNOS, which contributes to blood pressure regulation (Cortese-Krott et al., 2012; Wood et al., 2013). Therefore, research about the role of eNOS or nNOS in specific cells in the regulation of renal function in order to understand their specific contributions to the mechanisms involved is urgently needed.

1.6. The Cre/loxP system

The Cre/loxP system is a site-specific DNA recombination technology, which allows specific DNA modification in living organisms like deletion, inversion, and translocation of specific genes. It is based on the insertion of a loxP site and a Cre recombinase, both identified for the first time in 1981 by Sternberg in the bacteriophage P1 (Sternberg et al., 1981). The loxP site is characterised by 34 base pairs (bp) of DNA sequences, which consist of two 13 bp inverted repeat sequences flanking an 8 bp spacer region (ATAACTTCGTATA ATGTATGC TATACGAAGTTAT) (Abremski et al., 1983).

The Cre recombinase is a 38 kDa enzyme, which recognises the loxP site and catalyses the recombination of the DNA sequence between the two loxP sites (Abremski et al., 1984). In the bacteriophage P1, the loxP site and the Cre recombinase are separated by a region of 434 nucleotides containing an open reading frame, orfI, and at least three Cre promoters, pR1, pR2, and pR3 (Sternberg et al., 1986). Depending on the orientation of the loxP sites, the Cre recombinase can cause the deletion, inversion, or translocation of the flanked gene. When the two loxP sites are oriented in opposite directions, the DNA region is inverted (Fig. 2A); when they are oriented in the same direction, the DNA sequence is excised (Fig. 2B); when they are on separate DNA molecules, the DNA sequence is translocated, resulting in a reciprocal exchange of chromosome arms beyond the loxP sites (Fig. 2C). (Abremski et al., 1983; A. J. Smith et al., 1995). Thanks to this characteristic, the Cre/loxP system can inactivate (knock out or KO) or activate (knock in or KI) a specific gene in mice.

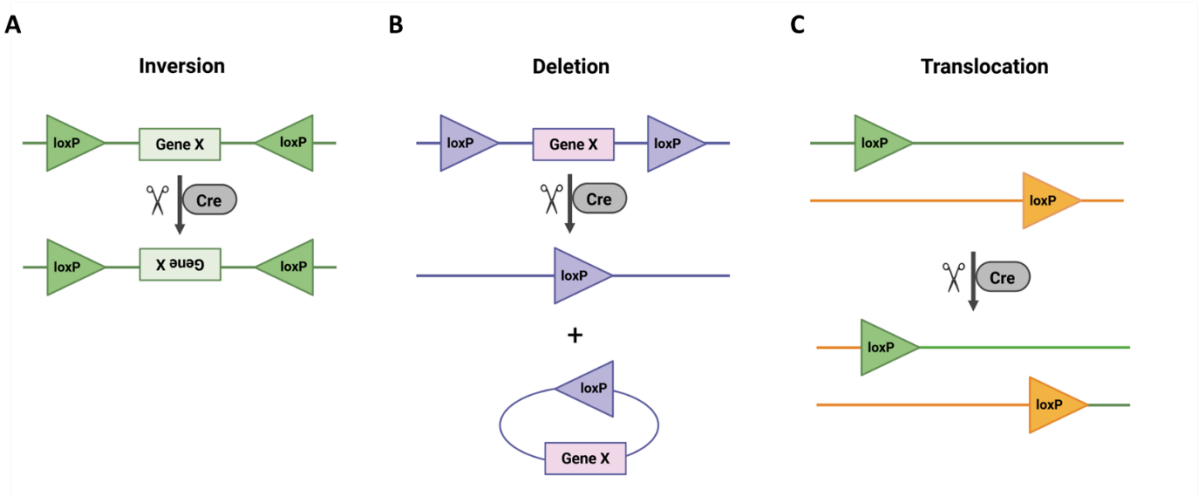

Figure 2 - Cre/loxP system for DNA recombination.

(A) When the loxP sites are oriented in opposite directions, the gene is inverted; (B) when the loxP sites are oriented in the same direction, the gene is excised; (C) when the loxP sites are in two different DNA molecules, the gene is translocated.

The Cre/loxP system method requires two strains of mice for this purpose, one expressing Cre recombinase in all cell types or in a specific cell, and the second carrying the gene of interest flanked (or floxed) by two loxP sites (Gu et al., 1994). To generate these two strains of mice, a plasmid encoding the floxed exon is designed and introduced into embryonic stem (ES) cells by electroporation or lipofection and injected into mouse blastocysts, which are then implanted to pseudopregnant female mice, generating chimeric mice (Fig. 3A). These are then crossed with wilde type (WT) mice to establish a stable line that carry the floxed gene in the germline (Fig. 3B). Finally, this mouse line is crossed with Cre recombinase expressing mice, allowing the generation of transgenic mice in which the targeted gene is excised or inverted (Fig. 3C).

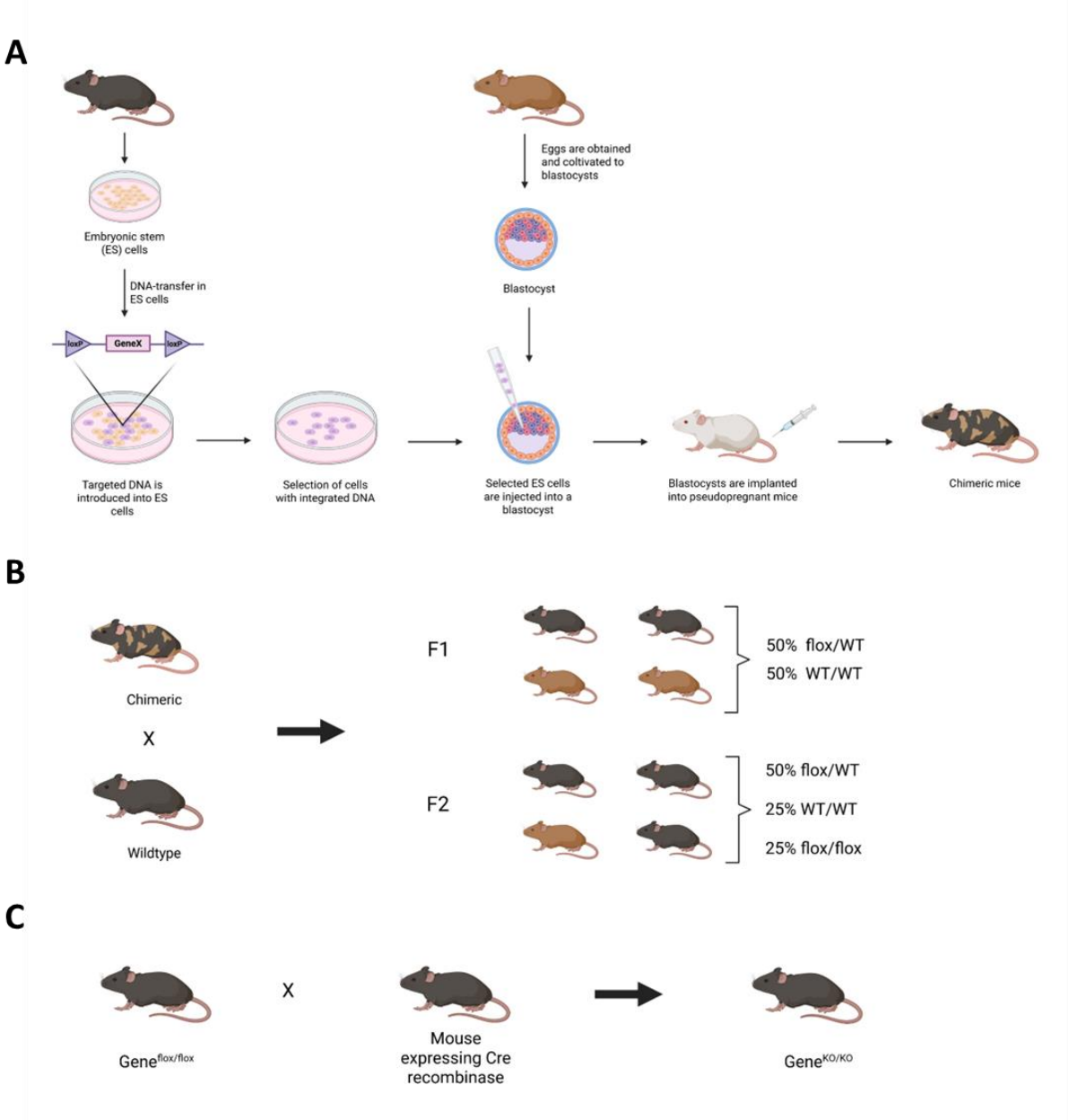

Figure 3 - Generation of floxed mice for Cre/loxP genetic recombination.

(A) A plasmid encoding the floxed gene is introduced into embryonic stem (ES) cells from a WT mouse (dark brown fur) by electroporation or lipofection and injected into mouse blastocysts (light brown fur), which are then implanted to pseudopregnant female mice (white fur), generating chimeric mice (dark and light brown fur). (B) Chimeric mice are crossed with WT mice to establish a stable line that carries the floxed gene. (C) Mice with the floxed gene are crossed with mice expressing Cre recombinase to generate KO mice for the targeted gene. Abbreviations: ES, embryonic stem; KO, knock out.

The Cre/loxP system allows the constitutive or inducible gene recombination depending on whether the Cre recombinase is constitutively expressed or its expression is regulated under the control of an external trigger, such as the administration of tamoxifen. The temporal expression of Cre recombinase is useful when the constitutive deletion of a specific gene can cause severe side effects. This approach is possible by fusing the Cre recombinase to a mutated hormone-binding domains of the estrogen receptor (CreER), which makes it insensitive to natural ligands and responsive to synthetic ligands (Feil et al., 1997). Therefore, Cre recombinase, initially inactive, can be activated by the administration of tamoxifen, which will bind the estrogen receptor, causing the translocation of the Cre recombinase from the cytoplasm to the nucleus; here the Cre recombinase will bind to the loxP sites, leading to DNA recombination (Metzger et al., 1995).

The Cre/loxP system offers several advantages, including its simplicity, its ability to recognise DNA in various conformations such as supercoiled, relaxed circle or linear forms, and it does not require the presence of additional cofactors or ATP (Abremski & Hoess, 1984). The ability to inactivate or reactivate the expression of a target gene in a specific cell allows a better understanding of gene function or disease mechanism. As compared to a global KO or KI approach, a cell-specific approach avoids unspecific adaptation mechanisms. By activating the gene only in specific cells, the phenotype can be investigated more accurately, excluding the influences of the gene expression in other tissues. Furthermore, this technique gives the ability to investigate the potential reversibility of a disease by activation of a specific gene in targeted cells. On the other hand, limitations of the Cre/loxP system include leaky Cre expression, which causes unspecific recombination events, requiring a careful characterization of off-target effects in other tissues.

2. Aim of the study

The kidney is one of the major regulators of blood pressure by water and sodium handling and by the renin-angiotensin-aldosterone system (RAAS). Lately, it was found that NO/sGC signalling is a crucial regulator of medullary blood flow and natriuresis, but the cells in which the regulation occurs are still unknown. In the juxtamedullary nephron, eNOS is expressed in the vasculature of the vasa recta and in the epithelial cells of the tubule. Moreover, RBCs also carry eNOS. NO produced in the tubulus by eNOS and nNOS can diffuse to the vasa recta and activate the NO/sGC signalling in the pericytes to induce vasodilation and increase RBF. On the other hand, NO produced by EC or RBC eNOS may diffuse to the tubulus and lead to natriuresis. In this way, NO mediates the tubulovascular crosstalk in the renal medulla. Furthermore, RBC eNOS, together with EC eNOS, may contribute to the modulation of GFR.

The aim of this study is to understand the role of eNOS in specific cells of the kidney in renal function.

To this aim $eNOS^{flox/flox}$ mice and $eNOS^{inv/inv}$ mice are generated and crossed with mice expressing Cre recombinase in all cells (Deleter Cre^{pos}), in ECs only, or in RBCs only, to generate global eNOS KO/WT and global eNOS KI/CondKO mice, EC eNOS KO/WT and EC eNOS KI/CondKO mice as well as RBC eNOS KO/WT and RBC eNOS KI/CondKO mice.

This work has three main goals:

(1) To verify that $eNOS^{inv/inv}$ = CondKO construct was efficient for reactivating eNOS expression in global eNOS KI mice and the effect of eNOS “gene dosage”, as proof of concept.

(2) To characterize the expression of eNOS in targeted and non-targeted tissues of the mouse lines as compared to the Cre-negative littermates.

(3) To investigate the role of eNOS expressed in ECs and RBCs in kidney function.

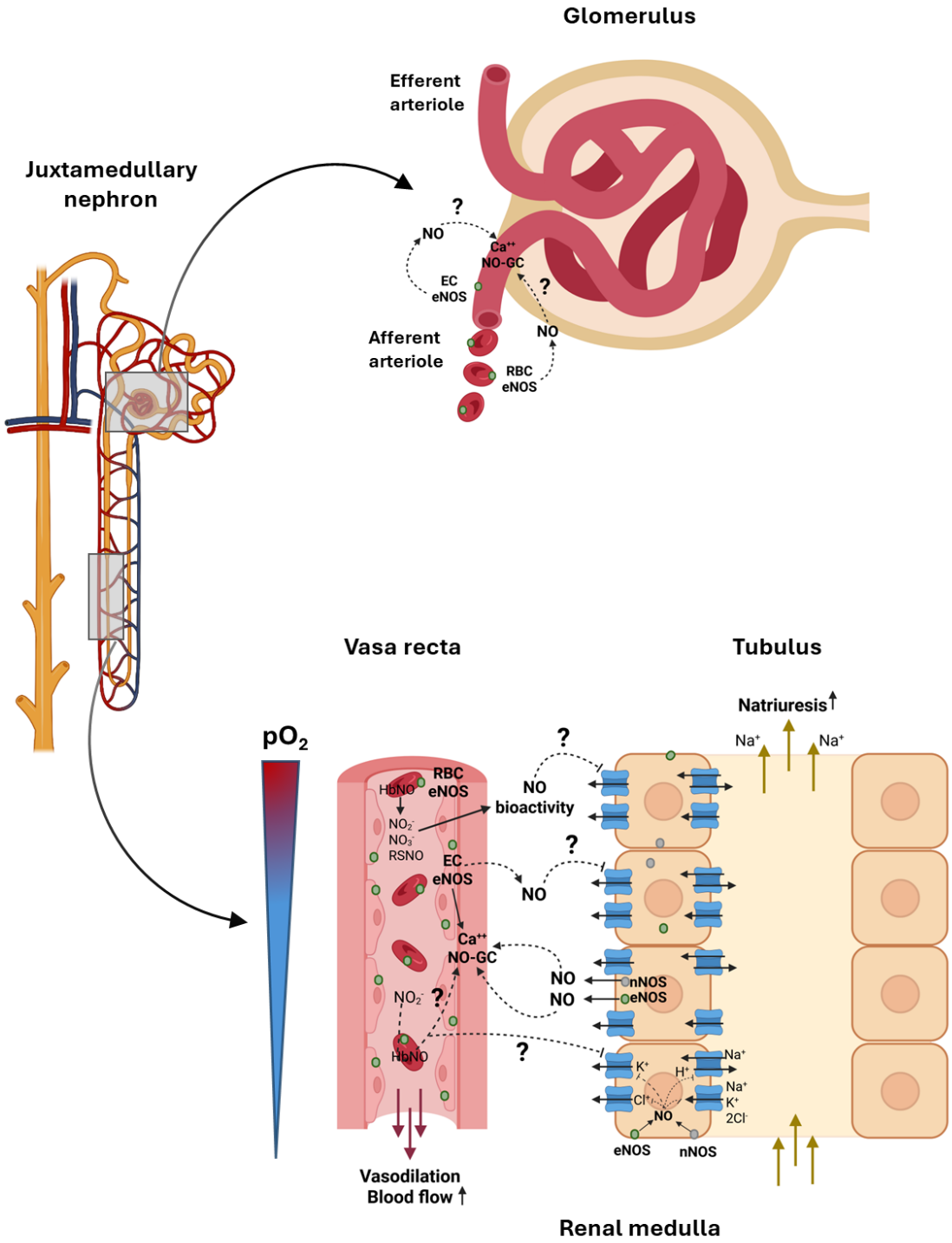

Figure 4 - Graphical abstract.

NO produced by eNOS regulates GFR by its vasodilator action primarily on the afferent arteriole of the glomerulus. Moreover, NO produced in the tubulus by eNOS and nNOS can diffuse to the vasa recta and activate the NO/sGC signalling in the pericytes to induce vasodilation and increase RBF. On the other hand, NO produced by EC or RBC eNOS in the vasa recta may diffuse to the tubulus and lead to natriuresis. In this way, NO mediates the tubulovascular crosstalk in the renal medulla. This study aims to understand the role of eNOS in ECs and RBCs in renal function regulation.

3. Materials and Methods

3.1. Materials

Table 1. Chemicals

Chemical	Manufacturer	Headquarter
Acetylcholine (Ach)	Merck	Darmstadt, Germany
Acrylamide	Carl Roth	Karlsruhe, Germany
Angiotensin II	Merck	Darmstadt, Germany
Bovine Serum Albumin (BSA)	Merck	Darmstadt, Germany
Buprenovet sine, buprenorphine	Bayer	Leverkusen, Germany
DNase I	Merck	Darmstadt, Germany
Ethylenediaminetetraacetic acid (EDTA)	Merck	Darmstadt, Germany
Ethanol	VWR Chemicals BDH	Radnor, US
Ferricyanide	Merck	Darmstadt, Germany
FITC-sinisitrin	MediBeacon GmbH	Mannheim, Germany
Glycine	Merck	Darmstadt, Germany
Hydroxyethylpiperazine ethanesulfonic acid (HEPES)	Merck	Darmstadt, Germany
Iodine	Merck	Darmstadt, Germany
Isoflurane	Piramal	Munich, Germany
KCl	Merck	Darmstadt, Germany
Ketaset, ketamine	Zoetis	Parsippany, US
methanol	Merck	Darmstadt, Germany
NaCl, powder	Carl Roth	Karlsruhe, Germany
NaCl, solution	Fresenius Kabi	Bad Homburg, Germany
N-ethylmaleimide (NEM)	Merck	Darmstadt, Germany
Phosphate-buffered saline (PBS)	Merck	Darmstadt, Germany
Peanut oil	Merck	Darmstadt, Germany
Phenylephrine (PE)	Merck	Darmstadt, Germany
Potassium ferricyanide	Merck	Darmstadt, Germany
Potassium hexacyanoferrate (III)	Merck	Darmstadt, Germany
Protease inhibitor cocktail	Roche	Basel, Switzerland
Proteinase K	Qiagen	Hilden, Germany
Sodium dodecyl sulfate (SDS)	Merck	Darmstadt, Germany
Skim milk powder	Merck	Darmstadt, Germany
Sodium nitrite	Merck	Darmstadt, Germany
Sodium nitroprusside (SNP)	Carl Roth	Karlsruhe, Germany

Sulfanilamide	Merck	Darmstadt, Germany
Tamoxifen	Merck	Darmstadt, Germany
Tetramethylethylenediamine (TEMED)	Carl Roth	Karlsruhe, Germany
Tris base	Merck	Darmstadt, Germany
Tween 20	Merck	Darmstadt, Germany
Rompun, xylazine	Bayer	Leverkusen, Germany
β-mercaptoethanol	Merck	Darmstadt, Germany

Table 2. Commercial kits

Kit	Manufacturer	Headquarter
Dynabeads antibody coupling kit	Thermo Fisher Scientific	Waltham, USA
Lowry assay	BioRad	Hercules, US
QuantiTect reverse transcription kit	Qiagen	Hilden, Germany
RNAeasy kit	Qiagen	Hilden, Germany
RNase-Free DNase Set	Qiagen	Hilden, Germany
SuperSignal™ West Femto Maximum chemiluminescent substrate	Thermo Fisher Scientific	Waltham, USA
SuperSignal™ West Pico Plus chemiluminescent substrate	Thermo Fisher Scientific	Waltham, USA

Table 3. Antibodies used for Western blots

Protein	Antibody	Dilution	Manufacturer	Code
eNOS	Purified Mouse anti-eNOS/NOS Type III	1:100 in 5% BSA	BD Biosciences	610297
eNOS	Purified Mouse anti-eNOS/NOS Type III	1:100 in 5% BSA	BD Biosciences	624086
Goat anti-mouse IgG	Goat anti-mouse IgG	1:5000 in 5% milk	BD Biosciences	554002
α-tubulin	Mouse anti-alpha-tubulin	1:5000 in 5% BSA	Sigma	T6199
β-actin	Mouse anti-beta actin	1:1000 in 5% BSA	Sigma	A1978

Table 4. Composition of solutions

Solution	Composition
Angiotensin II solution	8.182 mg Ang II in 1 mL 0.9 %NaCl
Blocking buffer for WB	Skim milk powder 5%, T-TBS 1x
FITC-sinistrin	15 mg per 100 g in 0.9% NaCl
Tri-iodide reductive solution	0.405 g KI, 0.143 g I_2, 3.75 mL dd H_2O, 50 mL glacial acetic acid
NEM/EDTA/PBS solution	0.5 mL EDTA 500 mM, 10 mL NEM 100 mM, PBS to 100 mL
PBS	8.54 mM Na_2HPO_4 and 1.46 mM KH_2HPO_4, 2.7 mM KCl and 137 mM NaCl
Potassium ferricyanide	1.646 g in 100 mL PBS
RIPA buffer	1 mL NP40, 500 mg sodium deoxycholate, 1 mL SDS 10%, PBS to 100 mL
Running buffer 10X	30.29 g 250 mM Tris base, 144 g 1.92 mM glycine, 10 g 35 mM SDS, dd H_2O to 1 L
Stripping buffer	10 mL SDS 10%, 3.33 mL 1.5 M Tris pH 8.8, 390 µL 2-mercaptohetanol, dd H_2O to 50 mL
Sulfanilamide	0.5 g in 10 mL 1 M HCl
Tamoxifen injection solution	60 mg tamoxifen in 1 mL EtOH at 60°C until dissolved, diluted 1:6 with peanut oil
TBS 20X	200 mM Tris base, 2 M NaCl in dd H_2O
Transfer buffer 10X	30.29 g 250 mM, 1.92 Glycine, dd H_2O to 1 L
Tris-buffer	50 mM Tris base
T-TBS	TBS 20X, Tween20 0.1% dd H_2O

Table 5. Table of instruments

Instrument	Manufacter	Headquarter
ChemiDOC™ Imaging System	Bio-Rad Laboratories GmbH	Hercules, CA, USA
FLUOstar OPTIMA	BMG LABTECH	Ortenberg, Germany
GeneExplorer	BIOER TECHNOLOGY	Hangzhou, China

iBright™ CL1500 Imaging System	Thermo Fisher Scientific	Waltham, USA
Millar pressure catheter	AD Instruments	Dunedin, New Zealand
MPVS ULTRA	AD Instruments	Dunedin, New Zealand
Nanodrop One	Thermo Fisher Scientific	Waltham, USA
Osmotic minipumps 1004	Alzet	Cupertino, CA, USA
PowerLab 16/35	AD Instruments	Dunedin, New Zealand
StepOnePlus Real-Time PCR System	AB Applied Biosystems	Waltham, USA
Transdermal Mini GFR Monitor	MediBeacon	Mannheim, Germany

Table 6. Table of softwares

Software	Manufacturer	Headquarter
ImageJ	National Institutes of Health	Rockville Pike Bethesda, MD, USA
Image Lab Software	Bio-Rad Laboratories GmbH	Munich, Germany
MediBeacon (MB Lab 2.26)	MediBeacon	Mannheim, Germany
Prism 10.4.2 (633)	GraphPad	San Diego, CA, USA
StepOne Software	AB Applied Biosystems	Waltham, USA

Table 7. Primers for DNA recombination.

Specific primers and probes for real-time PCR analysis designed by Transnetyx (Cordova, TN).

Allele	Forward Primers	Reverse Primers	Probes
		$eNOS^{inv/inv}$ mice	
$eNOS^{inv}$	ACCTCCTAAGGCTGTTGTGAGA	CTCCTCTTCCTGACACTTTCTGT	CCCTCACTAAAGGGCG
$eNOS^{fl}$	CTCCTCTTCCTGACACTTTCTGT	GCTTGCTGCAATTGATAACTTCGTA	CAGCTCATAACTTCGTATAGCAT
Intermediate1	AGGAAGGACCAGAGGGATCAAG	GGAACTTCAGATCTCCATAACTTCGT	GCAAGAACTTATAACTTCGTATAGTAT
Intermediate2	GGAACTTCAGATCTCCATAACTTCGT	ACCCTCCTCTTCCTGACACTTT	CTGTCAGCTCATAACTTC
Cre	TTAATCCATATTGGCAGAACGAAAACG	CAGGCTAAGTGCCTTCTCTACA	CCTGCGGTGCTAACC
		$eNOS^{flox/flox}$ mice	

eNOS^{flox}	GGCGGCCGCATAACTTC	CAGACTGCCTTGGGAAAAGC	CCGGTAGAATGAAGTTC
Δ-allele	ACCTCCTAAGGCTGTTGTGAGA	GCCAAAGGCTTGCTGCAATT	CCCTCACTAAAGGGCG
Cre	TTAATCCATATTGGCAGAACGAAAACG	CAGGCTAAGTGCCTTCTCTACA	CCTGCGGTGCTAACC

Table 8. Primers for mRNA expression

Gene	Assay ID	Manufacturer	Headquarter
Rplp0	Mm00725448_s1	Thermofisher	Waltham, USA
Nos3	Mm00435197_g1	ThermoFisher	Waltham, USA

3.2. Animals

All experiments were approved by the Landesamt für Natur, Umwelt und Verbraucherschutz (LANUV) according to the European Convention for the Protection of Vertebrate Animals used for Experimental and other Scientific Purposes (Council of Europe Treaty Series No. 123), under the O30/16, G406/21 and G488/24 project numbers. Animal care was provided according to the institutional guidelines. Tamoxifen-inducible endothelial-specific Cre mice (Tg(Cdh5-Cre/ERT2)1Rha; MGI:3848982) (Pitulescu et al., 2010) were kindly provided by Prof Dr E. Lammert (Heinrich-Heine-University of Düsseldorf). Mice expressing Cre recombinase in erythroid cells under the control of the promoter of the globin β-chain (C57BL/6-Tg(Hbb-Cre)12Kpe/J; MGI: J:89725) (Peterson et al., 2004) were obtained by Jackson Laboratory (JAX stock No. 008314) and crossed for >10 generations with C57BL/6J. DeleterCre (C57Bl/6.C-Tg(CMVCre)1Cgn/J) (DelCre) (Schwenk et al., 1995) mice expressing Cre in all cells were kindly provided by Prof Claus Pfeffer (Heinrich Heine University of Düsseldorf). Experimental planning and execution followed the ARRIVE recommendations (Animal Research: Reporting of In Vivo Experiments) (Kilkenny et al., 2010). For experiments, 2- to 31-month-old male mice up to 40 g were used. Mice of the same genotype and age were randomly assigned to the experimental groups.

3.2.1. Generation of eNOS$^{flox/flox}$ mice

To generate eNOS$^{flox/flox}$ mice, exon 2 of the *Nos3* genomic locus was targeted for Cre-mediated excision by inserting simultaneously an orphan loxP site and an FRT-neo-FRT-loxP resistance cassette, oriented in the same direction. The plasmid encoding the floxed gene was sequenced, linearized, and electroporated in A9 ES cells (hybrid C57/129), 100 clones were picked, and positive clones were screened by Southern blot at the 5′ arm and by long-range polymerase chain reaction (PCR). The ES cells were then injected into

mouse blastocysts and implanted into pseudopregnant female mice, generating chimeric mice. These mice were then backcrossed with C57BL/6J mice for 10 generations and finally crossed to generate $eNOS^{flox/flox}$ mice. By crossing $eNOS^{flox/flox}$ mice with Deleter Cre^{pos} ($DelCre^{pos}$) mice, exon 2 was excised, generating global eNOS KO mice (Δ-eNOS)

3.2.2. Generation of $eNOS^{inv/inv}$ mice

To generate the $eNOS^{inv}$ allele, a loxP-eNOS construct was generated by simultaneously inserting an orphan loxP site and an FRT-neo-FRT-loxP resistance cassette into the *Nos3* genomic locus to target exon 2 of *Nos3* by Cre recombinase-mediated excision; an inverted exon 2 was inserted in *Nos3,* and two additional loxP511 sites were inserted in the loxP-eNOS construct to generate a loxP-$eNOS^{inv}$ construct. The plasmid was sequenced, linearized, and electroporated in A9 ES cells (hybrid C57/129), 300 clones picked, and positive clones were screened by Southern blot at 5′ arm and by PCR. Heterozygous C57/129Sv chimera $eNOS^{wt/inv}$ mice were obtained from two independent clones, and two independent homozygous $eNOS^{inv/inv}$ mouse lines were generated. Genotyping was carried out by PCR. One line was selected by testing the efficiency of breeding, Cre-mediated recombination, and blood pressure response. These were then backcrossed for 10 generations with C57BL/6J mice. Homozygous $eNOS^{inv/inv}$ mice were then crossed with $DelCre^{pos}$ mice to generate $eNOS^{fl/fl}$ $Cre^{pos/neg}$ mice. After further crossing with $eNOS^{inv/inv}$ Cre^{neg} mice, $eNOS^{fl/inv}$ Cre^{neg} mice were generated and used for experiments described here.

3.2.3. Generation of EC eNOS KO/WT and EC eNOS KI/CondKO mice

To generate EC-specific eNOS KO and EC eNOS KI mice, $eNOS^{flox/flox}$ mice or $eNOS^{inv/inv}$ mice were crossed with $Cdh5Cre/ERT2^{pos}$ mice to generate $eNOS^{flox/flox}$ $Cdh5\text{-}Cre/ERT2^{pos}$ and $eNOS^{flox/flox}$ $Cdh5\text{-}Cre/ERT2^{neg}$ mice or $eNOS^{inv/inv}$ $Cdh5\text{-}Cre/ERT2^{pos}$ and $eNOS^{inv/inv}$ $Cdh5\text{-}Cre/ERT2^{neg}$ mice, respectively. To induce the EC-specific activation of Cre recombinase, the mice were treated by i.p. injection with tamoxifen for five consecutive days (75 mg/kg) and a waiting time of 21 days before experimentation was initiated.

3.2.4. Generation of RBC eNOS KO/WT and RBC eNOS KI/CondKO mice

To generate erythroid cell-specific eNOS KO mice (RBC eNOS KO/WT) and RBC eNOS KI/CondKO mice, $eNOS^{flox/flox}$ mice or $eNOS^{inv/inv}$ mice were crossed with erythroid-specific $Hbb\text{-}Cre^{pos}$ mice to generate $eNOS^{flox/flox}$ $Hbb\text{-}Cre^{pos}$ (RBC eNOS KO) and $eNOS^{flox/flox}$ $Hbb\text{-}Cre^{neg}$ (WT) mice or $eNOS^{inv/inv}$ $Hbb\text{-}Cre^{pos}$ (RBC eNOS KI) and $eNOS^{inv/inv}$ $Hbb\text{-}Cre^{neg}$ (CondKO), respectively.

3.3. Collections of mouse tissues, blood and cells

3.3.1. Tissues collection

The mice were i.p. injected with buprenorphine (0.1 mg/kg), anesthetized with 3% isoflurane, and killed by exsanguination. Organs were explanted after perfusion with phosphate-buffered saline (PBS) (Tab. 4), snap frozen in liquid nitrogen, and kept at -80°C until use.

3.3.2. Isolation of bone marrow

Bone marrow was isolated from the tibia and femur (4 bones per mouse) by placing the bones in a 0.5 mL tube with a small hole in the bottom, which was then mounted on a 2 mL tube, and centrifuged at max speed for 1 min. The bone marrow collected in the 2 mL tube was snap frozen in liquid nitrogen and kept at -80°C until use.

3.3.3. Blood collection and RBCs isolation

Blood was collected by heart puncture and transferred to tubes containing ethylenediaminetetraacetic acid (EDTA) as anticoagulant (final concentration 5 mM EDTA). Blood was centrifuged at 800 g for 10 min at 4°C. The supernatant (upper layer), the plasma, was collected and frozen. The second layer, the buffy coat, containing white blood cells and platelets, was discarded. The lowest layer, the RBCs, was collected and frozen or processed to obtain RBC membranes (ghosts).

3.3.4. Removal of white blood cells

RBCs used for immunoprecipitation of eNOS (see § 3.4.4) were first cleaned from white blood cells (WBCs) contamination by using Acrodisc WBC Filters (AP-4952, Pall Corporation, NY, USA). In detail, the filter (without the plunger) was attached to a 10 mL syringe and placed on top of a sterile 50 mL Falcon tube. 2 mL of PBS were used to wet the the membrane of the filter and afterwards 1 mL of blood was transferred to the empty syringe to proceed with filtration by gravity. 10 mL of PBS was added and filtered by gravity to wash the membrane. The washing step was repeated two times. The leukocyte-depleted filtrate was centrifuged at 250 g for 10 min at 4 °C, and the supernatant was discarded. Leukocyte-depleted RBCs were frozen at -80°C until use.

3.3.5. Ghost preparation

Ghosts were prepared from 250-350 µl fresh RBC pellet. RBCs were suspended at 40% Ht in a cold hypotonic buffered solution (PBS diluted 1:27) to a final volume of 2000 µL and incubated on ice (mixed with ethanol) at 0-2°C for 20 min. The ghosts were centrifuged for 10 min at 20000 g at 4°C, and the supernatant was discarded. The pellet was then carefully resuspended in the starting volume of hypotonic buffered solution and incubated for 20 min.

The washing steps were repeated in total three times. After the last centrifugation, the supernatant was discarded, and the ghosts were snap frozen in liquid nitrogen and kept at -80°C until use.

3.4. Molecular characterization of the transgenic mice lines

3.4.1. Analysis of DNA recombination

Recombination of the DNA locus by Cre recombinase was determined by extracting genomic DNA from targeted and non-targeted tissues and analyzed by real-time PCR conducted by Trasnetyx (Cordova, TN). Specific primers and probes were designed to recognize the WT allele ($eNOS^{WT}$), the floxed allele ($eNOS^{flox}$), the allele with targeted deletion ($eNOS^{\Delta}$), the floxed/inverted allele ($eNOS^{inv}$), the flipped allele ($eNOS^{fl}$), as well as the two intermediates of partial recombination (intermediate 1 and 2) (Transnetyx, Cordova, TN) (Tab. 7). Relative copies number (RCN) of the target gene was normalized to *cJun* as a housekeeping gene.

$$RCN1 = 2^{-(Target\ Ct1 - Average\ Housekeeping\ gene\ Ct)}$$

$$RCN2 = 2^{-(Target\ Ct2 - Average\ Housekeeping\ gene\ Ct)}$$

$$Reported\ \text{raw signal} = Average\ (RCN1, RCN2)$$

3.4.2. Analysis of eNOS expression in tissues by real-time RT-PCR

Extraction of total RNA, retrotranscription (RT), and real-time PCR were carried out on aorta and kidney lysates. In detail, the tissues were lysed and homogenized by using TissueRuptor in 400 µL or 3 mL (respectively for aorta and kidney) RLT Buffer (Qiagen, Hilden, Germany) containing 2-mercaptoethanol, followed by homogenization with a QIAshredder homogenizer and treatment with 10 µL of proteinase K for 10 min at 55°C. The total RNA was extracted by using RNAeasy Minikit and DNase I digestion (Qiagen). After treatment with ethanol (96-100%), the sample lysates were loaded into RNeasy Mini Spin columns to bind the total RNA and washed 3 times with RW1 and RPE/ethanol buffers. The total RNA was finally eluted with RNase-free water. RNA concentration and quality were assessed by using a NanoDrop spectrophotometer (Thermo Scientific) and an RNA NanoChip Agilent 2100 Bioanalyser (Santa Clara, CA, USA), respectively. The samples were incubated with gDNA wipe-out buffer for 2 min at 42°C to remove the remaining DNA. RT was carried out with QuantiTec reverse transcription kit (Qiagen). cDNA was generated from RNA MasterMix containing reverse transcriptase, RT-primers, and RT-buffer. The

samples were incubated for 15 minutes at 42°C, followed by incubation at 95°C for 3 min. To measure mRNA expression, cDNA was mixed with MasterMix containing 10 µL TaqMan Gene Fast Advanced Master Mix and 1 µL TaqMan Gene Expression Assay (Tab. 8). The qPCR run was built out of 2 minutes at 50°C and 2 minutes at 95°C, followed by 40 cycles consisting in 3 seconds at 95°C and 30 seconds at 60°C and was performed using the Applied Biosystems StepOnePlus Real-time PCR System. Data were analysed using the ΔΔCt method, as described previously (Livak et al., 2001). The mRNA expression of the gene of interest was normalized to that of *Rplp0* by subtracting the Ct of the housekeeping gene from the Ct of the gene of interest. The mean of Ct of the WT group was used to normalise the data according to the following calculation:

$$\Delta Ct = Gene\ Ct - Housekeeping\ Gene\ Ct$$

$$\Delta\Delta Ct = Sample\ \Delta Ct - Average\ Control\ Group\ \Delta Ct$$

$$2^{-\Delta\Delta Ct}$$

3.4.3. Determination of eNOS protein level in ghosts and tissues by immunoblotting

Kidneys, heart, lung and liver were lysed in 1 mL of RIPA buffer (150 µL for aorta), containing a cocktail of protease inhibitors (Roche, Basel, Switzerland), homogenized on ice by using Tissue Ruptor (Qiagen, Hilden, Germany), sonicated for 1 min at 4°C, and centrifuged at 10000 g for 10 min at 4°C. Ghosts were lysed in 2 volumes of RIPA buffer and then centrifuged at 10000 g for 10 min at 4°C. The total protein concentration of the supernatant was determined by the Lowry assay (Biorad). Lysates were loaded on a 10% Bis-Tris gel (Carl Roth, Karlsruhe; Germany) and transferred onto a nitrocellulose membrane (Amersham Biosciences, Munich, Germany). The membranes were blocked for 1 hour with 5 % Milk (Bio-Rad, Düsseldorf, Germany) in T-TBS and incubated overnight at 4°C with a mouse anti-eNOS (1:100), or monoclonal mouse anti-α-tubulin (1:5000) primary antibody in T-TBS. After washing for 1 hour in T-TBS, the membranes were incubated with HRP-conjugated goat anti-mouse secondary antibodies (1:5000), and bands were detected using West Pico or Femto Chemiluminescence Detection Reagents and detected by a ChemiDoc (Biorad) or by an iBright FL1000 (Thermo Fisher Scientific). Band intensity of eNOS was quantified by using ImageJ (National Institutes of Health, USA).

3.4.4. Determination of eNOS expression in RBC lysates by immunoprecipitation/immunoblotting

Lysis and extraction of eNOS from RBCs were carried out by immunoprecipitation by using Epoxy-Dynabeads cross-linked to an antibody anti-eNOS (dynabeads antibody coupling kit

#143.11D, Thermo Fisher Scientific; anti-eNOS/NOS type III antibody free from glycerol custom made from #624086, stock: 1 mg/ml in PBS pH 7.4, BD Bioscience, Erembodegem, Belgium BD Bioscience). After several washing steps of 10 mg of magnetic beads with solution C1, the antibody anti-eNOS was added to the beads. After washing with solution C2, the beads and the antibody were incubated on a roller at 37°C overnight to allow the coupling. The beads cross-linked to the antibody were washed with solutions HB, LB, and SB and resuspended in SB solution to a final concentration of 10 mg/mL and stored at 2-8°C until use. RBCs were lysed with 2 volumes of RIPA buffer, and the total protein concentration of the supernatant was determined by the Lowry assay (Bio-Rad, Feldkirchen, Germany). The lysate was diluted to a concentration of 100 µg/mL and incubated overnight with the Epoxy-Dynabeads crosslinked with an antibody anti-eNOS; after magnetic separation, proteins were eluted with LDS sample buffer and loaded on a 6-12 % Tris-Acetate pre-cast gels (Invitrogen, Carlsbad, US) and transferred onto nitrocellulose (Amersham Biosciences, Munich, Germany). The membranes were blocked for 1 hour with 5 % Milk (Bio-Rad, Feldkirchen, Germany) in T-TBS (10 mM Tris, 100 mM NaCl, 0.1% Tween) and incubated overnight at 4 °C with a mouse anti-eNOS (1:100) primary antibody in T-TBS. After washing for 1 hour in T-TBS (steps of 5-10 minutes), the membranes were incubated with HRP-conjugated goat anti-mouse secondary antibodies (1:5000; BD Biosciences, St Hose, CA) and bands were detected using West Femto Chemiluminescence Detection Reagent in a ChemiDoc (Bio-Rad, Feldkirchen, Germany).

3.4.5. Determination of eNOS by immunotransmission electron microscopy

RBCs were isolated by cardiac puncture and fixed in 4% PFA plus 0.05% glutaraldehyde. RBCs were spun down, embedded in LR White, and sectioned at 70 nm sections. Rabbit eNOS antibody (Abcam cat #ab199956) was added at 1:50 overnight, with donkey anti-rabbit secondary gold beads (18 nm; Jackson Labs cat #711-2125-152) used to resolve protein localization on the RBCs.

3.4.6. Determination of NO metabolites in blood and tissues

Nitrite, nitrate, nitrosyl heme (NO-heme), and nitrosated (S-nitroso and N-nitroso) product (RXNO) concentrations were measured in tissues, cells, and plasma using a chemiluminescence detector, as described previously (Bryan et al., 2004) and reviewed recently by us (J. Li et al., 2024).

In detail, blood was collected by heart puncture and transferred to a 2 mL tube containing 0.1 mL NEM/EDTA solution (100 mM). Whole blood was centrifuged at 3000 g for 2 minutes at 4°C. Plasma and RBCs were separated and frozen in liquid nitrogen. Organs were perfused with NEM/EDTA solution, weighed after collection, snap frozen in liquid nitrogen,

and stored at -80°C until use. The organs and tissues were homogenized in NEM/EDTA/PBS lysis buffer (Tab. 4), with a lysis factor of 1:12.5 (mg/µL) for all the organs, except the aorta 1:40 (mg/µL). RBCs were lysed in 2 volumes of NEM/EDTA/MilliQ water as lysis buffer. Plasma was injected without any further dilution. Nitrite was determined by reductive cleavage in 20 mL of tri-iodide solution (0.405 g KI, 0.143 g I_2, 3.75 mL Milli-Q water, 50 mL glacial acetic acid, Tab. 4) in a 60°C chamber. The NO released from these reactions was detected by chemiluminescent reaction with ozone. NO-heme levels were quantified by denitrosylation in 10 mL potassium hexacyanoferrate (III) solution (1.646 g in 100 mL PBS, Tab. 4) in a 37°C chamber. To detect nitroso species, sulfanilamide was added at a ratio of 1:10 and incubated for 15 minutes at room temperature, and then measured in a tri-iodide reductive solution in a 60°C chamber. For the quantification of nitrate levels, the samples were deproteinated with ice-cold methanol (1:1 v/v), cleared by centrifugation, and analysed by high-pressure liquid chromatography using a nitrite/nitrate analyzer (ENO20, Eicom).

3.5. Characterization of systemic hemodynamics and vascular function

3.5.1. Blood pressure measurements by Millar catheterization

Systemic hemodynamics were measured by invasive catheterization using a 1.4F Millar pressure-conductance catheter (SPR-839, Millar Instrument, Houston, TX, USA). The mice were intubated and anesthetized with 3% isoflurane controlled by using an anesthesia unit equipped with an isoflurane vaporizer, a flowmeter for compressed air with a flow of 0.2 L/min (Hugo Sachs Elektronik, Harvard Apparatus GmbH, March-Hugstetten, Germany). The respiration rate was controlled by a Minivent (Hugo Sachs). After neck incision and isolation of the right carotid, the Millar catheter was placed into the artery and fixed with silk sutures. Isoflurane was decreased to 2.5% before the measurement started. Mice were i.p. injected with buprenorphine (0.1 mg/kg) 30 minutes before surgery. The measurements of systolic blood pressure (SBP), diastolic blood pressure (DBP), and heart rate (HR) were recorded for 5 minutes with a Millar box, and LabChart 7 (AD Instruments, Oxford, UK) was used for analysis. Mean arterial pressure (MAP) was calculated with the following formula:

$$MAP = \frac{SBP + 2 * DBP}{3}$$

3.5.2. Measurement of endothelial function *ex vivo*

Functional activity of the thoracic aorta was analyzed in an organ bath as described before (Suvorava et al., 2005). The thoracic aorta was isolated, transferred into HEPES buffer, and

cut into 2 mm aortic rings. After a 60-min equilibration phase, the aortic rings were treated with 80 mM KCl. The vasoconstriction that developed during the last KCl application was taken as the maximal receptor-independent vasoconstriction. After submaximal precontraction with phenylephrine (PE), aortic rings were treated with cumulative concentrations of acetylcholine (ACh) (1 nM, 3 nM, 10 nM, 30 nM, 100 nM, 300 nM, 1 µM, 3 µM, 10 µM), followed by treatment with PE (1 nM, 3 nM, 10 nM, 30 nM, 100 nM, 300 nM, 1 µM, 3 µM, 10 µM), and subsequently with sodium nitroprusside (SNP) (0.1 nM, 0.3 nM, 1 nM, 3 nM 10 nM, 30 nM, 100 nM, 300 nM, 1 µM, 3 µM, 10 µM).

3.6. Characterization of renal function

3.6.1. GFR measurement

GFR was measured in mice by a noninvasive clearance device (NIC-Kidney Device; MediBeacon, Mannheim, Germany), which can detect fluorescent molecules. In detail, the fur was removed from the back of the mice by using an electric shaver and depilatory cream, and the skin was cleaned with warm water. The device was fixed on the depilated back of isoflurane-anesthetized mice (3-4% isoflurane for induction + 2.5% for maintenance) by using a double-sided adhesive patch. Baseline was recorded for 1 minute. FITC-sinistrin (15 mg per 100 g in 0.9% NaCl; MediBeacon) was injected intravenously, and transcutaneous measurement was carried out in awake mice for at least 60 minutes. Half-life value of the FITC-sinistrin was calculated by MediBeacon software (MB Lab Ver. 2.26), and GFR was calculated as follow (Schreiber et al., 2012):

$$GFR\ [\mu L * \min * 100\ g\ BW] = \frac{16416.8[\frac{\mu L}{100 g\ BW}]}{\frac{t1}{2}\ (FITC - sinistrin)[min]}$$

3.6.2. Preparation and filling of osmotic minipumps with Ang II

Ang II was dissolved in saline buffer (8181.82 ng/µL in 0.9% NaCl). Osmotic minipumps (model 1004, Alzet) were filled with around 100 µL of Ang II solution (the mean fill volume changes depending on the LOT). To verify that the minipumps were filled correctly, they were weighed before and after the filling. The difference in weights gives the net weight of the solution loaded, which must be over 90% of the reservoir volume (mean fill volume). Minipumps were then incubated in saline buffer at 37°C for at least 48 hours before implantation.

3.6.3. Osmotic pumps implantation

The mice were anesthetised with a combination of i.p. injection of ketamine/xylazine (100mg/kg and 10 mg/kg) and 1.5-2% of isoflurane. The minipumps were implanted subcutaneously on the back of anesthetized mice through a mid-scapular incision, which was finally sutured with a silk suture thread (18501G, Ethicon, New Jersey, US). Ang II (dose of 500 ng/kg/min) was delivered for 13 days.

3.6.4. Overnight urine collection in metabolic cages

Mice were placed individually in metabolic cages for overnight (14 hours) urine collection, with water and food ad libitum. Urines were collected throughout the period, weighed, and stored at -80°C until use. Urinary sodium concentrations were measured by the Central Laboratory of the Universitätsklinikum of Düsseldorf using a modular analyzer (Cobas 8000, Roche, Basel, Switzerland) and sodium excretion was normalized to the total urine volume.

3.6.5. Sodium excretion after salt and volume challenge

Mice were loaded with a volume of 0.9% NaCl equivalent to 10% of their body weight. Each mouse was placed in metabolic cages, and the urines were collected in two 2 mL collecting tubes. The collecting tubes were changed every hour for five hours. Urines were weighed and stored at -80°C until use. Sodium concentration in the urine was measured by the Central Laboratory of the Universitätsklinikum of Düsseldorf using a modular analyzer (Cobas 8000, Roche, Basel, Switzerland), and accumulated results of sodium (1) and urinary volume (2) excretion were expressed as a percentage of sodium and volume load injected. The sodium concentration in urine or the urinary volume at each point was added to the previous value to generate the accumulated curve, which was ultimately expressed as percentage.

$$Na^{+}\text{excretion}\ (\%) = \frac{mmol\ of\ Na^{+}\ excreted}{mmol\ of\ Na^{+}\ injected} * 100 \quad (1)$$

$$Urine\ \text{excretion}\ (\%) = \frac{mL\ of\ urine\ excreted}{mL\ of\ NaCl\ injected} * 100 \quad (2)$$

3.7. Statistical analysis

Unless otherwise specified, all results are presented as mean ± standard deviation (SD). Statistical analysis was carried out with GraphPad 10 for Windows (Version 10.4.2 (633)). Normal distribution was tested by D'Agostino-Pearson test. Unpaired Student's t-test with Welch's correction was used to determine statistical significance between two independent groups. For multiple comparisons, 1-way or 2-way ANOVA and Tukey post-hoc test were

used as indicated in the legends. Differences were considered statistically significant at $p < 0.05$. Specific statistic tests and numbers are indicated in the figure legends.

4. Results

4.1. Generation of the founder lines eNOS$^{flox/flox}$ and eNOS$^{inv/inv}$ mice

4.1.1. Gene-targeting strategy for the generation of eNOS$^{flox/flox}$ mice.

To generate eNOS$^{flox/flox}$ mice, exon 2 of the *Nos3* genomic locus was targeted for Cre-mediated excision by inserting simultaneously an orphan loxP site and an FRT-neo-FRT-loxP resistance cassette, oriented in the same direction. The plasmid encoding the floxed gene was sequenced, linearized, and electroporated in A9 ES cells (hybrid C57/129). 100 clones were picked, and positive clones were screened by Southern blot at the 5′ arm and by long-range PCR. These were then injected into mouse blastocysts and implanted into pseudopregnant female mice to generate chimeric mice, which were then backcrossed with C57BL/6J mice for 10 generations to generate eNOS$^{flox/flox}$ mice. By crossing eNOS$^{flox/flox}$ mice with mice expressing Cre recombinase, exon 2 is excised, generating global eNOS KO mice (Δ-eNOS) (Fig. 5).

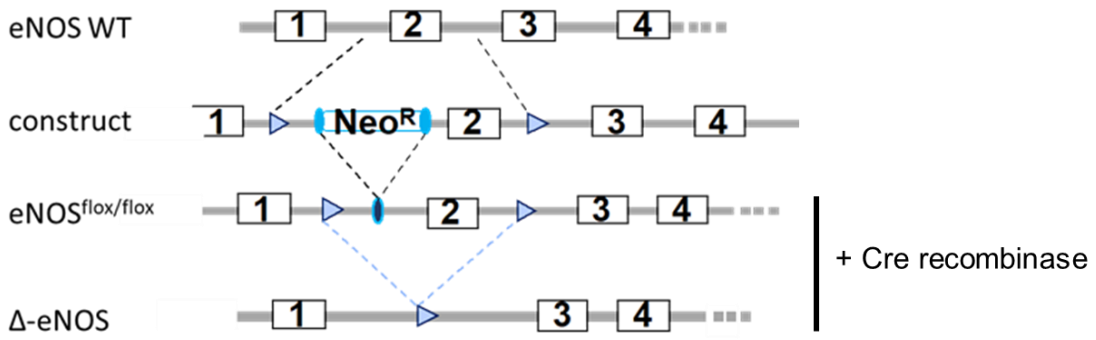

Figure 5 - Scheme describing the gene-targeting strategy for the generation of eNOS$^{flox/flox}$ mice.

To generate eNOS$^{flox/flox}$ mice, exon 2 of the Nos3 genomic locus was targeted for Cre-mediated excision by inserting simultaneously an orphan loxP site and an FRT-neo-FRT-loxP resistance cassette, oriented in the same direction. The plasmid encoding the floxed gene was sequenced, linearized, and electroporated in A9 ES cells (hybrid C57/129). 100 clones were picked, and positive clones were screened by Southern blot at the 5' arm and by long-range PCR. These were then injected into mouse blastocysts and implanted into pseudopregnant female mice, generating chimeric mice. These mice were then backcrossed with C57BL/6J mice for 10 generations to generate eNOS$^{flox/flox}$ mice. By crossing eNOS$^{flox/flox}$ mice with mice expressing Cre recombinase, exon 2 is excised, generating global eNOS KO mice (Δ-eNOS).

4.1.2. Gene–targeting strategy for the generation of eNOS$^{inv/inv}$ mice

To generate eNOS $^{inv/inv}$ mice, a gene-targeting construct was designed, in which an inverted (or “flipped”) exon 2 was inserted, followed by a second copy of a correctly oriented exon 2. Both copies were flanked by two pairs of loxP and loxP511 sequences (Fig. 6, Construct). After removal of the neomycin resistance cassette, this plasmid construct was used to generate eNOS$^{inv/wt}$ mice by gene targeting replacement. The generated mice were backcrossed for 10 generations with C57BL/6J mice and then crossed with each other to generate eNOS$^{inv/inv}$ mice.

In the presence of a Cre recombinase, two possible recombination reactions can occur, depending on which couple of loxP sites is targeted by the Cre recombinase. One reaction leads to the “flipping” of the inverted exon 2 (intermediate 1) (green), followed by the removal of the second exon 2 (black). The second type of reaction leads to the flipping of the whole sequence containing both the first and the second copy of exon 2 (intermediate 2) followed by the removal of the flipped exon (black). Both reactions lead to a final construct where only one exon 2 oriented in the correct direction remains, resulting in the “reactivation” of the gene (Fig 6).

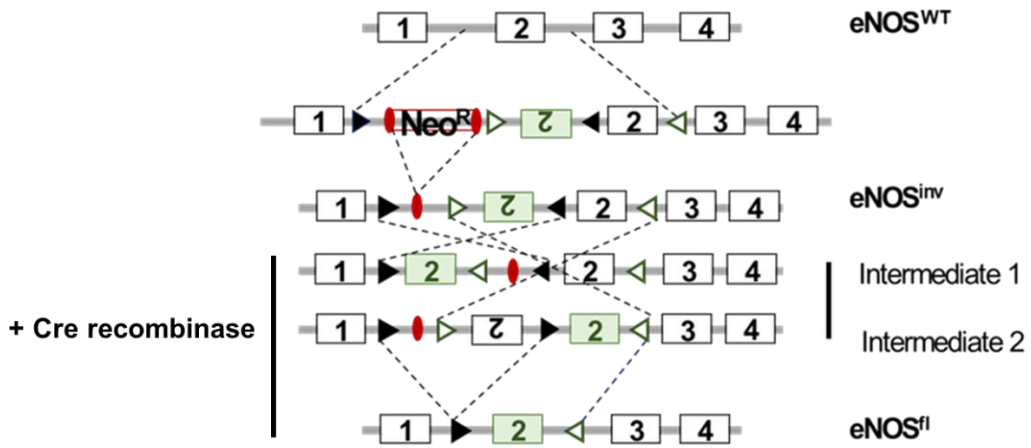

Figure 6 - Scheme describing the gene-targeting strategy for the generation of eNOS$^{inv/inv}$ mice.

To generate the eNOS^{inv} allele, exon 2 was targeted by the loxP-eNOS construct generated before; an inverted exon 2 was inserted in Nos3, and two additional loxP511 sites were inserted in the loxP-eNOS construct to generate a loxP-eNOS^{inv} construct. Homozygous eNOS$^{inv/inv}$ mice were then crossed with DelCre^{pos} mice to generate eNOS$^{fl/fl}$ Cre$^{pos/neg}$ mice.

4.1.3. Proof of concept: generation of eNOS$^{fl/inv}$ Cre^{neg} and eNOS$^{fl/fl}$ Cre^{neg} mice

As a proof of concept to see whether eNOS could be reactivated *in vivo* by the presence of a Cre recombinase, eNOS$^{inv/inv}$ mice were crossed with DelCre^{pos} mice. The goal was to generate eNOS$^{fl/inv}$ Cre^{neg} and eNOS$^{fl/fl}$ Cre^{neg} mice, which are respectively heterozygous and homozygous for eNOS for the "flipped" allele, i.e., with the reactivated gene.

The generation of eNOS$^{fl/fl}$ mice required many crossing steps; in particular, four different generations of progeny were created (F1-4). As shown in Table 9, by crossing eNOS$^{inv/inv}$ Cre^{neg} mice with WT (eNOS$^{wt/wt}$) Cre^{pos} mice, the first generation (F1) are heterozygous eNOS$^{wt/inv}$ Cre^{pos} or eNOS$^{wt/inv}$ Cre^{neg} mice. Only when the Cre recombinase is present, the eNOS^{inv} allele is flipped, resulting in eNOS$^{fl/wt}$ Cre^{pos} mice and eNOS$^{inv/wt}$ Cre^{neg} mice. The F2 was generated by crossing eNOS$^{inv/inv}$ Cre^{neg} mice with eNOS$^{fl/wt}$ Cre^{pos} mice (from F1). In this case, four different results are possible: eNOS$^{fl/inv}$ Cre^{pos} or Cre^{neg} mice, and eNOS$^{inv/wt}$ Cre^{pos} or Cre^{neg} mice. Again, when the Cre recombinase is expressed, the eNOS^{inv} allele is "flipped", leading to a F2 characterized by: eNOS$^{fl/fl}$ Cre^{pos} mice, eNOS$^{fl/inv}$ Cre^{neg} mice, eNOS$^{fl/wt}$ Cre^{pos} mice, and eNOS$^{inv/wt}$ Cre^{neg} mice. At this point (F3), eNOS$^{fl/inv}$ Cre^{neg} mice can be crossed between them to obtain the mice needed for the experiments, i.e., eNOS$^{fl/fl}$ Cre^{neg} mice, eNOS$^{fl/inv}$ Cre^{neg} mice, and eNOS$^{inv/inv}$ Cre^{neg} mice (F4).

Table 9. Generation of heterozygous and homozygous eNOS KI mice.
eNOS$^{inv/inv}$ were crossed with DelCre^{pos} mice to generate heterozygous (eNOS$^{fl/inv}$) and homozygous (eNOS$^{fl/fl}$) eNOS KI mice.

Pairing	Crossing	Progeny			Frequency
P1	eNOS$^{inv/inv}$ Cre^{neg} X eNOS$^{wt/wt}$ Cre^{pos}	F1	1	eNOS$^{inv/wt}$ Cre^{pos} → **eNOS$^{fl/wt}$ Cre^{pos}**	1/2
			2	**eNOS$^{inv/wt}$ Cre^{neg}**	1/2
P2	eNOS$^{inv/inv}$ Cre^{neg} X eNOS$^{fl/wt}$ Cre^{pos}	F2	1	eNOS$^{fl/inv}$ Cre^{pos} → **eNOS$^{fl/fl}$ Cre^{pos}**	1/4
			2	**eNOS$^{fl/inv}$ Cre^{neg}**	1/4
			3	eNOS$^{inv/wt}$ Cre^{pos} → eNOS$^{fl/wt}$ Cre^{pos}	1/4
			4	eNOS$^{inv/wt}$ Cre^{neg}	1/4
P3	eNOS$^{inv/inv}$ Cre^{neg} X eNOS$^{fl/fl}$ Cre^{pos}	F3	1	eNOS$^{fl/inv}$ Cre^{pos} → **eNOS$^{fl/fl}$ Cre^{pos}**	1/2
			2	**eNOS$^{fl/inv}$ Cre^{neg}**	1/2
P4	eNOS$^{fl/inv}$ Cre^{neg} X eNOS$^{fl/inv}$ Cre^{neg}	F4	1	**eNOS$^{fl/fl}$ Cre^{neg}**	1/3
			2	**eNOS$^{fl/inv}$ Cre^{neg}**	1/3
			3	**eNOS$^{inv/inv}$ Cre^{neg}**	1/3

4.2. Characterization of eNOS$^{inv/inv}$ mice

The recombination of the *Nos3* DNA locus was analysed in ear tissue from eNOS$^{inv/inv}$, eNOS$^{fl/inv,}$ and eNOS$^{fl/fl}$ mice by real-time PCR using specific primers and probes recognising the eNOS^{inv} and the eNOS^{fl} alleles (Fig. 7), and the recombined DNA locus was expressed as $2^{-(\text{Target } \Delta Ct - \text{Average Housekeeping gene } \Delta Ct)}$. This analysis demonstrated the presence of the recombined eNOS^{fl} DNA locus only in eNOS$^{fl/inv}$ and eNOS$^{fl/fl}$ mice (Fig. 7A). Vice versa, eNOS^{inv} allele was present in eNOS$^{fl/inv}$ and eNOS$^{inv/inv}$ mice, and not in the eNOS$^{fl/fl}$ mice.

Further characterization was done by immunoblotting of eNOS in aorta lysates from eNOS$^{fl/fl}$, eNOS$^{fl/inv}$, eNOS$^{inv/inv}$ mice, and WT mice (Fig. 7B-D). eNOS$^{fl/fl}$ and eNOS$^{fl/inv}$ mice expressed eNOS in the aorta, while in eNOS$^{inv/inv}$ mice, eNOS was absent (Fig. 7C, D representative Western blot). Moreover, the eNOS expression was at the same level in eNOS$^{fl/fl}$ and eNOS$^{fl/inv}$ mice as compared to the WT controls (Fig. 7B, semiquantitative analysis). Taken together, these results showed that eNOS was successfully reactivated in the aorta of the eNOS$^{fl/fl}$ and eNOS$^{fl/inv}$ mice and that the presence of one allele can compensate for the lack of eNOS in the other allele by up-regulation of eNOS expression.

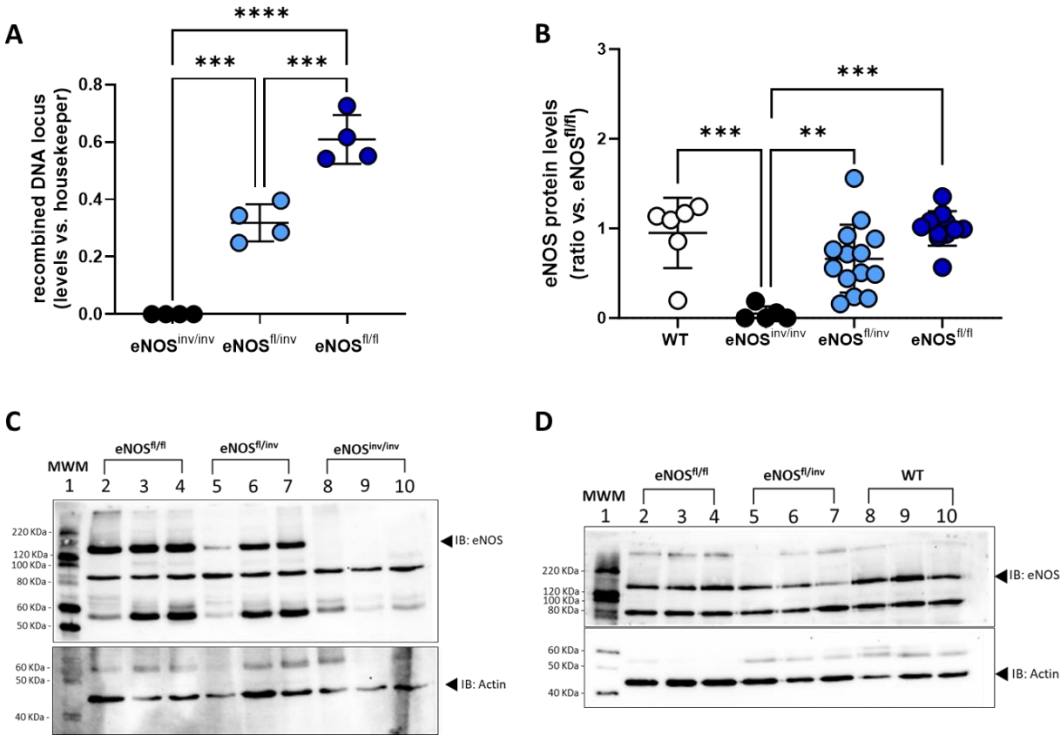

Figure 7 - Characterization of eNOS$^{inv/inv}$, eNOS$^{fl/inv}$ and eNOS$^{fl/fl}$ mice.

eNOS$^{inv/inv}$, eNOS$^{fl/inv,}$ and eNOS$^{fl/fl}$ mice were characterized by (A) real-time PCR in ear tissue and (B-D) immunoblotting of aorta lysates, showing the expression of eNOS in eNOS$^{fl/inv}$ and eNOS$^{fl/fl}$ mice and demonstrating that the reactivation of eNOS in eNOS$^{fl/inv}$ and eNOS$^{fl/fl}$ mice was successful.

DNA recombination: eNOS$^{inv/inv}$ (n = 4), eNOS$^{fl/inv}$ (n = 4), eNOS$^{fl/fl}$ (n = 4). Protein quantification: WT (n = 6), eNOS$^{inv/inv}$ (n = 5), eNOS$^{fl/inv}$ (n = 14), eNOS$^{fl/fl}$ (n = 11). One-way ANOVA p < 0.0001; post hoc Tukey; ∗∗p < 0.01, ∗∗∗p < 0.001. C) Representative Western blot of three independent experiments; D) Representative Western blot of two independent experiments.

Vascular endothelial function of eNOS$^{inv/inv}$, eNOS$^{fl/fl}$, and eNOS$^{fl/inv}$ and mice was also investigated. Aortic rings from eNOS$^{fl/fl}$ and eNOS$^{fl/inv}$ mice showed a fully restored endothelium-dependent relaxation (EDR) in response to ACh as compared to eNOS$^{inv/inv}$ mice, which instead showed a lack of ACh-induced vasodilation (Fig. 8A, B). The contractile response to PE was decreased in eNOS$^{fl/fl}$ and eNOS$^{fl/inv}$ mice as compared to eNOS$^{inv/inv}$ mice (Fig. 8C). The vasodilatory response to the NO donor SNP was increased in eNOS$^{fl/fl}$ and eNOS$^{fl/inv}$ mice as compared to eNOS$^{inv/inv}$ mice (Fig. 8D). These findings demonstrate that the vascular endothelial function is fully restored in eNOS$^{fl/fl}$ and eNOS$^{fl/inv}$ mice.

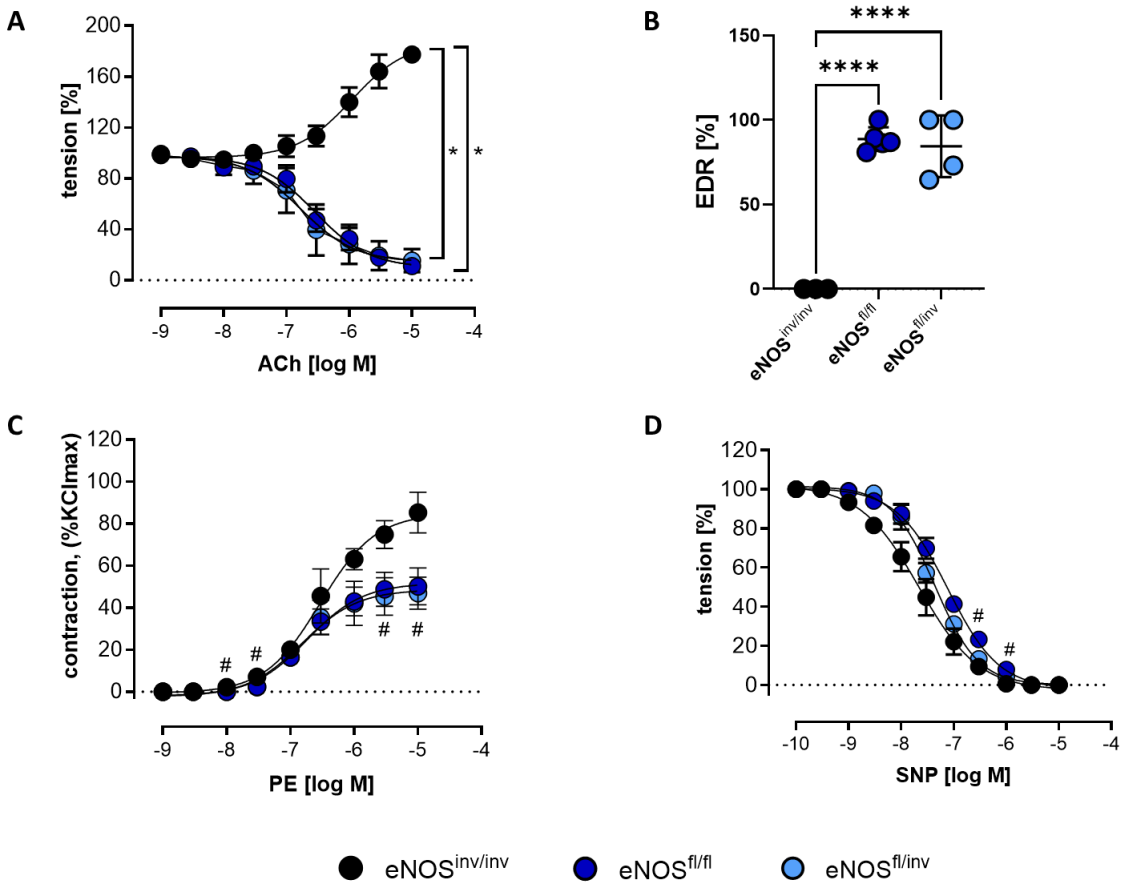

Figure 8 - Vascular endothelial function in aortic rings of eNOS$^{fl/fl}$, eNOS$^{fl/inv}$ and eNOS$^{inv/inv}$ mice.

(A) eNOS$^{fl/fl}$ and eNOS$^{fl/inv}$ mice showed a fully preserved endothelium-dependent relaxation (EDR) in response to ACh as compared to eNOS$^{inv/inv}$ mice. Two-way ANOVA concentration p = 0.0003, genotype p = 0.0003; post hoc Tukey ∗p < 0.05 vs. eNOS$^{inv/inv}$. (B) EDR in response to ACh

*(calculated as the percentage of the maximal ACh response) is fully preserved in eNOS$^{fl/fl}$ and eNOS$^{fl/inv}$ mice. One-way ANOVA p < 0.0001; post hoc Tukey; ***p < 0.001. (C) The contractile response to PE was decreased in eNOS$^{fl/fl}$ and eNOS$^{fl/inv}$ mice as compared to eNOS$^{inv/inv}$ mice. (D) The vasodilatatory response to SNP was increased in eNOS$^{fl/fl}$ and eNOS$^{fl/inv}$ mice as compared to eNOS$^{inv/inv}$ mice, as shown in the shift of the curves of eNOS$^{fl/fl}$ and eNOS$^{fl/inv}$ mice to the right. Unpaired t-test with Welch's correction; no correction for multiple comparisons; #p < 0.05. ACh, acetylcholine; PE, phenylephrine; SNP, sodium nitroprusside.*

To analyse whether the reactivation of eNOS in one or both alleles may rescue the hypertensive phenotype of global eNOS KO mice (gene dosage effect), blood pressure was determined in anesthetised eNOS$^{fl/fl}$, eNOS$^{fl/inv}$ and eNOS$^{inv/inv}$ mice by Millar catheter. As expected, eNOS$^{inv/inv}$ mice showed high blood pressure, while eNOS$^{fl/inv}$ and eNOS$^{fl/fl}$ mice showed a significant decrease in SBP as compared to eNOS$^{inv/inv}$ mice. For comparison, also WT (eNOS$^{flox/flox}$ mice) and global eNOS KO (eNOS$^{\Delta/\Delta}$) are shown in the same graph. Moreover, HR was the same among all lines (Fig. 9 B). These results demonstrate that the reintroduction of eNOS in only one allele is enough to rescue the hypertensive phenotype, as the SBP is comparable to the WT mice (Fig. 9A).

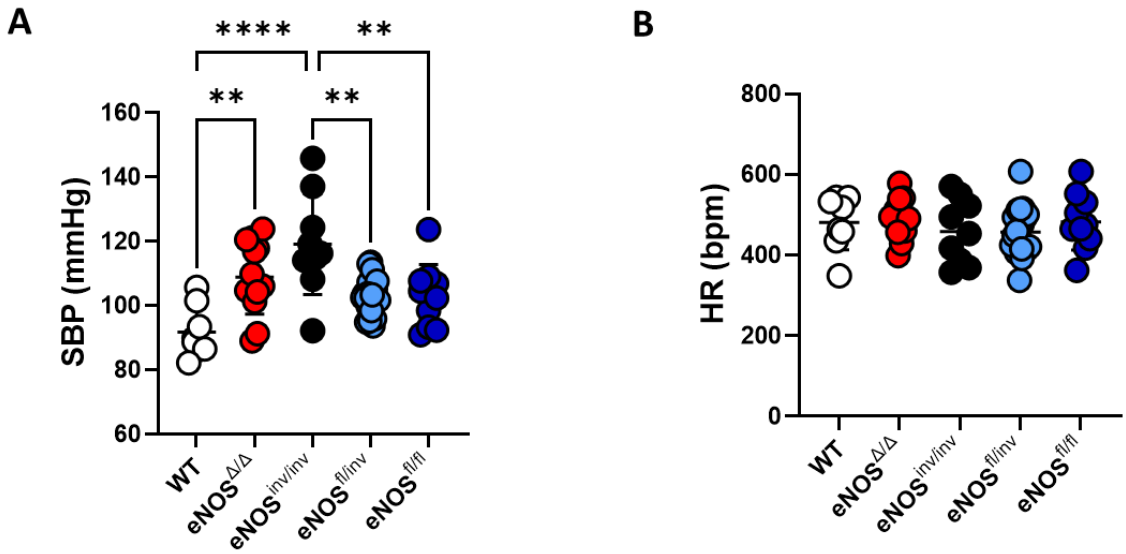

Figure 9 - SBP of eNOS$^{fl/fl}$, eNOS$^{fl/inv}$ and eNOS$^{inv/inv}$ mice.

(A) SBP measurements were assessed in anesthetized eNOS$^{fl/fl}$, eNOS$^{fl/inv}$, eNOS$^{inv/inv,}$ mice as well as in WT and global eNOS KO mice by using a Millar catheter; both eNOS$^{fl/inv}$ and eNOS$^{fl/fl}$ mice showed a decrease in SBP as compared to eNOS$^{inv/inv}$ mice. The data show that eNOS$^{inv/inv}$ had higher SBP as compared to WT mice, while eNOS$^{fl/inv}$ and eNOS$^{fl/fl}$ mice had the same SBP as WT mice. (B) No differences in HR were shown among eNOS$^{inv/inv}$, eNOS$^{fl/inv}$, eNOS$^{fl/fl}$, WT, and eNOS$^{\Delta/\Delta}$

mice. One-way ANOVA p < 0.0001; post hoc Tukey; ∗∗p < 0.01; ∗∗∗p < 0.001. SBP, systolic blood pressure; HR, heart rate.

4.3. Generation and characterization of EC eNOS KO and KI mice

To generate EC-specific eNOS KO mice, $eNOS^{flox/flox}$ mice were crossed with $Cdh5Cre/ERT2^{pos}$ mice (Sorensen et al., 2009), expressing Cre recombinase under the control of a Cadherin5 promoter. In this case, the Cre recombinase is fused to a muted hormone-binding domains of the estrogen receptor to make it insensitive to natural ligands and responsive to synthetic ligands like tamoxifen, in order to keep the Cre recombinase inactive in the cytoplasm (Feil et al., 1997). The activation of the Cre recombinase can occur as soon as tamoxifen binds to the estrogen receptor, causing the translocation of the Cre recombinase to the nucleus. Thus, to induce the removal of the floxed exon 2, the mice were treated by i.p. injection with tamoxifen for five consecutive days (75 mg/kg) (Fig. 10A). Real-time PCR was performed with specific primers and probes designed to recognise the eNOS-Δ-allele, and the recombined DNA locus was quantified as $2^{-(\text{Target } \Delta Ct - \text{Average Housekeeping gene } \Delta Ct)}$. Real-time PCR analysis carried out on DNA extracted from aorta lysates showed that DNA recombination occurred only in the EC eNOS KO mice, while the WT mice did not show any DNA recombination (Fig. 10B). These data demonstrate that the tamoxifen-inducible eNOS deletion occurred only in the mice expressing Cre recombinase (EC eNOS KO Cre-positive), while the mice that did not express Cre recombinase were phenotypically WT (EC eNOS KO Cre-negative).

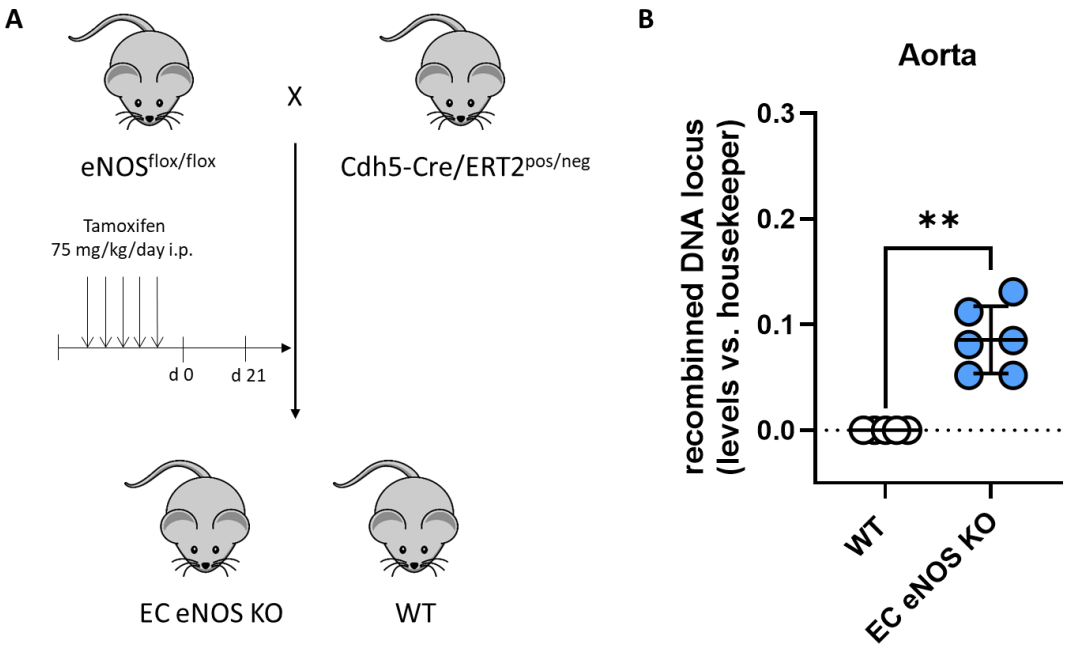

Figure 10 - Generation of EC eNOS KO mice.

*A) To generate EC eNOS KO mice, eNOS$^{flox/flox}$ mice were crossed with Cdh5Cre/ERT2^{pos} mice. At 8 weeks of age, mice underwent a five-day-treatment with tamoxifen (75 mg/kg). (B) Real-time PCR analysis performed on DNA extracted from aorta lysates showed DNA recombination only in the EC eNOS KO mice as compared to the WT control mice. WT (n = 5), EC eNOS KO (n = 6). Unpaired t-test with Welch's correction, **p < 0.01.*

To generate EC-specific eNOS KI mice, eNOS$^{inv/inv}$ mice were crossed with Cdh5Cre/ERT2^{pos} mice, following by five-day treatment with tamoxifen (75 mg/kg) to induce the flipping of exon 2 (Fig. 11A). Real-time PCR analysis, with specific primers and probes designed to recognise the eNOS^{inv} allele, was performed on aorta lysates of EC eNOS KI mice showing that DNA recombination occurred only in the EC eNOS KI mice and not in the CondKO control mice (Fig. 11B), demonstrating that the reactivation of eNOS was successful.

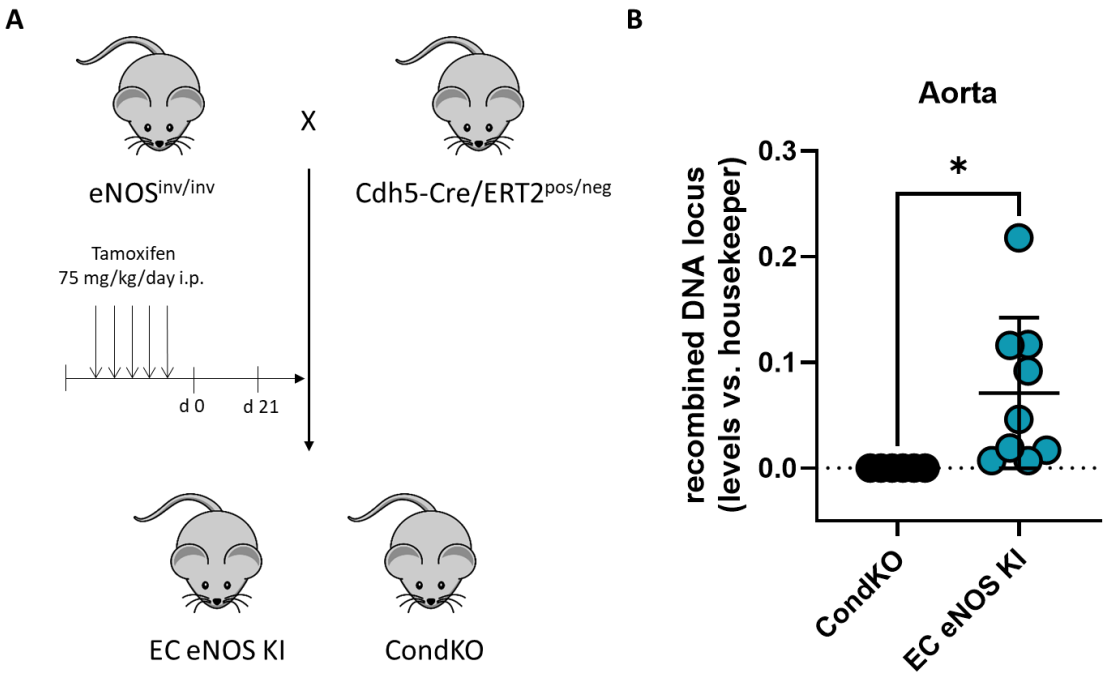

Figure 11 - Generation of EC eNOS KI mice.

*To generate EC eNOS KI mice, eNOS$^{inv/inv}$ mice were crossed with Cdh5Cre/ERT2^{pos} mice, followed by 5-day tamoxifen treatment (75 mg/kg). Real-time PCR analysis on DNA extracted from aorta lysates showed DNA recombination only in the EC eNOS KI mice as compared to the control CondKO mice. CondKO (n = 6), EC eNOS KI (n = 9). Unpaired t-test with Welch's correction, *p < 0.05.*

In this study, the cell-specific eNOS KO and KI models will be used for kidney function analysis; thus, the major characterization of these lines was done on aorta (tissue rich in ECs) and kidney. To investigate whether the treatment with tamoxifen altered the mRNA expression of eNOS in the kidney, real-time RT-PCR of total mRNA extracted from kidney lysates of tamoxifen-treated WT mice was compared to the one from tamoxifen-untreated WT mice (Fig. 12). The results show that tamoxifen treatment significantly decreased the eNOS expression in the whole kidney in WT mice.

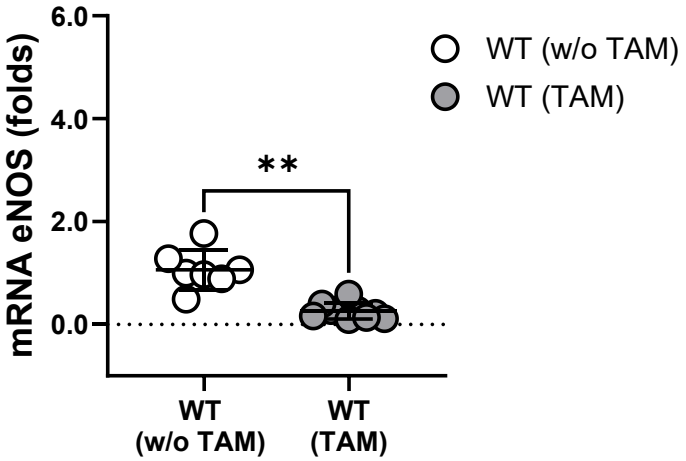

Figure 12 - Effect of tamoxifen on eNOS mRNA expression in kidney of WT mice.
Real-time RT-PCR performed on total mRNA extracted from kidneys of tamoxifen-treated WT (n = 10) and untreated WT (n = 7) mice showed that tamoxifen significantly decreased mRNA eNOS expression in the kidney. Unpaired t-test with Welch's correction, ***p < 0.01. Abbreviations: w/o TAM, without tamoxifen; TAM, tamoxifen.*

EC eNOS KO and KI mice were characterized by real-time RT-PCR carried out on total mRNA extracted from aorta and kidney lysates, as well as by Western blot in the same tissues (Fig. 13). Western blot of aorta lysates showed lack of eNOS in EC eNOS KO mice and CondKO mice, while WT and EC eNOS KI mice expressed eNOS. This was confirmed by real-time RT-PCR analysis (Fig. 13A). Immunoblotting of kidney lysates showed the presence of eNOS also in EC eNOS KO mice, but at a lower level as compared to WT mice. This is due to the expression of eNOS in non-ECs, likely tubular epithelial cells (Wu et al., 1999; Plato et al., 2000; Baines & Ho, 2002). CondKO mice did not show any presence of eNOS in kidney lysates as assessed by Western blot, while EC eNOS KI mice expressed eNOS. Real-time RT-PCR analysis was also performed, confirming the expression of eNOS only in EC eNOS KI mice and not in the CondKO controls (Fig. 13B).

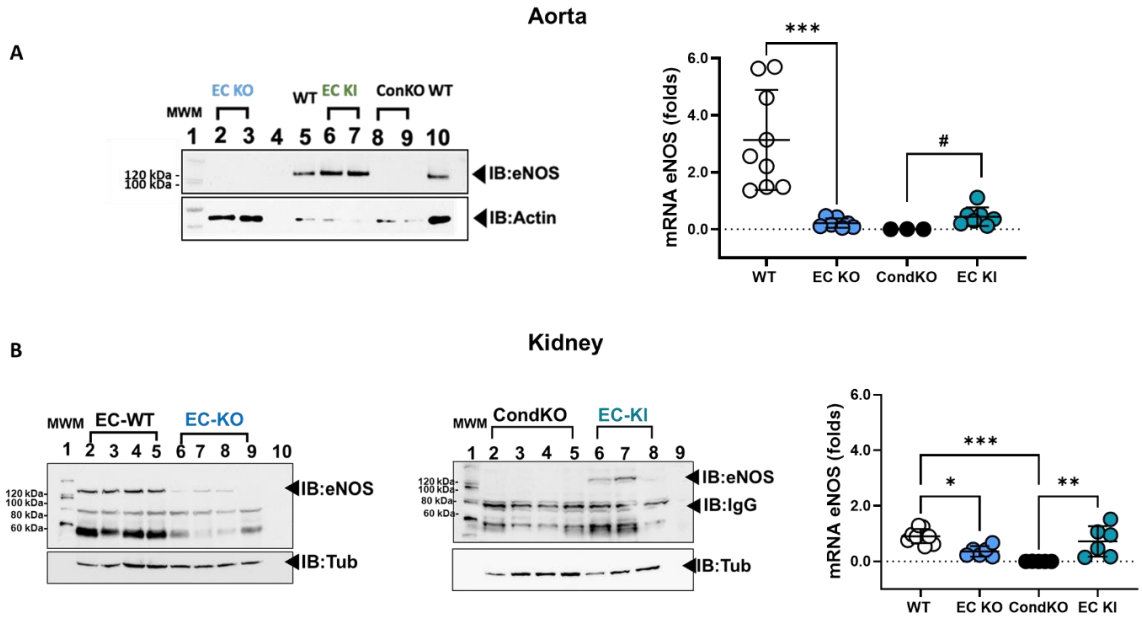

Figure 13 - Characterization of EC eNOS KO and KI mice.

*(A) Immunoblotting and real-time RT-PCR of aorta lysates showing the lack of eNOS in EC eNOS KO mice and the reactivation of eNOS in EC eNOS KI mice. (B) Immunoblotting of kidney lysates showed a low level of eNOS in EC eNOS KO mice due to its expression in non-ECs; CondKO mice did not show eNOS expression, while eNOS was reactivated in EC eNOS KI mice as assessed by immunoblot and real-time RT-PCR. Each Western blot is representative of three independent experiments. mRNA eNOS in aorta: WT (n = 9), EC eNOS KO (n = 7), CondKO (n = 3), EC eNOS KI (n = 7). One-way ANOVA p < 0.0001, post hoc Tukey, ***p < 0.001; Unpaired t-test with Welch's correction, #p < 0.05. mRNA expression in kidney: WT (n = 9), EC eNOS KO (n = 6), CondKO (n = 5), EC eNOS KI (n = 6). One way ANOVA p = 0.0002, post hoc Tukey, *p < 0.05, ** p < 0.01, ***p < 0.001.*

The expression of eNOS in both models was also measured by immunoblotting in heart, liver, and lung, showing again a lack of expression of eNOS in all three compartments of EC eNOS KO and CondKO mice, while EC eNOS KI and WT mice expressed eNOS (Fig. 14). In the lung lysates, a faint band was detectable also in the EC eNOS KO mice lines. This is likely due to the presence of eNOS not only in the ECs of pulmonary arteries and veins, but also in the airway and in the bronchiolar and alveolar epithelial cells (Shaul et al., 1994; Giaid & Saleh, 1995). These data show that the removal and reactivation of eNOS in ECs was successful and specific.

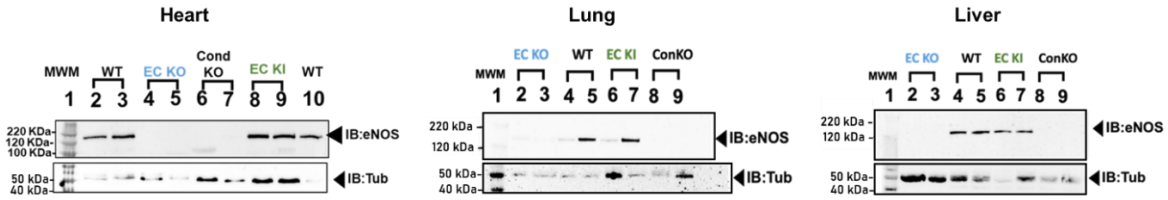

Figure 14 - Expression of eNOS in different tissues of EC eNOS KO and KI mice.
Immunoblotting of heart, liver, and lung lysates of EC eNOS KO and KI mice, and their WT and CondKO littermate control mice, showing the lack of eNOS in the EC eNOS KO and its reactivation in the EC eNOS KI mice. A faint band of eNOS was also detectable in the lung lysates of EC eNOS KO mice due to its expression in non-ECs. Each Western blot is representative of three independent experiments.

4.4. Generation and characterization of RBC eNOS KO and KI mice

To generate erythroid cell-specific eNOS KO mice (RBC eNOS KO) and their respective WT littermates, eNOS$^{flox/flox}$ mice were crossed with erythroid-specific Hbb-Cre$^{pos/neg}$ mice, expressing the Cre recombinase under the control of the human beta haemoglobin promoter (HBB) (Peterson et al., 2004), resulting in the generation of RBC eNOS KO mice and the Cre-negative WT littermates (Fig. 15A). Real-time PCR was carried out on DNA extracted from bone marrow by using specific primers and probes designed to recognise the eNOS-Δ-allele. The data showed that DNA recombination occurred only in RBC eNOS KO mice and not in WT mice (Fig. 15B).

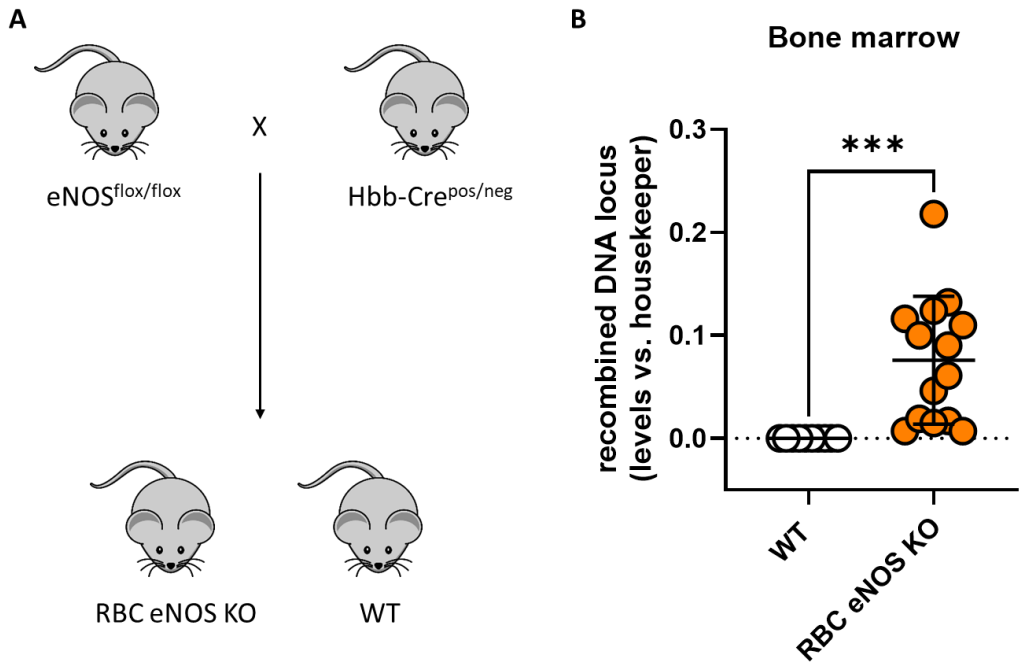

Figure 15 - Generation of RBC eNOS KO mice.

*To generate RBC eNOS KO mice, eNOS$^{flox/flox}$ mice were crossed with Hbb-Cre$^{pos/neg}$ mice. Real-time PCR analysis in bone marrow showed DNA recombination only in the RBC eNOS KO mice as compared to the WT controls. WT (n = 10), RBC eNOS KO (n = 14). Unpaired t-test with Welch's correction, ***p < 0.001.*

To generate RBC-specific eNOS KI mice and the CondKO littermates, eNOS$^{inv/inv}$ mice were crossed with erythroid-specific Hbb-Cre$^{pos/neg}$ mice (Fig. 16A). Real-time PCR was performed by using specific primers and probes designed to recognise the eNOS^{inv} allele, and the recombined DNA locus was expressed as $2^{-(\text{Target } \Delta Ct - \text{Average Housekeeping gene } \Delta Ct)}$. RBC eNOS KI mice showed DNA recombination in bone marrow, whereas no DNA recombination was detected in the same tissue of CondKO mice (Fig. 16B). These data show the specificity of reactivation of eNOS in Cre-positive mice in bone marrow.

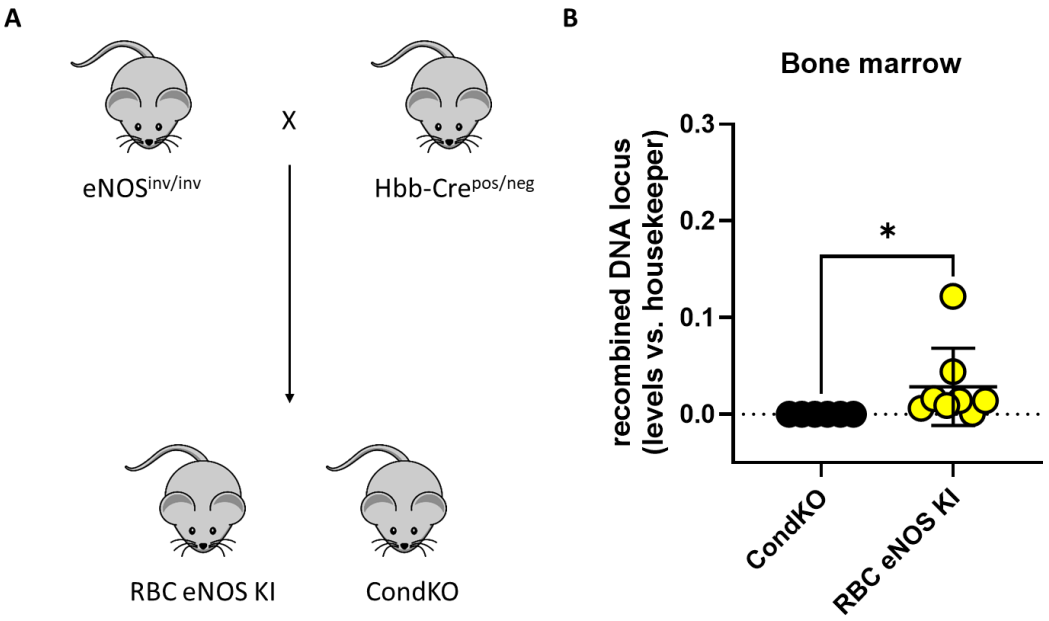

Figure 16 - Generation of RBC eNOS KI mice.

*To generate RBC eNOS KI mice, eNOS$^{inv/inv}$ mice were crossed with Hbb-Cre$^{po/neg}$ mice. Real-time PCR analysis of DNA extracted from bone marrow showed DNA recombination only in RBC eNOS KI mice and not in CondKO mice. CondKO (n = 6), RBC eNOS KI (n = 8). Unpaired t-test with Welch's correction, *p < 0.05.*

To further characterize these models, Western blotting of ghost lysates from RBC eNOS KO mice was carried out, showing a lack of eNOS in RBC eNOS KO mice and its presence in WT mice (Fig. 17A). Additionally, immunoprecipitation of eNOS was performed on RBC lysates of RBC eNOS KO and KI mice, as well as of the WT and global eNOS KO (gKO or eNOS$^{\Delta/\Delta}$) controls (Fig. 17B, C). The data showed the lack of eNOS expression in RBCs of RBC eNOS KO mice and gKO mice, while eNOS was detectable in aorta of RBC eNOS KO mice and WT used as a positive control (Fig. 17B). Taken together, the data show that the removal of eNOS from RBCs was successful. RBC lysates from RBC eNOS KI mice showed a band at 135 kDa corresponding to eNOS, while this band was not detected in CondKO mice (Fig. 17C), showing that eNOS was specifically reactivated in RBCs. Immunoblotting was carried out also on kidney lysates, showing the expression of eNOS in RBC eNOS KO mice, but not in RBC eNOS KI mice (Fig. 17D). These findings were further confirmed by performing real-time RT-PCR on kidney lysates, showing expression of mRNA eNOS in RBC eNOS KO mice as well as in WT controls, and the absence of eNOS in RBC eNOS KI mice and CondKO littermates (Fig. 17E). Taken together, these data showed that the deletion or reactivation of eNOS was successful and specific for RBC in Cre-positive mice (the specificity for RBC is shown in the next set of experiment).

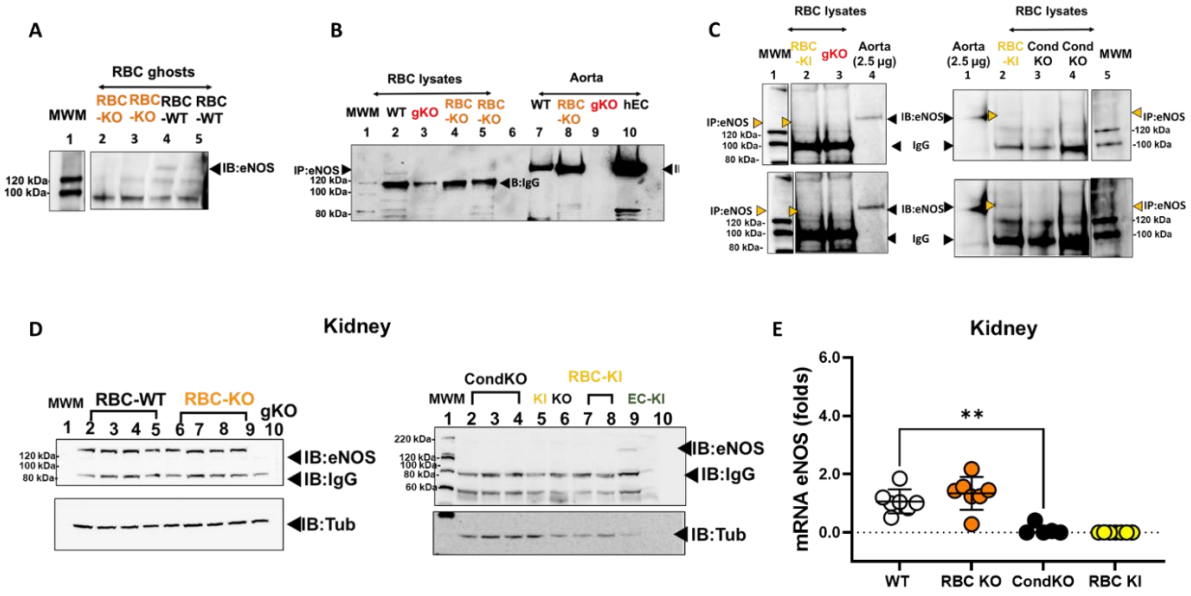

Figure 17 - Characterization of RBC eNOS KO and KI mice.

(A) *Western blot carried out on ghosts lysates showed lack of eNOS in RBC eNOS KO mice; (B, C) Immunoprecipitation of eNOS from RBC lysates of RBC eNOS KO and KI mice showed lack of eNOS in RBC eNOS KO mice and its expression in RBC eNOS KI mice. (D) Immunoblot performed on kidney lysates showed the presence of eNOS in RBC eNOS KO mice, while it was not detected in RBC eNOS KI mice. (E) Real-time RT-PCR performed on kidney lysates showed eNOS expression in RBC eNOS KO mice but not in RBC eNOS KI mice. mRNA eNOS: WT (n = 7), RBC eNOS KO (n = 7), CondKO (n = 5), RBC eNOS KI (n = 7). One way ANOVA $p < 0.0001$, post hoc Tukey, ** $p < 0.01$. Each Western blot is representative of three independent experiments.*

Immunotransmission electron microscopy was also performed on RBCs of RBC eNOS KO and KI mice, as well as on the respective WT and CondKO littermate control mice (Fig. 18). In this way, it was possible to visualize and localize eNOS in RBCs of WT and RBC eNOS KI mice, while eNOS was not detectable in RBC eNOS KO and CondKO mice. This data definitely demonstrated the specificity of the KO/KI mouse models.

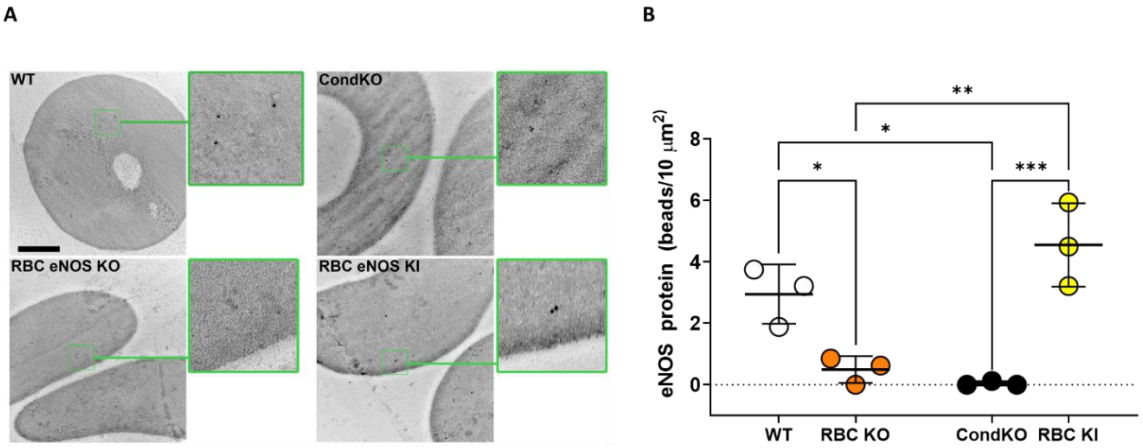

Figure 18 - Immunotransmission electron microscopy in RBC eNOS KO and KI mice.
(A) *Immunotransmission electron microscopy was performed on RBCs of RBC eNOS KO, RBC eNOS KI, WT, and CondKO mice. (B) The quantification showed eNOS expression in WT and RBC eNOS KI mice, while RBC eNOS KO and CondKO mice showed a lack of eNOS. One way ANOVA p = 0.0006; post hoc Tukey *p < 0.05; **p < 0.01; ***p < 0.001. Each data point is the average of 5 fields of view from one mouse.*

To exclude “off-target effects”, the two lines were further investigated by immunoblotting of tissues such as heart, aorta, lung, and liver lysates. The RBC eNOS KO mice showed the presence of eNOS in all the tissues at the same level as WT mice, while eNOS was not detected in tissues from RBC eNOS KI mice and CondKO mice (Fig. 19). These data show that the removal and reactivation of eNOS specifically in RBCs of RBC eNOS KO and RBC eNOS KI mice were specific for the targeted cells and there were no off-target effects.

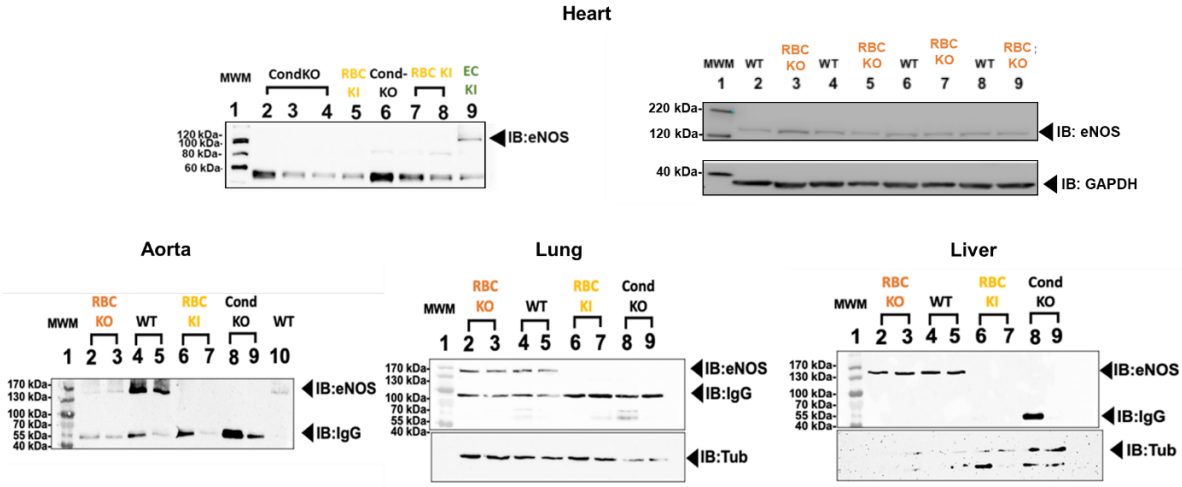

Figure 19 - Expression of eNOS in different tissues of RBC eNOS KO and KI mice.

Immunoblotting of heart, aorta, lung, and liver lysates from RBC eNOS KO and KI mice, showing the presence of eNOS in the tissues of RBC eNOS KO mice and the WT controls, and the lack of eNOS in RBC eNOS KI mice and the CondKO littermates. Each Western blot is representative of three independent experiments.

4.4.1. Determination of NO metabolites in EC eNOS KO and EC eNOS KI mice

To test whether the deletion or reactivation of eNOS in RBCs or ECs influenced NO bioavailability, the concentrations of NO metabolites in blood and tissues of all KO and KI lines were analysed. A decrease in nitrite and nitrate levels in plasma was found in EC eNOS KO mice, as well as a decrease in total NO species in plasma, aorta, and lung as compared to the WT controls. Nitrate was increased only in the liver. CondKO mice showed a decrease in NO metabolites in plasma and tissues as compared with WT mice. Instead, the reactivation of eNOS specifically in ECs did not restore nitrite levels in plasma.

NO-heme levels were fully preserved in EC eNOS KO mice as compared to WT littermates and did not show any changes in EC eNOS KI mice or CondKO mice (Tab. 10). These data show that EC eNOS contributes to the level of systemic NO metabolites, but not of NO-Heme.

Table 10. NO metabolites in EC eNOS KO, EC eNOS KI and relative WT and CondKO littermate. *t-test vs respective control group. * p < 0.05, **p < 0.01, *** p < 0.001, § One value excluded as outlier according to the Tukey test, or not determined/available, † two values were not determined/available, or one was excluded as an outlier according to Tukey test.*

	WT	**EC eNOS KO**		**CondKO**	**EC eNOS KI**	
Metabolite	$eNOS^{flox/flox}$ $Cdh5Cre/ERT2^{neg}$	$eNOS^{flox/flox}$ $Cdh5/ERT2Cre^{pos}$	p	$eNOS^{inv/inv}$ $Cdh5/ERT2Cre^{neg}$	$eNOS^{inv/inv}$ $Cdh5/ERT2Cre^{pos}$	p
n	5	5		8	7	
Heart						
Nitrite, µmol/L	1.10±0.30	1.27±0.25	0.3557	2.27±0.14§	2.24±0.48	0.8745
Nitrate, µmol/L	93.86±26.51	77.84±14.97	0.2818	N.D.	N.D.	
RXNO, nmol/L	81.94±26.31	102.74±37.20	0.3406	34.86±16.40	32.50±3.38	0.7043
NO-heme, nmol/L	475.21±320.85	97.74±24.20	0.0579*	26.57±12.00	32.67±8.46	0.2865
Total NO species, µmol/L	95.09±26.43	79.31±14.91	0.2871	N.D.	N.D.	

Lung						
Nitrite, µmol/L	0.88±0.51[§]	0.71±0.11	0.5100	2.42±0.52[§]	3.05±0.62	0.0626
Nitrate, µmol/L	35.62±6.74[§]	19.49±5.52	0.0035**	N.D.	N.D.	
RXNO, nmol/L	94.01±19.94[§]	79.43±20.31	0.3173	71.73±35.40	54.26±12.34	0.2237
NO-heme, nmol/L	228.44±92.18[§]	463.51±121.30	0.0131*	27.62±14.30	29.86±7.76	0.7090
Total NO species, µmol/L	34.25±5.57[§]	20.74±5.62	0.0096**	N.D.	N.D.	
Liver						
Nitrite, µmol/L	0.63±0.34	0.83±0.15	0.2798	3.32±1.44	2.72±0.36[§]	0.2921
Nitrate, µmol/L	38.47±22.34	71.02±20.84	0.0445*	N.D.	N.D.	
RXNO, nmol/L	1378.28±749.29	1038.64±283.33	0.3857	617.11±336.52	496.28±193.14	0.4046
NO-heme, nmol/L	1190.08±722.98	310.85±104.09	0.0523	118.74±46.90[§]	79.44±3.42[†]	0.0686
Total NO species, µmol/L	40.65±22.39	73.20±21.08	0.0456*	N.D.	N.D.	
Aorta						
Nitrite, µmol/L	138.12±62.10	141.36±39.21	0.9243	9.56±4.74	6.20±2.06	0.0995
Nitrate, µmol/L	10191.95±7764.94	5473.15±4015.51	0.2730	N.D.	N.D.	
RXNO, nmol/L	2058.42±1653.39	1870.34±1002.49	0.8344	79.10±46.81	55.80±47.50	0.3579
NO-heme, nmol/L	N.D.	N.D.		11.49±3.97[†]	21.28±5.55	0.0037**
Total NO species, µmol/L	10331.13±7805.42	5616.38±4052.67	0.2758	N.D.	N.D.	
Plasma						
Nitrite, µmol/L	0.81±0.18	0.44±0.10	0.0065**	0.45±0.23	0.28±0.13[§]	0.1218
Nitrate, µmol/L	41.35±15.75	20.65±4.25	0.0402*	N.D.	N.D.	
RXNO, nmol/L	22.24±4.58	16.34±11.15	0.3268	15.64±15.77	12.89±13.12	0.7160
Total NO species, µmol/L	36.66±11.28	21.11±4.30	0.0642	N.D.	N.D.	
RBCs						

Nitrite, µmol/L	0.49±0.16	0.43±0.16	0.6088	0.15±0.04	0.21±0.10	0.2011
Nitrate, µmol/L	35.23±14.27	17.64±3.14	0.0880	N.D.	N.D.	
RXNO, nmol/L	475.06±158.27	225.04±76.99	0.0201*	88.78±47.89	103.57±72.60	0.6562
NO-heme, nmol/L	62.92±9.99§	83.12±39.12	0.3209	3.06±0.66	2.67±0.41	0.1904
Total NO species, µmol/L	32.02±21.79§	18.38±3.33	0.2999	N.D.	N.D.	

4.4.2. Determination of NO metabolites in RBC eNOS KO and RBC eNOS KI mice

RBC eNOS KO mice showed a significant decrease in nitrite and nitrate levels in plasma and increased nitrite concentration in the aorta. On the other hand, they also showed an increase in RXNO compared to WT mice. The total NO species in plasma of RBC eNOS KO mice were decreased as compared to WT mice. Surprisingly, RBC eNOS KO mice showed an increase in nitrite in the aorta compared to WT mice, but no significant changes in the other tissues. Also in this case, CondKO mice showed a decrease in NO metabolites as compared to WT mice. These results show that RBC eNOS is involved mainly in the regulation of circulating NO metabolites.

To analyse NO bioavailability in RBCs, the level of NO-heme was significantly lower in RBCs of RBC eNOS KO mice and CondKO mice as compared to WT mice. Accordingly, the NO-heme levels were completely restored in RBC eNOS KI mice as compared to the CondKO littermate controls. This shows that the levels of NO-heme in RBCs depend on the presence of eNOS in RBCs and not on EC eNOS (Tab. 11).

Table 11. NO metabolites in RBC eNOS KO, RBC eNOS KI and relative WT and CondKO littermates.

*t-test vs. respective control group. * p < 0.05, **p < 0.01, ***p < 0.001, § one value excluded as outlier according to the Tukey test, or not determined/available, † two values were not determined/available, or one was excluded as an outlier according to Tukey test.*

	WT	**RBC eNOS KO**		**CondKO**	**RBC eNOS KI**	
Metabolite	$eNOS^{flox/flox}$ $HbbCre^{neg}$	$eNOS^{flox/flox}$ $HbbCre^{pos}$	p	$eNOS^{inv/inv}$ $HbbCre^{neg}$	$eNOS^{inv/inv}$ $HbbCre^{pos}$	p
n	7	6		8	8	
Heart						

Nitrite, µmol/L	0.69±0.15	0.92±0.60§	0.4463	0.64±0.23	0.67±0.18†	0.7817
Nitrate, µmol/L	65.16±19.11	86.82±54.70	0.3914	13.86±6.27	13.98±6.08†	0.9715
RXNO, nmol/L	54.00±19.06	43.81±10.47	0.2528	15.54±4.38	20.65±6.23	0.0810
NO-heme, nmol/L	125.04±37.83	38.82±20.11	0.0005***	6.94±1.49	8.40±2.09	0.1303
Total NO species, µmol/L	66.02±19.14	87.66±54.33	0.3890	14.52±6.31	14.68±6.09†	0.9628
Lung						
Nitrite, µmol/L	0.71±0.24	0.50±0.13§	0.0801	0.70±0.26	0.70±0.65†	0.9796
Nitrate, µmol/L	44.01±13.20	40.10±22.66	0.7202	28.75±14.78	21.31±9.03†	0.2674
RXNO, nmol/L	62.99±29.43	122.80±106.30	0.2331	3783.51±2023.74†	3666.83±2476.96	0.9244
NO-heme, nmol/L	282.16±166.87	104.77±61.72	0.0316*	425.90±238.14†§	443.89±88.30†	0.8792
Total NO species, µmol/L	45.06±13.40	33.78±16.50§	0.2450	39.21±16.11†§	25.28±9.53†	0.1378
Liver						
Nitrite, µmol/L	0.20±0.06	0.16±0.04§	0.2483	0.65±0.52	0.31±0.08	0.1050
Nitrate, µmol/L	57.69±17.70	33.88±7.05§	0.0116*	17.56±9.23	14.68±5.38	0.4606
RXNO, nmol/L	366.42±71.71	1836.38±1541.77	0.0666	672.09±412.26	377.99±47.68†	0.0842
NO-heme, nmol/L	1149.31±323.81	494.14±573.76	0.0396*	342.06±207.87	353.56±136.61	0.8981
Total NO species, µmol/L	59.41±17.54	36.68±8.85§	0.0159*	19.23±9.47	14.52±4.20†	0.2389
Aorta						
Nitrite	57.57±16.44§	118.71±42.34	0.0147*	2.90±1.05	2.28±1.21†	0.3407
Nitrate	2931.00±1184.00§	3408.00±1888.00	0.6357	126.67±104.88	100.97±97.25†	0.6451
RXNO	2103.00±980.10§	3067.00±1737.00	0.2712	141.72±106.74	191.45±106.22§	0.3834
NO-heme, nmol/L	N.D.	N.D.		129.71±105.59	67.44±48.22†	0.1780
Total NO species	3020.34±1181.83§	2455.27±1651.94	0.5126	N.D.	N.D.	
Plasma						
Nitrite, µmol/L	1.52±0.42	0.78±0.07	0.0031**	0.32±0.12	0.24±0.09§	0.1542

Nitrate, µmol/L	57.63±9.22	25.40±10.93	0.0002***	55.72±48.50	43.47±21.12	0.5279
RXNO, nmol/L	9.39±1.57†	39.65±22.64	0.0220*	34.46±11.52	29.16±7.14	0.2909
Total NO species, µmol/L	59.96±9.07†	26.22±10.91	0.0003***	56.06±48.53	44.71±22.62§	0.5668
RBCs						
Nitrite, µmol/L	0.94±0.14§	1.09±0.35§	0.4063	3.29±1.24§	2.94±1.51§	0.6435
Nitrate, µmol/L	67.95±15.61	68.43±29.82	0.9727	N.D.	N.D.	
RXNO, nmol/L	196.32±123.29	125.32±28.68	0.1846	1.26±0.52	0.72±0.25	0.0253*
NO-heme, nmol/L	74.76±24.84	45.06±13.31	0.0220*	23.86±8.89†	41.547±12.94§	0.0150*
Total NO species, µmol/L	56.34±31.65§	75.91±28.53§	0.3097	4.66±1.43§	3.78±1.72†	0.3425

4.4.3. Blood pressure and hemodynamics in EC eNOS KO/KI and RBC eNOS KO/KI mice

To verify whether the presence or absence of eNOS specifically in ECs or RBCs may affect the blood pressure and systemic hemodynamics, measurements were performed in all the mouse lines by Millar catheter (Tab. 12). As expected, EC eNOS KO mice showed high blood pressure, confirming the well known role of endothelial eNOS in controlling blood pressure. Surprisingly, also RBC eNOS KO mice were hypertensive. Moreover, CondKO mice showed hypertension as expected (as compared to WT mice). The reactivation of eNOS specifically in ECs or RBCs rescued the hypertensive phenotype, as EC eNOS KI and RBC eNOS KI were normotensive (Tab. 12). These results show that eNOS expressed in ECs and RBCs independently contribute to blood pressure regulation.

Table 12. Blood pressure and heart rate in all strains investigated.

All mice investigated were 4-6 month old. Abbreviations: SBP, systolic blood pressure; DBP, diastolic blood pressure; MAP, mean arterial pressure; HR, heart rate; RPP, rate pressure product.

Strain	Genotype	Body weight (g)	SBP (mmHg)	DBP (mmHg)	MAP (mmHg)	HR (bpm)	RPP (mmHg*bpm)	n
WT	$eNOS^{flox/flox}$	30.3 ± 2.5	92±8	62±9	71±1	543±67	49591±5512	14

WT (TAM)	$eNOS^{flox/flox}$ $Cdh5Cre/ERT2^{neg}$ +TAM	29.3 ± 3.6	86±5	57±8	67±7	564±53	48413±5018	12
EC eNOS KO	$eNOS^{flox/flox}$ $Cdh5Cre/ERT2^{pos}$ +TAM	29.4 ± 3.1	104±8	72±7	83±7	535±58	55696±6929	19
WT	$eNOS^{flox/flox}$ $HbbCre^{neg}$	29.1 ± 2.1	89±9	61±1	70±1	528±56	46622±5306	15
RBC eNOS KO	$eNOS^{flox/flox}$ $HbbCre^{pos}$	29.7 ± 2.6	103±1	69±7	80±8	476±93	48506±9392	16
gKO	$eNOS^{flox/flox}$ $DelCre^{pos}$	30.2 ± 2.6	115±1	79±1	91±1	516±76	56275±20504	10
CondKO	$eNOS^{inv/inv}$	27.8 ± 1.8	127±1	84±1	98±1	465±44	59046±8299	11
CondKO (TAM)	$eNOS^{inv/inv}$ $Cdh5Cre/ERT2^{neg}$ +TAM	28.7 ± 2.2	122±6	81±1	94±9	547±49	66562±5285	11
EC eNOS KI	$eNOS^{inv/inv}$ $Cdh5Cre/ERT2^{pos}$ +TAM	28.3 ± 2.2	94±7	58±8	70±7	540±48	50849±5346	13
CondKO	$eNOS^{inv/inv}$ $HbbCre^{neg}$	28.7 ± 1.2	119±1	75±1	90±11	494±45	58845±5542	18
RBC eNOS KI	$eNOS^{inv/inv}$ $HbbCre^{pos}$	31.1 ± 2.5	95±8	56±9	69±8	469±67	47022±7322	10

4.5. Role of eNOS in renal function

NO in the kidney is a key molecule in the renal function regulation. Specifically, NO plays a role in the renal autoregulatory mechanism and in the pressure-natriuresis response. Both mechanisms are activated in response to an increase in blood pressure to maintain stable RBF and GFR (autoregulatory mechanism) and induce sodium and water excretion (pressure-natriuresis response). The cell-specific role of eNOS as source of NO in the regulation of renal function is still not fully understood and needs further investigation.

In this part of the thesis, the aim is to investigate renal function in all cell-specifc eNOS KO and KI lines. The same experimental setting was used for all the cohorts, and it is depicted in Fig. 20.

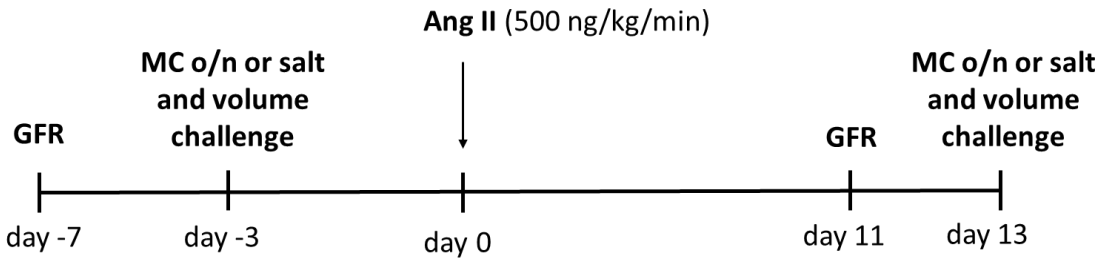

Figure 20 - Experimental setting.

Basal GFR and overnight sodium excretion or after salt challenge were investigated at day -7 and day -3, respectively. Osmotic minipumps releasing Ang II (500 ng/kg/min) were subcutaneously implanted at day 0, followed by GFR and overnight sodium excretion or after salt challenge measurements at day 11 and day 13, respectively. Abbreviations: Ang II, angiotensin II; GFR, glomerular filtration rate; MC o/n, metabolic cage overnight.

Mice were treated with Ang II (500 ng/kg/min), and GFR and sodium excretion (basal and after salt and volume challenge) were measured before and after Ang II treatment. In detail, GFR was measured at baseline (day -7) followed by overnight urine collection or after salt and volume challenge (day -3) to investigate sodium and urine excretion. At day 0, osmotic minipumps filled with Ang II in 0.9% NaCl (500 ng/kg/min) were implanted subcutaneously. GFR and overnight sodium excretion or after salt and volume challenge were again investigated after respectively 11 and 13 days of Ang II infusion.

4.5.1. Effect of Ang II on heart weight index in EC eNOS KO/KI and RBC eNOS KO/KI mice

Ang II plays a significant role in cardiac hypertrophy, and thus in an increase in heart weight index, via the combination of its direct effect on cardiomyocytes and the elevation of blood pressure (Geisterfer et al., 1988; Dostal et al., 1992; Crowley et al., 2006; Xu et al., 2010).

To understand whether the total or a cell-specific deletion of eNOS may worsen the hypertrophy effect of Ang II, a comparison of the heart weight indexes (heart weight/body weight) before and after 13 days of Ang II treatment was done in all the cell-specific eNOS KO and KI mice and the littermate control groups (Tab. 13). 4-6-month-old mice were used for comparisons with Ang II-treated mice.

To understand whether tamoxifen may have an effect on heart weight index per se, a first comparison was done between tamoxifen-treated and untreated WT mice. The results showed that at baseline, the tamoxifen-treated group had a significantly lower heart weight index as compared to the untreated WT group. However, after Ang II infusion, there were no differences between the two groups, as Ang II led to a significant increase in heart weight

index only in the tamoxifen-treated WT mice. Tamoxifen-treated CondKO mice showed the same heart weight index as the untreated control group at baseline and after Ang II treatment. However, Ang II led to an increase in heart weight index only in tamoxifen-treated CondKO mice. CondKO mice treated with tamoxifen, showed a significantly higher heart weight index as compared to tamoxifen-treated WT mice at baseline. After Ang II treatment, both CondKO and WT mice showed increased heart-to-body weight ratio, which was similar in both groups. These results show that at baseline, tamoxifen decreases heart weight index, while after Ang II it leads to an increase in heart weight index, which is independent from eNOS.

Treatment with Ang II did not affect the heart weight index in EC eNOS KO mice. These results suggest that the lack of eNOS in ECs did not affect the heart-to-body weight ratio. Moreover, there were no differences in heart weight index between them before and after Ang II treatment. Tamoxifen-untreated WT and CondKO mice did not show any difference in heart weight index at baseline. Moreover, Ang II treatment did not lead to any changes in either group. RBC eNOS KO mice did not show any difference as compared to WT mice at baseline and after Ang II treatment. Additionally, Ang II infusion did not affect the heart weight index in both RBC eNOS KO and WT mice. Surprisingly, RBC eNOS KI mice showed a lower heart weight index as compared to CondKO littermates at baseline. However, after treatment with Ang II, the two groups did not show any differences. Moreover, Ang II did not affect the heart to body weight index in both RBC eNOS KI and CondKO mice as compared to baseline. However, due to the limited sample size, these results need further investigation.

Table 13. Heart weight indexes.

*The heart weight index was calculated in all cell-specific eNOS KO and KI lines and the relative control mice, before and after Ang II treatment. For RBC eNOS KO, RBC eNOS KI mice, and their respective WT and CondKO controls, only data from 4-6 months old groups are shown. Statistical analyses are referred to the heart weight indexes. unpaired t-test with Welch's correction; [a] Baseline vs. Ang II; [b] CondKO (TAM) vs. WT (TAM) at baseline; [c] WT (w/o TAM) vs. WT (TAM) at baseline; [d] RBC eNOS KI vs. CondKO at baseline; * p < 0.05, ** p < 0.01.*

		Baseline			Ang II			
Strain	**Genotype**	**Body weight (n)**	**Heart weight (n)**	**Heart weight index (n)**	**Body weight (n)**	**Heart weight (n)**	**Heart weight index (n)**	**p**
		g	**mg**	**mg/g**	**g**	**mg**	**mg/g**	

WT (TAM)	$eNOS^{flox/flox}$ Cdh5-Cre/$ERT2^{neg}$ + TAM	30.3±1.7 (7)	155.6±12.8 (7)	5.2±0.5 (7)	31.1±1.9 (7)	192.5±19.2 (7)	6.2±0.5 (7)	[a] 0.0037**
EC eNOS KO	$eNOS^{flox/flox}$ Cdh5-Cre/$ERT2^{pos}$ + TAM	29.5±2.1 (7)	167.9±21.0 (7)	5.7±0.5 (7)	29.8±3.2 (8)	189.5±24.9 (8)	6.4±1.0 (8)	[a] 0.2496
CondKO (TAM)	$eNOS^{inv/inv}$ Cdh5-Cre/$ERT2^{neg}$ + TAM	31.4±2.9 (12)	188.6±23.0 (12)	6.0±0.4 (12)	26.8±3.9 (15)	182.1±30.8 (15)	6.8±1.0 (15)	[a] 0.0176* [b] 0.0025*
EC eNOS KI	$eNOS^{inv/inv}$ Cdh5-Cre/$ERT2^{pos}$ + TAM	32.0±2.1 (11)	189.4±19.0 (11)	5.9±0.5 (11)	30.4±4.0 (21)	189.0±37.5 (21)	6.3±1.5 (21)	[a] 0.3125
WT (w/o TAM)	$eNOS^{flox/flox}$ $HbbCre^{neg}$	31.1±1.6 (11)	181.2±21.2 (11)	5.8±0.7 (11)	33.0±2.3 (7)	199.1±15.5 (7)	6.1±0.6 (7)	[a] 0.3725 [c] 0.0333*
RBC eNOS KO	$eNOS^{flox/flox}$ $HbbCre^{pos}$	32.4±1.3 (13)	186.1±26.9 (13)	5.7±0.8 (13)	33.8±3.6 (7)	197.8±19.5 (7)	5.9±0.3 (7)	[a] 0.4619
CondKO (w/o TAM)	$eNOS^{inv/inv}$ $HbbCre^{neg}$	30.6 ±1.8 (11)	191.0±23.7 (11)	6.2±0.6 (11)	29.8±2.9 (6)	185.7±18.5 (6)	6.3±0.8 (6)	[a] 0.9781
RBC eNOS KI	$eNOS^{inv/inv}$ $HbbCre^{pos}$	29.5±3.3 (8)	160.0±19.1 (8)	5.5±0.7 (8)	26.7±2.2 (10)	186.5±26.5 (10)	7.0±1.3 (10)	[a] 0.0652 [d] 0.0259*

4.5.2. The role of eNOS in sodium and urine excretion: basal measurements

NO has a central role in sodium and water handling by regulating the pressure-natriuresis response and, therefore, the long-term blood pressure.

To investigate whether tamoxifen has a role in sodium excretion in basal conditions, tamoxifen-treated and untreated WT mice were compared. As shown in Tab. 14, tamoxifen did not affect sodium excretion as the two groups of WT mice showed similar natriuresis before and after Ang II treatment. Also tamoxifen-treated and untreated CondKO mice showed the same sodium excretion with/without Ang II. These results show that tamoxifen does not have an effect on sodium excretion under a normal sodium intake.

To analyse whether the lack of eNOS might have an impact on sodium excretion under basal conditions, the urine of all the cell-specific eNOS KO and KI lines was collected overnight, and excreted sodium concentrations were analysed before and after Ang II treatment, as shown in Table 14. Ang II did not affect sodium excretion in WT mice as compared to baseline. Moreover, also EC eNOS KO mice did not show any difference in sodium excretion after treatment with Ang II. EC eNOS KO mice showed the same basal overnight sodium excretion as WT control mice before and after Ang II treatment. CondKO mice did not show any difference as compared to WT mice before and after Ang II in both

tamoxifen-treated and untreated groups. Also EC eNOS KI mice showed similar sodium excretion as CondKO littermates with/without Ang II (Tab. 14). These data suggest that eNOS in ECs does not play a significant role in sodium excretion in regular sodium intake conditions.

RBC eNOS KO mice showed the same overnight sodium excretion as WT control mice with/without Ang II, and no changes in both groups after Ang II as compared to baseline. RBC eNOS KI mice showed no difference in basal sodium excretion as compared to the CondKO littermates, both before and after Ang II. However, due to the limited sample size, these results need further investigation.

Table 14. Overnight urinary sodium excretion.

Basal urinary sodium excretion was analysed in all the cell-specific eNOS KO and KI lines, as well as in the respective WT and CondKO control mice at baseline and after Ang II treatment. t-test with Welch's correction; [a] Baseline vs. Ang I.

Urinary sodium excretion overnight (mmol)				
Strain	**Genotype**	**Baseline (n)**	**Ang II (n)**	**p**
WT (TAM)	$eNOS^{flox/flox}$ Cdh5-Cre/$ERT2^{neg}$ + TAM	0.152 ± 0.083 (11)	0.194 ± 0.099 (4)	[a] 0.8296
EC eNOS KO	$eNOS^{flox/flox}$ Cdh5-Cre/$ERT2^{pos}$ + TAM	0.144 ± 0.061 (10)	0.168 ± 0.056 (4)	[a] 0.2023
CondKO (TAM)	$eNOS^{inv/inv}$ Cdh5-Cre/$ERT2^{neg}$ + TAM	0.140 ± 0.060 (4)	0.173 ± 0.123 (3)	[a] 0.8119
EC eNOS KI	$eNOS^{inv/inv}$ Cdh5-Cre/$ERT2^{pos}$ + TAM	0.162 ± 0.086 (14)	0.116 ± 0.078 (10)	[a] 0.0678
WT (w/o TAM)	$eNOS^{flox/flox}$ $HbbCre^{neg}$	0.143 ± 0.055 (4)	0.207 ± 0.089 (5)	[a] 0.4060
RBC eNOS KO	$eNOS^{flox/flox}$ $HbbCre^{pos}$	0.144 ± 0.061 (4)	0.133 ± 0.036 (5)	[a] 0.4036
CondKO (w/o TAM)	$eNOS^{inv/inv}$ $HbbCre^{neg}$	0.177 ± 0.070 (5)	0.230 ± 0.034 (3)	[a] 0.8256
RBC eNOS KI	$eNOS^{inv/inv}$ $HbbCre^{pos}$	0.101 ± 0.044 (4)	0.168 ± 0.046 (5)	[a] 0.2282

To investigate whether tamoxifen influences urine excretion, urines from tamoxifen-treated and untreated WT mice were collected overnight, before and after Ang II treatment. Tamoxifen did not have any effect on urine excretion, both before and after Ang II infusion, as treated WT mice showed the same urine excretion as the untreated group with/without Ang II. Similarly, tamoxifen did not affect urine excretion in CondKO mice, as treated and untreated groups showed the same urine excretion before and after Ang II. These data show that tamoxifen did not have any effect on basal sodium excretion in both WT and CondKO mice.

To analyse whether the lack of eNOS specifically in ECs or RBCs has an effect on basal urine excretion, urines from all the cell-specific eNOS KO and KI lines were collected overnight, before and after Ang II (Tab. 15). EC eNOS KO mice did not show any difference in basal urine excretion as compared to WT mice at both baseline and after Ang II infusion. Furthermore, Ang II treatment did not affect urine excretion in both EC eNOS KO and WT mice as compared to baseline. EC eNOS KI mice did not show any difference in urine excretion as compared to CondKO mice, before and after Ang II infusion. Moreover, Ang II treatment did not have any effect, as both EC eNOS KI and CondKO mice showed unchanged urine excretion as compared to baseline. Additionally, CondKO mice (which are treated with tamoxifen) had the same urine excretion as compared to tamoxifen-treated WT mice with/without Ang II. These results show that eNOS in ECs does not modulate basal urine excretion and that Ang II affected only WT mice.

RBC eNOS KO mice showed the same urine excretion as compared to WT littermates with/without Ang II treatment (Tab. 15). However, Ang II treatment led to a decrease in urine excretion only in RBC eNOS KO mice and not in WT controls. RBC eNOS KI mice showed lower urine excretion as compared to CondKO littermates at baseline, but this difference was abolished after treatment with Ang II. However, Ang II did not affect urine excretion in both RBC eNOS KI and CondKO mice, as both groups showed unchanged urine excretion as compared to baseline. Moreover, tamoxifen-untreated CondKO and WT mice had the same urine excretion both with/without Ang II. These results were unexpected, and further investigations are needed as the sample size was limited.

Table 15. Overnight urinary excretion.

Basal urinary excretion was analysed in all the cell-specific eNOS KO and KI lines, as well as in the respective WT and CondKO control mice at baseline and after Ang II treatment. t-test with Welch's corrections. [a] *Baseline vs. Ang II;* [b] RBC eNOS KI vs. CondKO at baseline*; *p < 0.05.*

Urinary excretion overnight (mL)				
Strain	**Genotype**	**Baseline (n)**	**Ang II (n)**	**p**
WT (TAM)	$eNOS^{flox/flox}$ Cdh5-Cre/$ERT2^{neg}$ + TAM	1.278 ± 0.637 (12)	1.696 ± 0.947 (7)	[a] 0.6855
EC eNOS KO	$eNOS^{flox/flox}$ Cdh5-Cre/$ERT2^{pos}$ + TAM	1.186 ± 0.405 (11)	1.322 ± 0.553 (9)	[a] 0.9126
CondKO (TAM)	$eNOS^{inv/inv}$ Cdh5-Cre/$ERT2^{neg}$ + TAM	1.393 ± 0.546 (6)	2.395 ± 1.671 (7)	[a] 0.2787
EC eNOS KI	$eNOS^{inv/inv}$ Cdh5-Cre/$ERT2^{pos}$ + TAM	1.460 ± 1.235 (16)	1.612 ± 1.629 (14)	[a] 0.7587
WT (w/o TAM)	$eNOS^{flox/flox}$ $HbbCre^{neg}$	1.040 ± 0.550 (4)	2.204 ± 0.879 (5)	[a] 0.1754
RBC eNOS KO	$eNOS^{flox/flox}$ $HbbCre^{pos}$	1.618 ± 0.719 (4)	1.264 ± 0.624 (5)	[a] 0.0037**
CondKO (w/o TAM)	$eNOS^{inv/inv}$ $HbbCre^{neg}$	2.251 ± 1.096 (5)	3.840 ± 1.032 (3)	[a] 0.1278
RBC eNOS KI	$eNOS^{inv/inv}$ $HbbCre^{pos}$	0.876 ± 0.405 (4)	3.461 ± 2.088 (5)	[a] 0.1110 [b] 0.0463*

4.5.3. The role of eNOS in sodium excretion: salt and volume challenge

Cumulative urinary sodium and urine volume excretion were analysed after salt and volume challenge before and after treatment with Ang II. To perform the experiment, mice were injected with 0.9% NaCl i.p. (volume corresponding to 10% of the body weight) and urines collected every hour for five hours.

4.5.4.1 Effect of tamoxifen on sodium and urine excretion

As a first step, the effect of tamoxifen on sodium excretion was investigated in WT mice. $eNOS^{flox/flox}HbbCre^{neg}$ mice were used as untreated WT controls, while $eNOS^{flox/flox}$Cdh5-Cre/$ERT2^{neg}$ mice were used as tamoxifen-treated WT group. Tamoxifen treatment induced a very weak increase in sodium excretion, which was only significant at the third hour of urine collection and was not significant for all other time points (Fig. 21A). The effects of tamoxifen were investigated also after treatment with Ang II, which challenges the kidney both locally and systemically, because of its vasoconstrictor and hypertensive effects. There was no difference between the groups in sodium excretion after Ang II treatment (Fig. 21B). Moreover, by comparing the results before and after Ang II for each group (data in Fig. 21A

vs. B), the data show that treatment with Ang II did not affect sodium excretion in WT mice with or without tamoxifen as determined by paired t-test corrected for Holm-Šidák multiple comparisons. Therefore, these data show that tamoxifen did not affect sodium excretion in WT mice before or after Ang II treatment.

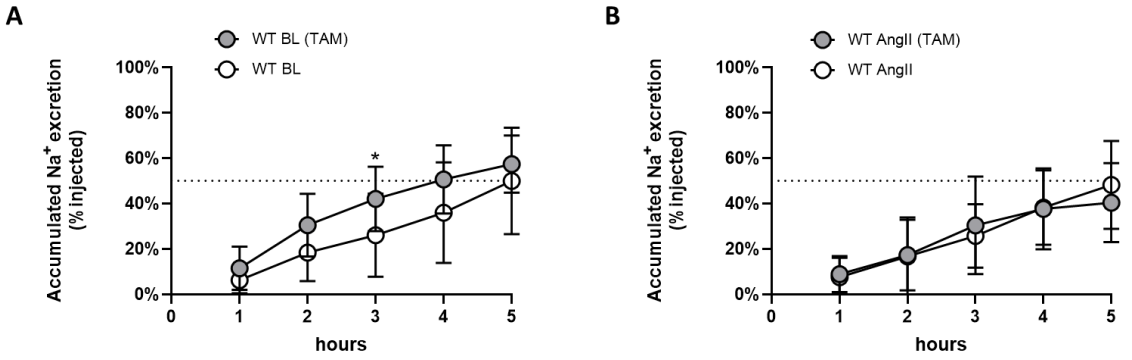

Figure 21 - Effect of tamoxifen on sodium excretion in WT mice after salt and volume challenge.

*Cumulative sodium excretion in urine was measured at (A) baseline and (B) after Ang II infusion in tamoxifen-treated and untreated WT mice, showing a significant increased sodium excretion in WT mice treated with tamoxifen at baseline. Baseline: WT TAM (n = 9), WT (n = 11); Ang II: WT TAM (n = 7), WT (n = 8). 2-way ANOVA, baseline: time p < 0.0001, TAM treatment p = ns, subject p < 0.0001, Ang II: time p < 0.0001, TAM treatment p = ns, subject p < 0.0001; Welch's t test (non-adjusted for multiple comparison), * p < 0.05. Abbreviations: Ang II, angiotensin II; BL, baseline; ns, not significant; TAM, tamoxifen; WT, wild type.*

The effect of tamoxifen on urine volume excretion was investigated in tamoxifen-treated and untreated WT mice as well. Before Ang II, tamoxifen-treated WT mice showed a higher volume of urine excretion as compared to the untreated WT mice. These data show that tamoxifen has an effect on urine excretion at baseline (Fig. 22A). By comparing the data obtained after Ang II treatment (panel B) with baseline data (panel A) Ang II treatment did not show any effect on urine excretion both in tamoxifen-treated and untreated WT mice as determined by paired t-test corrected for Holm-Šidák multiple comparisons. Taken together, tamoxifen affects urine excretion at baseline but not after Ang II treatment; this needs to be taken into account for the interpretation of data in tamoxifen-treated mice.

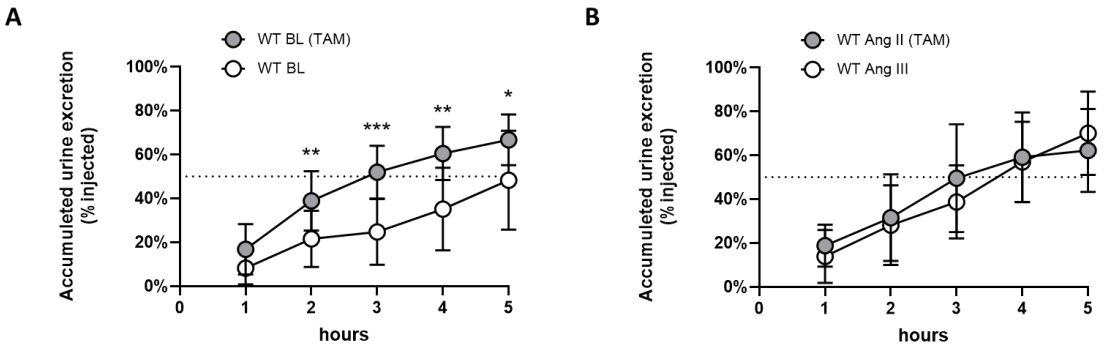

Figure 22 - Effect of tamoxifen on urine volume excretion in WT mice after salt and volume challenge.

*Cumulative urine excretion was measured at (A) baseline and (B) after Ang II infusion in tamoxifen-treated and untreated WT mice, showing a significant increased urine excretion in WT mice treated with tamoxifen only at baseline. Baseline: WT TAM (n = 9), WT (n = 11); Ang II: WT TAM (n = 7), WT (n = 7). 2-way ANOVA, baseline: time p < 0.0001, treatment p = 0.0009, subject p < 0.0001, Ang II: time p < 0.0001, TAM treatment p = ns, subject p < 0.0001; post hoc Tukey, * p < 0.05, **p < 0.01, ***p < 0.001. Abbreviations: Ang II, angiotensin II; BL, baseline; ns, not significant; TAM, tamoxifen; WT, wild type.*

To understand whether the effect of tamoxifen on sodium excretion was eNOS dependent, tamoxifen-treated and untreated CondKO mice were used for this purpose. eNOS$^{inv/inv}$HbbCre^{neg} mice were used as untreated control group, while eNOS$^{inv/inv}$Cdh5-Cre/ERT2^{neg} mice were used as tamoxifen-treated group. Treatment with tamoxifen led to an increase in sodium excretion at baseline, which was not statistically significant (2h, p = 0.0795; 3h, p = 0.0618; 4h, p = 0.0574) (Fig. 23A). After Ang II, treated and untreated CondKO mice showed the same sodium excretion (Fig. 23B). Moreover, the comparison between baseline (panel A) and Ang II (panel B) data showed that Ang II decrease sodium excretion only in tamoxifen-treated CondKO mice, but it was statistically significant only if not corrected for Holm-Šidák multiple comparisons. These results show that tamoxifen had a weak effect on sodium excretion in CondKO mice after Ang II treatment.

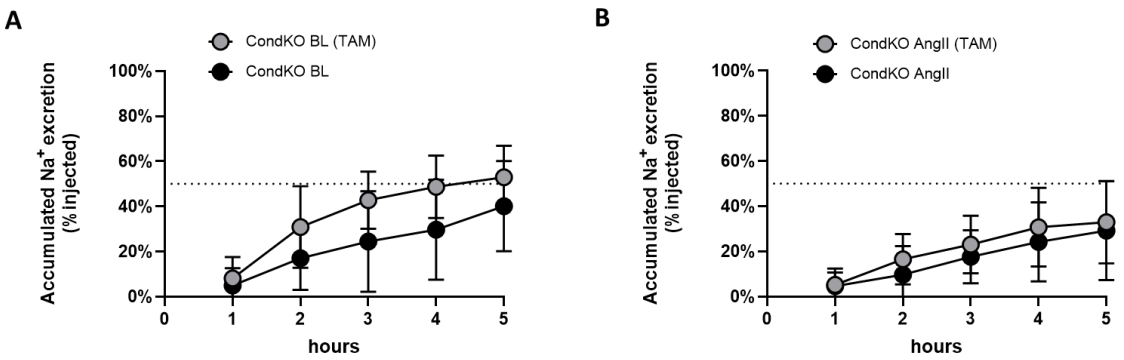

Figure 23 - Effect of tamoxifen on sodium excretion in CondKO mice after salt and volume challenge.

Cumulative sodium excretion in urine was measured (A) at baseline and (B) after Ang II infusion in tamoxifen-treated and untreated CondKO mice, showing an increase in sodium excretion in tamoxifen-treated CondKO mice at baseline, which was not statistically significant. Baseline: CondKO TAM (n = 11), CondKO (n = 8); Ang II: CondKO TAM (n = 19), CondKO (n = 6). 2-way ANOVA, baseline: time p < 0.0001, TAM treatment p = ns, subject p < 0.0001, Ang II: time p < 0.0001, TAM treatment p = ns, subject p < 0.0001; Welch's t test (non-adjusted for multiple comparison) ns. Abbreviations: Ang II, angiotensin II; BL, baseline; CondKO, conditional eNOS knock out or eNOS$^{inv/inv}$; ns, not significant; TAM, tamoxifen.

The effect of tamoxifen on urine excretion in the absence of eNOS was also investigated. Tamoxifen-treated CondKO mice showed a significant increased urine volume excretion as compared to the untreated control group at baseline (Fig. 24A) but not after Ang II treatment (Fig. 24B). Moreover, by comparing the urine excretion data at baseline (panel A) and after Ang II (panel B), Ang II treatment did not cause any change in both treated and untreated groups ad determined by paired t-test corrected for Holm-Šidák multiple comparison. These data show that tamoxifen has an effect on urine excretion, which is independent from eNOS.

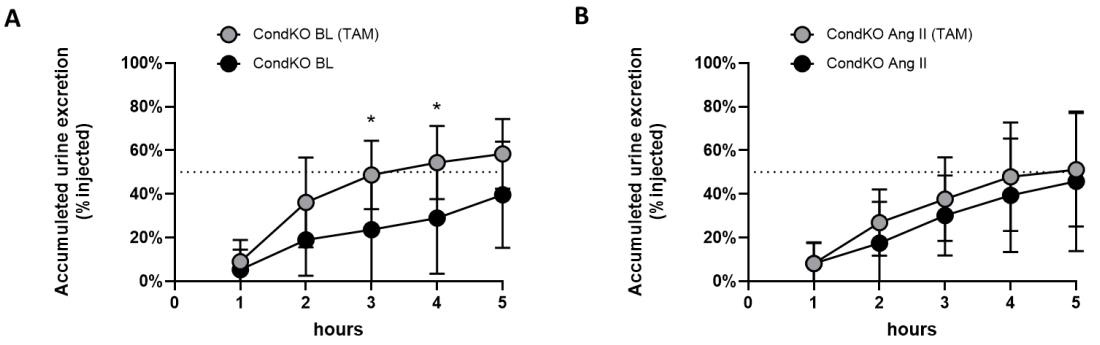

Figure 24 - Effect of tamoxifen on urine excretion in CondKO mice after salt and volume challenge.

*Cumulative urine excretion was measured (A) at baseline and (B) after Ang II infusion in tamoxifen-treated and untreated CondKO mice, showing a significant increase in urine excretion in tamoxifen-treated CondKO mice at baseline. Baseline: CondKO TAM (n = 11), CondKO (n = 9); Ang II: CondKO TAM (n = 10), CondKO (n = 6). 2-way ANOVA, baseline: time p < 0.0001, TAM treatment p = 0.0250, subject p < 0.0001; Ang II: time < 0.0001, TAM treatment = ns, subject p < 0.0001; post hoc Tukey, *p < 0.05. Abbreviations: Ang II, angiotensin II; BL, baseline; CondKO, conditional eNOS knock out or eNOS$^{inv/inv}$; TAM, tamoxifen; ns, not significant.*

4.5.4.2 Sodium and urine excretion in EC eNOS KO mice and WT littermates

To better understand the role of eNOS in ECs, sodium excretion after salt and volume challenge was investigated in EC eNOS KO and littermate WT mice. EC eNOS KO mice showed a significant decreased sodium excretion as compared to WT control mice at baseline (Fig. 25A). After the administration of Ang II, there were no differences in sodium excretion between the groups (Fig. 25B). By comparing the sodium excretion before (panel A) and after Ang II (panel B), there were no significant differences in the EC eNOS KO or WT mice as tested by paired t-test corrected for Holm-Šidák multiple comparisons (Fig. 25A vs. B). This data show that eNOS in ECs plays a role in sodium reabsorption/excretion when the kidney is challenged with a high sodium load, and that Ang II does not have an effect in the absence of eNOS.

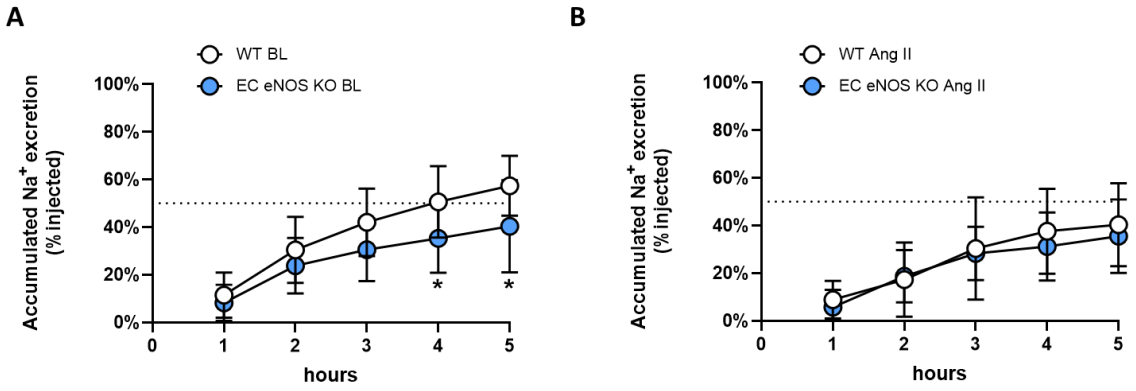

Figure 25 – Accumulated sodium excretion in EC eNOS KO mice after salt and volume challenge.

*Cumulative sodium excretion in urine was measured at (A) baseline and (B) after Ang II treatment in EC eNOS KO and WT mice, showing a significant decreased sodium excretion in EC eNOS KO mice as compared to WT mice at baseline. Baseline: WT (n = 7), EC eNOS KO (n = 9); Ang II: WT (n = 5), EC eNOS KO (n = 6). 2-way ANOVA, baseline: time p < 0.0001, genotype p = 0.0492, subject p < 0.0001, Ang II: time p < 0.0001, genotype p = ns, subject p < 0.0001; post hoc Tukey, *p < 0.05. Abbreviations: Ang II, angiotensin II; BL, baseline; EC eNOS KO, endothelial cell eNOS knock out; ns, not significant; WT, wild type.*

Cumulative urine excretion was also analysed in EC eNOS KO and WT mice before and after Ang II treatment. EC eNOS KO mice showed a significant decrease in urine excretion (3h, 4h, and 5h) as compared to WT control mice at baseline (Fig. 26A), but no difference after administration of Ang II (Fig. 26B). As shown before in Figure 22A, tamoxifen caused an increase in urine excretion in WT mice; thus, the lower urine excretion in EC eNOS KO mice as compared to the WT control mice is not a tamoxifen artifact but it is due to the lack of eNOS in ECs.

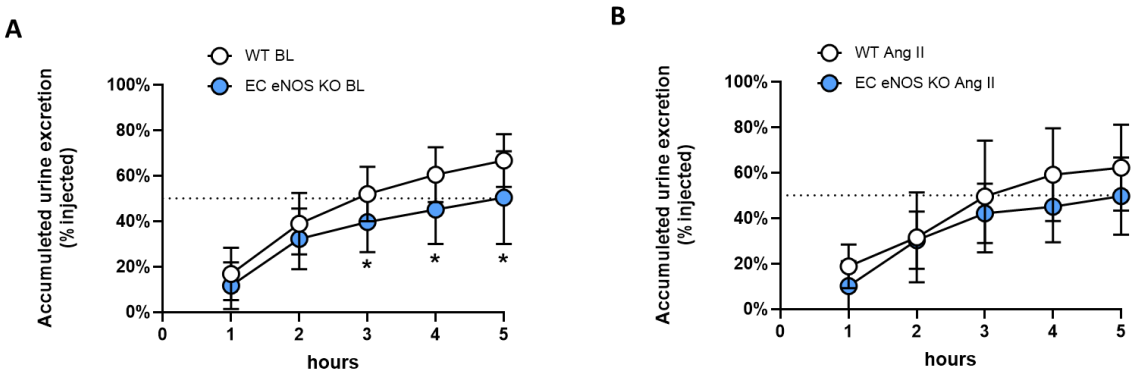

Figure 26 – Accumulated urine excretion in EC eNOS KO mice after salt and volume challenge. *Cumulative urine excretion was measured at (A) baseline and (B) after Ang II treatment in EC eNOS KO and WT mice, showing a significant decreased urine excretion in EC eNOS KO as compared to WT mice at baseline. Baseline: WT (n = 7), EC eNOS KO (n = 9); Ang II: WT (n = 5), EC eNOS KO (n = 6). 2-way ANOVA, baseline: time p < 0.0001, genotype p = 0.0492, subject < 0.0001, Ang II: time p < 0.0001, genotype p = ns, subject p < 0.0001; post hoc Tukey, *p < 0.05.* Abbreviations: *Ang II, angiotensin II; BL, baseline; EC eNOS KO, endothelial cell eNOS knock out; ns, not significant; WT, wild type.*

4.5.4.3 Sodium and urine excretion in EC eNOS KI mice and CondKO littermates

To better understand the role of EC eNOS in the regulation of sodium excretion, in the absence of eNOS expression in other cellular compartments, urine from EC eNOS KI mice and CondKO littermates was collected after salt and volume challenge, and the sodium concentration in urine was analysed before and after Ang II infusion. The cumulative urinary sodium concentration was the same between EC eNOS KI mice and CondKO control mice at baseline (Fig. 27A). After administration of Ang II only CondKO mice showed a weak decrease in sodium excretion, while natriuresis was preserved in EC eNOS KI mice (Fig. 27B). As shown above, the decreased sodium excretion after Ang II in CondKO mice is a tamoxifen artifact, which is counterbalanced by the reactivation of eNOS in ECs, as EC

eNOS KI showed a preserved sodium excretion after Ang II treatment. However, the differences between the CondKO before (panel A) and after AngII (panel B) were only significant if Holm-Šidák t-test was carried out without correction for multiple comparisons, indicating that the effect was weak.

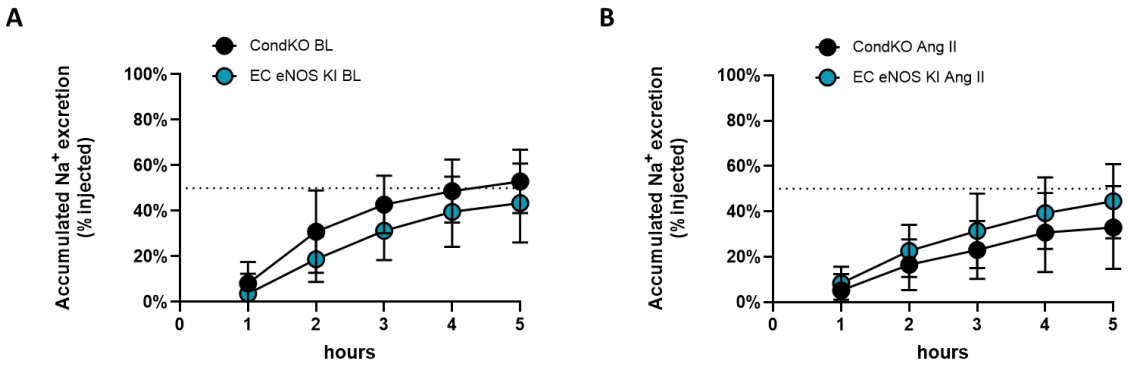

Figure 27 – Accumulated sodium excretion in EC eNOS KI mice after salt and volume challenge.

*Cumulative sodium excretion was measured at (A) baseline and (B) after Ang II treatment in EC eNOS KI and CondKO mice, showing no changes in sodium excretion between EC eNOS KI mice and CondKO mice at baseline. After Ang II administration, sodium excretion was preserved in EC eNOS KI mice. Baseline: CondKO (n =11), EC eNOS KI (n = 9); Ang II: CondKO (n = 10), EC eNOS KI (n = 8). 2-way ANOVA, baseline: time p < 0.0001, genotype p = ns, subject p < 0.0001, Ang II: time p < 0.0001, genotype p = ns, subject p < 0.0001; Welch's t test (*non-adjusted *for multiple comparison) ns. Abbreviations: Ang II, angiotensin II; BL, baseline; CondKO, conditional eNOS knock out or eNOS$^{inv/inv}$; EC eNOS KI, endothelial cell eNOS knock in; ns, not significant.*

Cumulative urine excretion was analysed in EC eNOS KI and CondKO mice before and after Ang II infusion (Fig. 28). EC eNOS KI and CondKO control mice did not show any difference between them both before (Fig. 28A) and after Ang II (Fig. 28B). Also the comparison of urine excretion of CondKO before (panel A) or after AngII treatment (panel B) or EC eNOS KI before (green, panel A) or after Ang II (green, panel B) were not significant as tested by paired t-test Holm-Šidák multiple comparisons. Also, the comparison of CondKO (data in Fig. 28) with WT (data in Fig. 26) before and after Ang II did not show any difference as tested by paired t-test corrected for Holm-Šidák multiple comparisons.

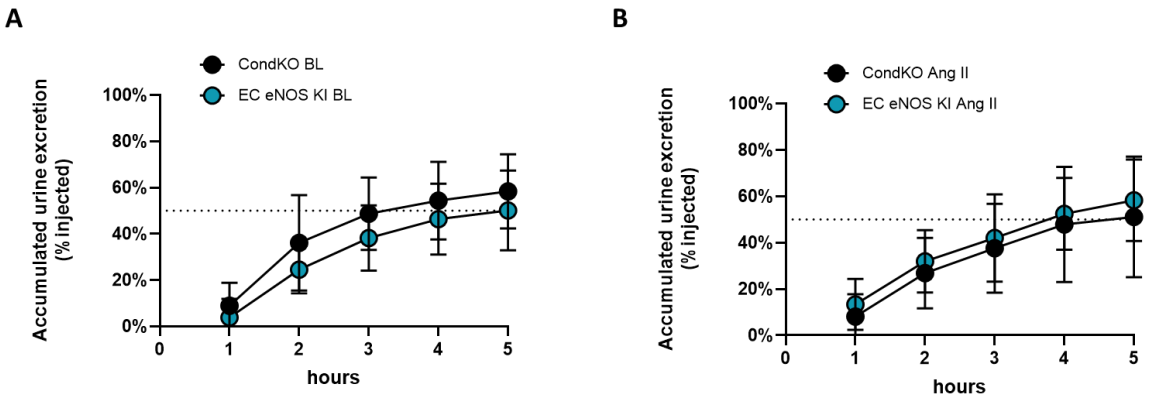

Figure 28 - Accumulated urine excretion in EC eNOS KI mice after salt and volume challenge. *Cumulative urine excretion was measured at (A) baseline and (B) after Ang II treatment in EC eNOS KI and CondKO mice, showing no changes between the two groups at both baseline and after Ang II treatment. Baseline: CondKO (n = 12), EC eNOS KI (n = 9); Ang II: CondKO (n = 10), EC eNOS KI (n = 8). 2-way ANOVA, baseline: time p < 0.0001, genotype p = ns, subject p < 0.0001; Ang II: time p < 0.0001, genotype p = ns, subject p < 0.0001; Welch's t test (*non-adjusted *for multiple comparison) ns. Abbreviations: Ang II, angiotensin II; BL, baseline; CondKO, conditional eNOS knock out or eNOS$^{inv/inv}$; EC eNOS KI, endothelial cell eNOS knock in;* ns, *not significant.*

In conclusion, the reactivation of eNOS in ECs in a global eNOS KO mouse contributes to preserving sodium excretion in global eNOS KO mice after Ang II treatment but does not affect urine excretion.

4.5.4.4 Sodium and urine excretion in RBC eNOS KO and RBC eNOS KI mice

To determine whether eNOS in RBCs has a role in sodium excretion, salt and volume challenge was performed in RBC eNOS KO and WT mice at baseline and after Ang II administration. As shown before in Figure 25, Ang II has no effect on sodium excretion in WT mice. RBC eNOS KO mice did not show any difference in sodium excretion as compared to WT littermates at both baseline (Fig. 29A) and after Ang II treatment (Fig. 29B). Moreover, Ang II did not affect sodium excretion also in RBC eNOS KO mice, as determined by paired t-test corrected for Holm-Šidák multiple comparisons. These findings show that RBC eNOS is not involved in the regulation of sodium excretion in mice.

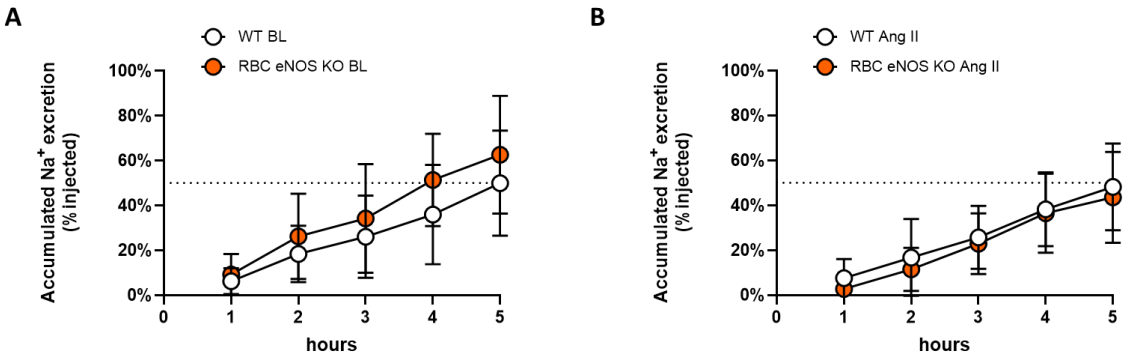

Figure 29 - Accumulated sodium excretion in RBC eNOS KO mice after salt and volume challenge.

Cumulative sodium excretion was measured at (A) baseline and (B) after Ang II treatment in RBC eNOS KO and WT mice, showing no differences between the two groups at both baseline and after Ang II treatment. Baseline: WT (n = 11), RBC eNOS KO (n = 10); Ang II: WT (n = 8), RBC eNOS KO (n = 12). 2-way ANOVA, baseline: time p < 0.0001, genotype p = ns, subject p < 0.0001, Ang II: time p < 0.0001, genotype p = ns, subject p < 0.0001; Welch's t test (non-adjusted for multiple comparison) ns. Abbreviations: Ang II, angiotensin II; BL, baseline; ns, not significant; RBC eNOS KO, red blood cell eNOS knock out; WT, wild type.

Cumulative urine excretion was also investigated in RBC eNOS KO mice and WT littermates after salt and volume challenge at baseline and after the administration of Ang II. Ang II did not affect sodium excretion in both WT and RBC eNOS KO mice (Fig. 30A vs. B) as tested by paired t-test corrected for Holm-Šidák multiple comparisons. Moreover, RBC eNOS KO mice showed the same urine excretion as WT control mice both before and after Ang II treatment (Fig. 30).

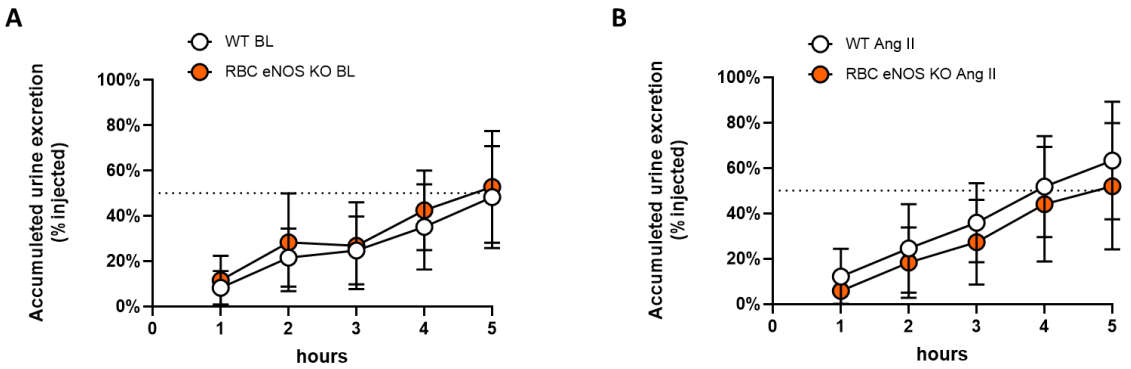

Figure 30 – Accumulated urine excretion in RBC eNOS KO mice after salt and volume challenge.

Cumulative urine excretion was measured in RBC eNOS KO and WT mice at (A) baseline and (B) after Ang II treatment, showing no differences between the two groups at both baseline and after

Ang II. Baseline: WT (n = 11), RBC eNOS KO (n = 10); Ang II: WT (n = 8), RBC eNOS KO (n = 12). 2-way ANOVA baseline: time p < 0.0001, genotype p = ns, subject p < 0.0001, Ang II: time p < 0.0001, genotype p = ns, subject p < 0.0001; Welch's t test (non-adjusted for multiple comparison) ns. Abbreviations: Ang II, angiotensin II; BL, baseline; ns, not significant; RBC eNOS KO, red blood cell eNOS knock out; WT, wild type.

To further understand the role of RBC eNOS in the regulation of sodium reabsorption/excretion, in the absence of eNOS expression in other cellular compartments, cumulative sodium excretion after salt and volume challenge was investigated in RBC eNOS KI mice and CondKO littermates at baseline and after treatment with Ang II. RBC eNOS KI mice did not show any difference as compared to CondKO mice at baseline (Fig. 31A) and after Ang II treatment (Fig. 31B). By comparing the data of baseline (panel A) and after Ang II (panel B), Ang II did not affect both CondKO and RBC eNOS KI mice as determined by paired t-test corrected for Holm-Šidák multiple comparisons. These results show that eNOS in RBC does not modulate sodium excretion.

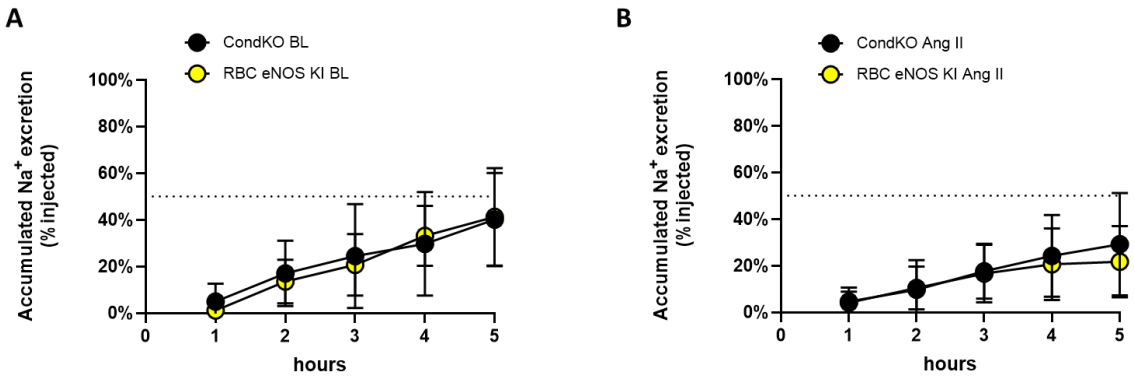

Figure 31 – Accumulated sodium excretion in RBC eNOS KI mice after salt and volume challenge.

Cumulative sodium excretion was measured at (A) baseline and (B) after Ang II treatment in RBC eNOS KI and CondKO mice, showing no difference in sodium excretion between RBC eNOS KI mice and CondKO littermates at baseline, as well as after Ang II. Baseline: CondKO (n = 8), RBC eNOS KI (n = 11); Ang II: CondKO (n = 6), RBC eNOS KI (n = 10). 2-way ANOVA, baseline: time p < 0.0001, genotype p = ns, subject p < 0.0001, Ang II: time p < 0.0001, genotype p = ns, subject p < 0.0001, Welch's t test (non-adjusted for multiple comparison) ns. Abbreviations: Ang II, angiotensin II; BL, baseline; CondKO, conditional eNOS knock out or $eNOS^{inv/inv}$; ns, not significant; RBC eNOS KI, red blood cell eNOS knock in.

Cumulative urine excretion was also analysed in RBC eNOS KI mice and CondKO mice after sodium and volume challenge with/without Ang II. RBC eNOS KI mice showed no difference in cumulative urine excretion as compared to the CondKO mice at baseline (Fig. 32A), as well as after Ang II treatment (Fig. 32B). Moreover, Ang II did not affect both CondKO and RBC eNOS KI mice as tested by paired t-test corrected for Holm-Šidák multiple comparisons. These data show that eNOS in RBCs does not play any role in urine excretion.

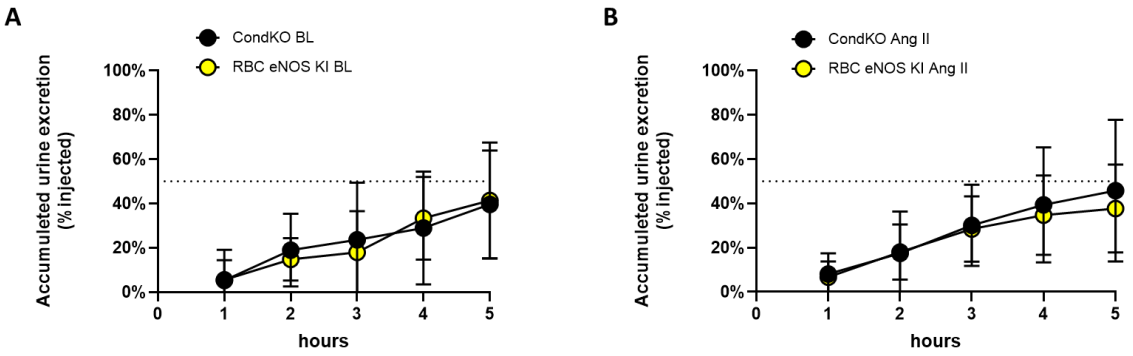

Figure 32 – Accumulated urine excretion in RBC eNOS KI mice after salt and volume challenge.

Cumulative urine excretion was measured in RBC eNOS KI and CondKO mice at (A) baseline and (B) after Ang II treatment, showing no differences in urine excretion between the two groups at both baseline and after Ang II infusion. Baseline: CondKO (n = 9), RBC eNOS KI (n = 11); Ang II: CondKO (n = 6), RBC eNOS KI (n = 10). 2-way ANOVA baseline: time p < 0.0001, genotype p = ns, subject p < 0.0001, Ang II: time p < 0.0001, genotype p = ns, subject p < 0.0001, Welch's t test (non-adjusted for multiple comparison) ns. Abbreviations: Ang II, angiotensin II; BL, baseline; CondKO, conditional eNOS knock out or eNOS$^{inv/inv}$; ns, not significant; RBC eNOS KI, red blood cell eNOS knock in.

4.5.4. Role of eNOS in GFR

The aim of this set of experiments was to understand whether the presence or the absence of eNOS specifically in ECs or RBCs may influence the GFR. To this aim, control experiments to determine the effect of tamoxifen on GFR were also performed. Moreover, also the role of age in GFR in WT, CondKO, RBC eNOS KO, and RBC eNOS KI mice models was also investigated.

The EC eNOS KO/KI mice and their littermate controls could not be used for this purpose since in these models the activation of the Cre recombinase is tamoxifen-inducible and transient; thus, all the experiments have to be performed on 12-week-old mice within three weeks.

To have an overview in order to better understand the role of eNOS on GFR regulation as well as the effect of tamoxifen treatment, data from all the mouse lines are summarized in Table 16. For RBC eNOS KO and KI mice and the respective WT and CondKO littermates, only data from 4-6-month-old groups are reported for comparison (Tab. 16). Here, statistical comparisons were performed using t-test with Welch's correction as indicated in the legend. For a comprehensive statistical analysis (2-way ANOVA) among cell-specific eNOS KO/KI mice with their respective Cre-negative littermates, both before and after Ang II treatment, refer to the respective figures.

Table 16. Glomerular filtration rate.

*GFR was investigated in all cell-specific eNOS KO and KI lines, and the respective littermate control mice at baseline and after Ang II treatment. For RBC eNOS KO, RBC eNOS KI mice, and their respective WT and CondKO controls, only 4-6-month-old groups are shown. t test with Welch's corrections. [a] Baseline vs. Ang II; [b] CondKO (TAM) vs. WT (TAM) after Ang II; [c] EC eNOS KI vs. CondKO (TAM) after Ang II; [d] CondKO (w/o TAM) vs. WT (w/o TAM) at baseline; [e] CondKO (w/o TAM) vs. WT (w/o TAM) after Ang II. * p < 0.05, ** p < 0.01, *** p < 0.001.*

Glomerular filtration rate (GFR), µL/min/gBW				
Strain	**Genotype**	**Baseline (n)**	**Ang II (n)**	**p**
WT (TAM)	$eNOS^{flox/flox}$ Cdh5-Cre/$ERT2^{neg}$ + TAM	6.383 ± 1.651 (20)	8.304 ± 2.752 (9)	[a] 0.0156*
EC eNOS KO	$eNOS^{flox/flox}$ Cdh5-Cre/$ERT2^{pos}$ + TAM	7.565 ± 2.441 (27)	7.796 ± 2.016 (15)	[a] 0.8434
CondKO (TAM)	$eNOS^{inv/inv}$ Cdh5-Cre/$ERT2^{neg}$ + TAM	6.026 ± 1.468 (37)	4.431 ± 1.592 (17)	[a] 0.1470 [b] 0.0025**
EC eNOS KI	$eNOS^{inv/inv}$ Cdh5-Cre/$ERT2^{pos}$ + TAM	6.524 ± 1.662 (40)	7.403 ± 2.152 (14)	[a] 0.0758 [c] 0.0003***
WT (w/o TAM)	$eNOS^{flox/flox}$ $HbbCre^{neg}$	7.272 ± 1.355 (15)	8.348 ± 2.671 (10)	[a] 0.8355
RBC eNOS KO	$eNOS^{flox/flox}$ $HbbCre^{pos}$	6.723 ± 1.509 (15)	6.813 ± 2.522 (12)	[a] 0.8461
CondKO (w/o TAM)	$eNOS^{inv/inv}$ $HbbCre^{neg}$	6.052 ± 1.170 (16)	4.386 ± 1.915 (11)	[a] 0.0878 [d] 0.0124* [e] 0.0013**
RBC eNOS KI	$eNOS^{inv/inv}$ $HbbCre^{pos}$	5.834 ± 1.252 (15)	3.824 ± 1.283 (10)	[a] 0.0006***

4.5.4.1 Effect of tamoxifen on GFR

To understand whether treatment with tamoxifen may influence the GFR, a comparison between tamoxifen-treated and untreated WT mice was done before and after Ang II infusion. The eNOS$^{flox/flox}$HbbCre^{neg} (4-6 months old) were used as untreated control group, while eNOS$^{flox/flox}$Cdh5-Cre/ERT2^{neg} mice were used as tamoxifen-treated WT group for this comparison.

Tamoxifen-treated WT mice showed the same GFR as compared to the untreated group at baseline (Fig. 33). Ang II increased GFR only in the WT mice treated with tamoxifen, while GFR did not change in WT without tamoxifen after the administration of Ang II (Fig. 33). These results show that the use of tamoxifen increases GFR after administration of Ang II in WT mice.

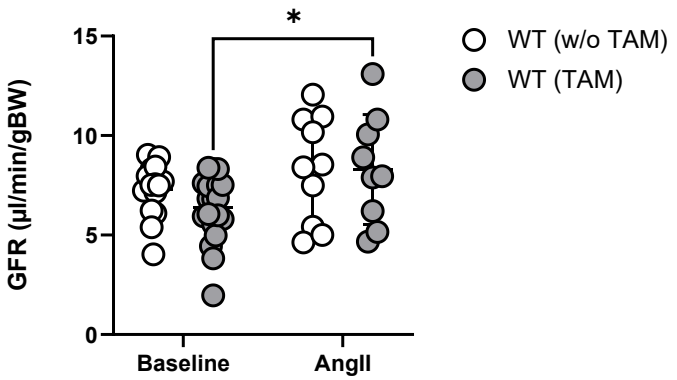

Figure 33 - Effect of tamoxifen on GFR in WT mice before and after Ang II treatment.
*GFR measurements were performed on tamoxifen-treated and untreated WT mice before and after Ang II treatment. Ang II treatment led to a significant increased GFR only in tamoxifen-treated WT mice. Baseline: WT w/o TAM (n = 22), WT TAM (n = 20). Ang II: WT w/o TAM (n = 10), WT TAM (n = 9). Mixed-effect 2-way ANOVA, Ang II treatment p = 0.0135, TAM treatment = ns, uncorrected Fisher's LSD, *p < 0.05. Abbreviations: Ang II, angiotensin II; GFR, glomerular filtration rate; ns, not significant; TAM, tamoxifen; w/o TAM, without tamoxifen; WT, wild type.*

The same comparison was also done in CondKO mice in order to understand whether tamoxifen could exacerbate or ameliorate the GFR in global absence of eNOS. eNOS$^{inv/inv}$HbbCre^{neg} mice were used as untreated control group, while eNOS$^{inv/inv}$Cdh5-Cre/ERT2^{neg} mice were used as tamoxifen-treated group. Tamoxifen-treated CondKO mice showed the same GFR as CondKO mice not treated with tamoxifen at baseline (Fig. 34). Treatment with Ang II decreased GFR in both treated and untreated CondKO mice in a

similar way. These results show that tamoxifen does not affect GFR in CondKO mice, both with/without Ang II.

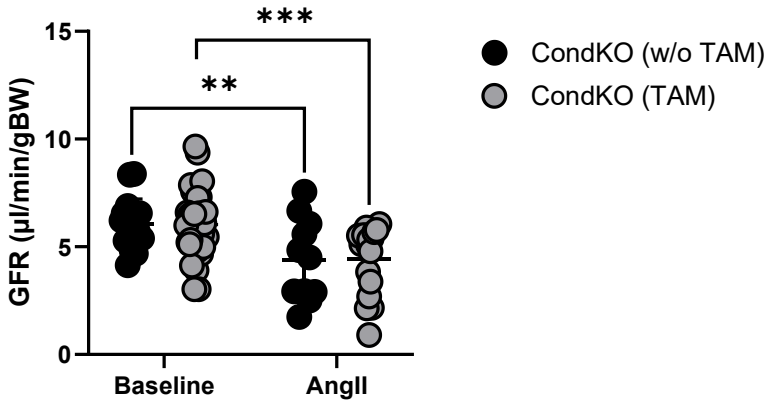

Figure 34 - Effect of tamoxifen on GFR in CondKO mice before and after Ang II treatment.
*Baseline GFR measurements were performed on tamoxifen-treated and untreated CondKO mice, showing no difference in GFR between the two groups of CondKO mice at baseline. After Ang II treatment, both groups showed a decreased GFR without any difference between each other. Baseline: CondKO TAM (n = 37), CondKO w/o TAM (n = 16); Ang II: CondKO TAM (n = 17), CondKO w/o TAM (n = 11). Mixed-effect 2-way ANOVA Ang II treatment p < 0.0001, TAM treatment p = ns, uncorrected Fisher's LSD, ** p < 0.01, *** p < 0.001. Abbreviations: Ang II, angiotensin II; CondKO, conditional eNOS knock out or eNOS$^{inv/inv}$; GFR, glomerular filtration rate; ns, not significant.*

4.5.4.2 GFR in EC eNOS KO and EC eNOS KI mice

To understand whether eNOS in ECs is involved in the regulation of the GFR, basal measurements as well as after Ang II treatment were carried out on EC eNOS KO and EC eNOS KI mice, and their WT and CondKO control mice, respectively. As mentioned before, the investigation of the age effect was not possible with these mouse models because of the transient effect of tamoxifen. Thus, the mice used for this experiment were about 3 months old. EC eNOS KO mice did not show any difference compared to WT mice at baseline. After Ang II treatment, only WT mice showed an increase in GFR while EC eNOS KO mice showed a lack of the compensatory response to Ang II (Fig. 35). However, there was no difference between the groups after Ang II treatment; therefore the effect was weak. These results are probably confounded by the unspecific effects of tamoxifen treatment. As shown in Fig. 33, the increase in GFR in the WT is measurable only in WT treated with tamoxifen and not observed in untreated WT mice.

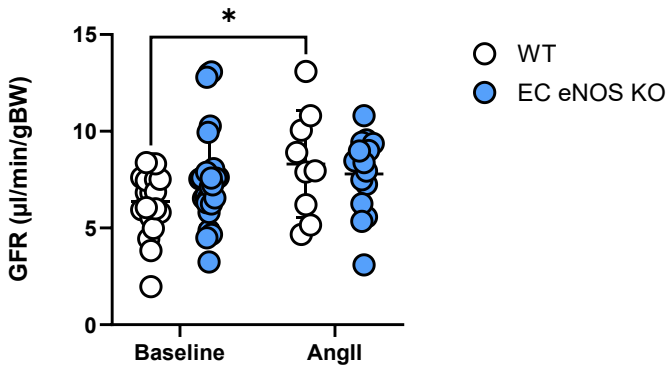

Figure 35 - GFR in EC eNOS KO mice before and after Ang II treatment.

*GFR was measured before and after Ang II treatment in EC eNOS KO and WT mice. EC eNOS KO mice did not show any difference as compared to WT mice at baseline. Ang II increased GFR only in WT mice, while EC eNOS KO mice lacked this compensatory response. Baseline: WT (n = 20), EC eNOS KO (n = 27); Ang II: WT (n = 9), EC eNOS KO (n = 15). Mixed-effect 2-way ANOVA Ang II treatment p = 0.0372, TAM treatment p = ns, uncorrected Fisher's LSD, *p < 0.05. Abbreviations: Ang II, angiotensin II; EC eNOS KO, endothelial cell eNOS knock out; GFR, glomerular filtration rate; ns, not significant; WT, wild type.*

GFR was also measured in EC eNOS KI mice and CondKO littermates at baseline and after Ang II infusion. GFR in basic conditions was the same between EC eNOS KI mice and the littermate CondKO mice. After Ang II administration, only CondKO mice showed a significant decrease in GFR, while the phenotype was preserved in EC eNOS KI. These data show that EC eNOS is involved in the regulation of GFR (Fig. 36).

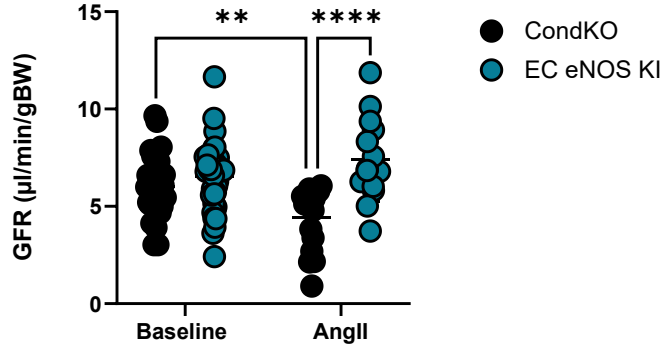

Figure 36 - GFR in EC eNOS KI mice before and after Ang II treatment.

*GFR was measured in EC eNOS KI and CondKO mice at baseline and after Ang II treatment. EC eNOS KI mice did not show any difference as compared to CondKO controls at baseline. After Ang II administration, the GFR was preserved in EC eNOS KI mice. Baseline: WT (n = 37), EC eNOS KI (n = 40); Ang II: CondKO (n = 17), EC eNOS KI (n = 14). Mixed-effect 2-way ANOVA Ang II treatment p = ns, genotype p < 0.0001, treatment x genotype p = 0.0007; uncorrected Fisher's LSD, **p < 0.01,*

*****p < 0.0001. Abbreviations: Ang II, angiotensin II; CondKO, conditional eNOS KO or eNOS$^{inv/inv}$; EC eNOS KI, endothelial cell eNOS knock in; GFR, glomerular filtration rate; ns, not significant.*

4.5.4.3 GFR in RBC eNOS KO and RBC eNOS KI mice

To understand whether eNOS in RBCs plays a role in GFR regulation, basal measurements were carried out on RBC eNOS KO and RBC eNOS KI mice, and their WT and CondKO control mice, respectively, as well as after Ang II treatment. The role of age in GFR was also investigated. Three different sets of RBC eNOS KO and WT mice grouped by age (4-6 month old, 9-12 month old, and 21-31 month old mice) were analysed. Age did not affect GFR in WT mice. Similarly, the lack of eNOS specifically in RBCs did not affect the GFR with age. Moreover, the deletion of eNOS from RBCs did not affect the GFR as there were no changes among all three groups of RBC eNOS KO mice and their respective age-matched WT mice controls (Fig. 37).

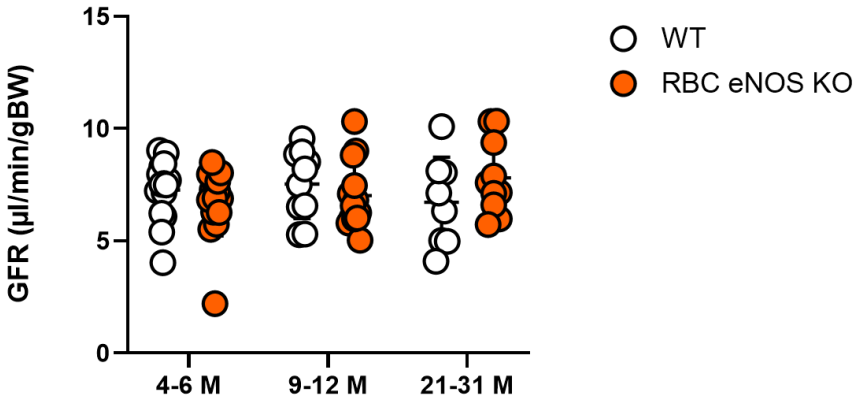

Figure 37 - GFR in different sets of RBC eNOS KO and WT mice grouped by age.
Baseline GFR measurements were performed on three different RBC eNOS KO and WT groups (4-6-month-old (M), 9-12 M, and 21-31 M mice), showing no differences in GFR with aging. 4-6 M: WT (n = 22), RBC eNOS KO (n = 23); 9-12 M: WT (n = 24), RBC eNOS KO (n = 22); 21-31 M: WT (n = 10), RBC eNOS KO (n = 10). Mixed-effect 2-way ANOVA age p = ns, genotype p = ns. Abbreviations: GFR, glomerular filtration rate; M, month old; ns, not significant; RBC eNOS KO, red blood cell eNOS knock out; WT, wild type.

The effect of Ang II was investigated only in 4-6-month-old and 9-12-month-old groups of RBC eNOS KO mice and WT littermates. 21-31-month-old mice were excluded from the experiment due to high mortality following Ang II treatment. 4-6 month old RBC eNOS KO mice did not show any difference in GFR as compared to WT mice at both baseline and after Ang II treatment (Fig. 38A). Also 9-12 month old RBC eNOS KO mice did not show

any phenotype as compared to WT before and after Ang II infusion (Fig. 38B). These data show that eNOS in RBCs does not play any role in GFR regulation.

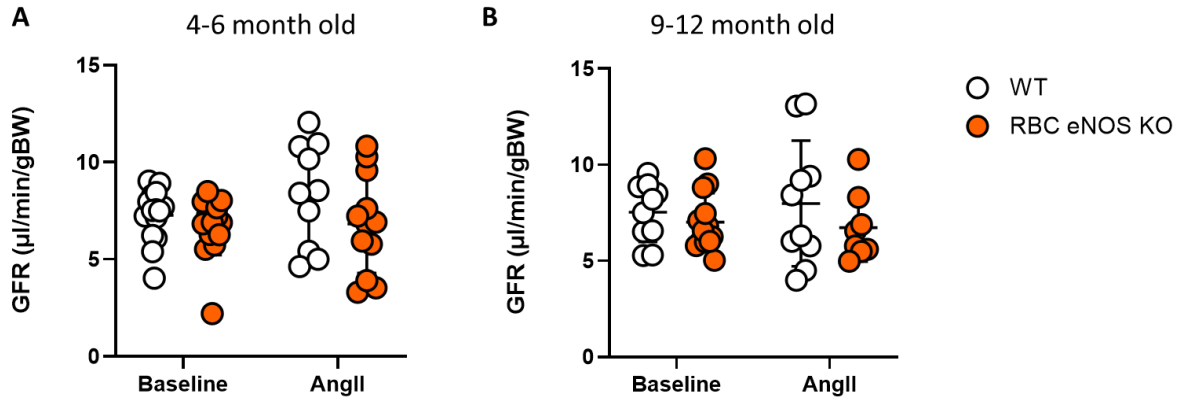

Figure 38 - GFR in different sets of RBC eNOS KO and WT mice grouped by age, before and after Ang II treatment.

GFR measurements were performed on two different RBC eNOS KO and WT groups (4-6 month old (A) and 9-12 month old (B)) before and after Ang II treatment. Both RBC eNOS KO groups showed no difference in GFR as compared to WT mice before and after Ang II treatment. 4-6 M, baseline: WT (n = 22), RBC eNOS KO (n = 23); 4-6 M, Ang II: WT (n = 10), RBC eNOS KO (n = 12); 9-12 M, baseline: WT (n = 25), RBC eNOS KO (n = 22); 9-12 M, Ang II: WT (n = 10), RBC eNOS KO (n = 8). Mixed-effect 2-way ANOVA, 4-6 M: Ang II treatment p = ns, genotype p = ns; 9-12 M: Ang II treatment p = ns, genotype p = ns. Abbreviations: Ang II, angiotensin II; GFR, glomerular filtration rate; M, month old; ns, not significant; RBC eNOS KO, red blood cell eNOS knock out; WT, wild type.

To further investigate the role of age and eNOS in RBCs on GFR, two different sets of RBC eNOS KI and CondKO mice grouped by age were used (4-6-month-old and 9-12-month-old mice). Surprisingly, RBC eNOS KI mice showed a significant decrease in GFR with age, but they did not show any changes as compared to the CondKO control mice (Fig.39).

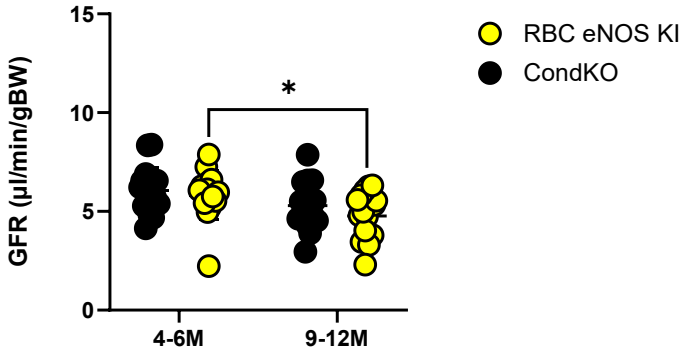

Figure 39 - GFR in different sets of RBC eNOS KI and CondKO mice grouped by age.
*Basal GFR measurements were performed on two different RBC eNOS KI and CondKO groups (4-6-month-old and 9-12-month-old mice), showing a decreased GFR in RBC eNOS KI mice with age. 4-6 M: CondKO (n = 16), RBC eNOS KI mice (n = 15); 9-12 M: CondKO (n = 15), RBC eNOS KI (n = 17). Mixed-effect 2-way ANOVA, age p = 0.0040, genotype p = ns; uncorrected Fisher's LSD *p < 0.05. Abbreviations: CondKO, conditional eNOS knock out or eNOS$^{inv/inv}$; GFR, glomerular filtration rate; M, month old; RBC eNOS KI, red blood cell eNOS knock in.*

The effect of Ang II was investigated in both sets of RBC eNOS KI and CondKO mice grouped by age. RBC eNOS KI mice showed the same GFR as compared to CondKO mice at baseline in both groups (Fig. 40). After administration of Ang II, both 4-6-month-old RBC eNOS KI and CondKO mice showed a significant decrease in GFR as compared to baseline, but there were no differences between RBC eNOS KI and CondKO controls (Fig. 40A). 9-12-month-old RBC eNOS KI mice did not show any difference in GFR as compared to CondKO at baseline, as well as after Ang II treatment. However, the administration of Ang II decreased GFR in the RBC eNOS KI mice but not in the CondKO mice (Fig. 40B).

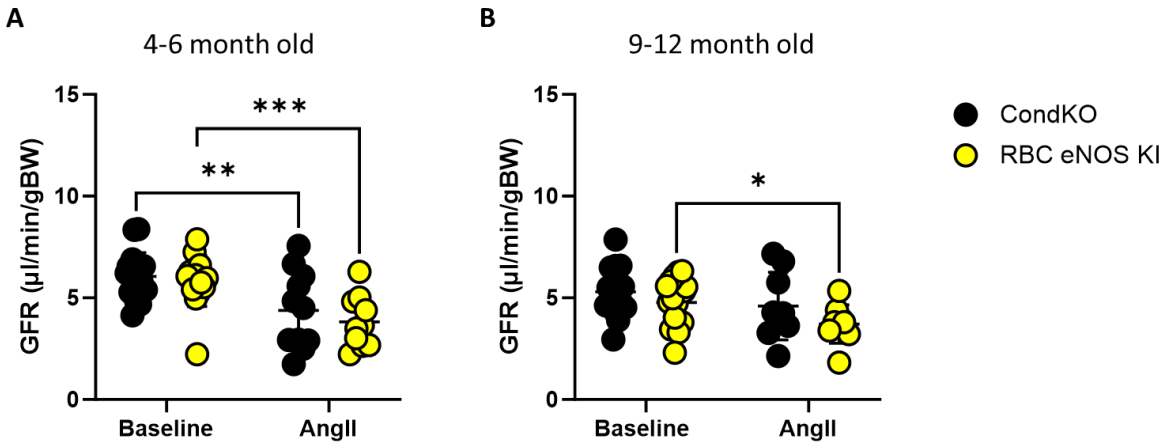

Figure 40 - GFR in different sets of RBC eNOS KI and CondKO mice grouped by age, before and after Ang II treatment.

*GFR measurements were performed on two different RBC eNOS KI and CondKO groups (4-6-month-old and 9-12-month-old mice). (A) 4-6-month-old RBC eNOS KI and CondKO mice showed a decreased GFR after Ang II. (B) In the group of 9-12-month-old mice, only RBC eNOS KI showed a decrease in GFR as compared to baseline. 4-6 M, baseline: CondKO (n = 16), RBC eNOS KI (n = 15); 4-6 M, Ang II: CondKO (n = 11), RBC eNOS KI (n = 10); 9-12 M, baseline: CondKO (n = 15), RBC eNOS KI (n = 17); 9-12 M, Ang II: CondKO (n = 9), RBC eNOS KI (n = 9). Mixed-effect 2-way ANOVA, 4-6 M: Ang II treatment p < 0.0001, genotype p = ns; 9-12 M: Ang II treatment p = 0.0089, genotype p = ns; uncorrected Fisher's LSD, *p < 0.05, **p < 0.01, ***p < 0.001. Abbreviations: Ang II, angiotensin II; CondKO, conditional eNOS knock out or eNOS$^{inv/inv}$; GFR, glomerular filtration rate; M, month old; RBC eNOS KI, red blood cell eNOS knock in.*

4.5.4.4 Role of age in GFR

The effect of age on basal GFR was investigated in WT and CondKO mice. To exclude any effect of tamoxifen, the eNOS$^{flox/flox}$HbbCre^{neg} mice were used as WT group, and eNOS$^{inv/inv}$HbbCre^{neg} mice were used as CondKO group. Two different sets of WT and CondKO mice grouped by age were used: 4-6 month old mice and 9-12 month old mice. The results show that age did not affect GFR between the two groups of WT mice. CondKO mice showed a significant decrease in GFR in both groups as compared to the respective WT control mice, but there were no changes in GFR between the two groups of CondKO mice. These data show that age does not affect GFR in WT mice and the absence of eNOS does not worsen the phenotype with age (Fig. 41).

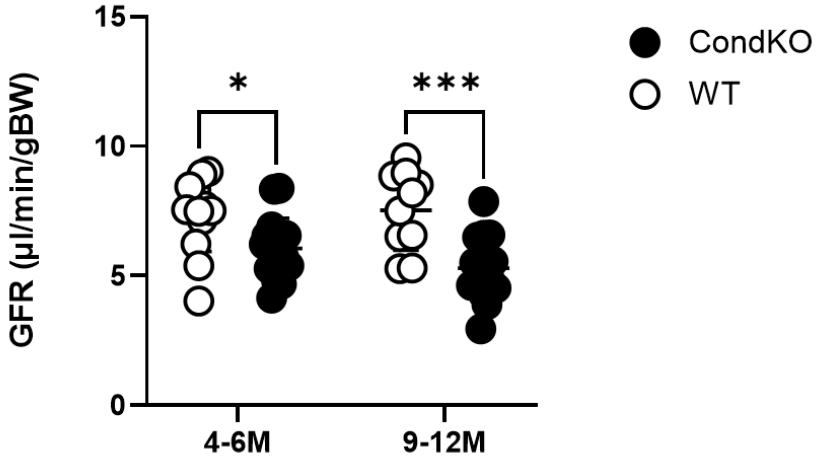

Figure 41 - GFR in different sets of CondKO and WT mice grouped by age.

Basal GFR measurement were performed on two different CondKO and WT groups (4-6 month old and 9-12 month old mice), showing a significant decreased GFR in both groups of CondKO mice as compared to age-matched WT mice, but no differences in GFR with age. 4-6M: WT (n = 22), CondKO

*(n = 16). 9-12M: WT (n = 10), CondKO (n = 15). Mixed-effect 2-way ANOVA, age p = ns, genotype < 0.0001, uncorrected Fisher's LSD, **p < 0.01. ***p < 0.001. Abbreviations: CondKO, conditional eNOS knock out or eNOS$^{inv/inv}$; GFR, glomerular filtration rate; M, month old; ns, not significant; WT, wild type.*

A comparison among these groups after Ang II treatment was also performed. Ang II treatment exacerbated the difference in GFR between WT and CondKO mice as compared to baseline in both sets of mice (Fig. 42). Moreover, the 4-6 month old CondKO mice showed a significant decreased GFR after Ang II infusion as compared to baseline (Fig. 42A), as also shown in Figure 41.

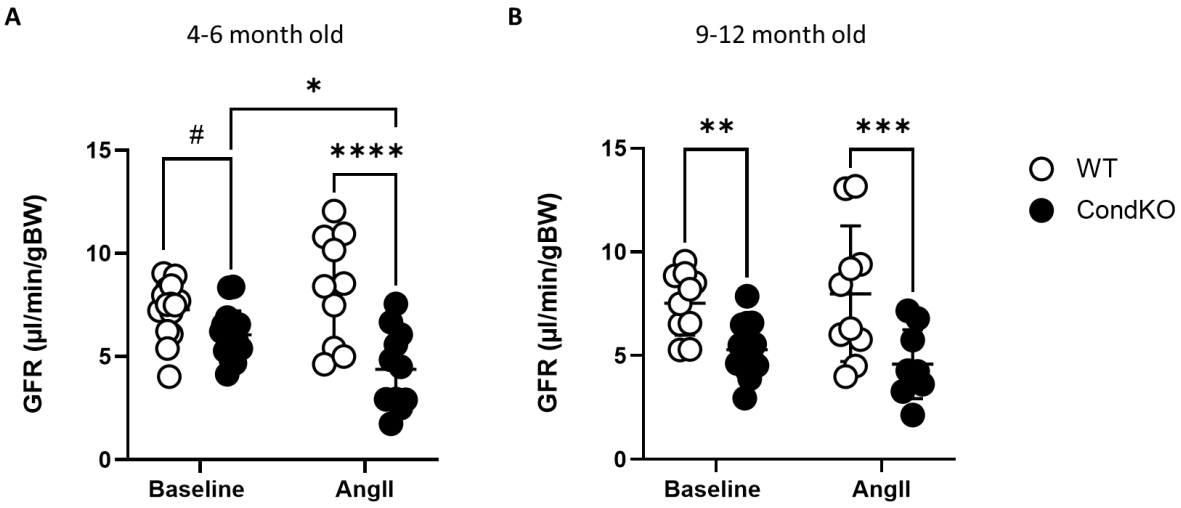

Figure 42 – GFR in different sets of CondKO and WT mice grouped by age before and after Ang II treatment.

*GFR was measured before and after Ang II treatment in (A) 4-6 month old and in (B) 9-12 month old WT and CondKO mice. Ang II worsened the GFR in CondKO as compared to WT mice in both sets of mice. Moreover, the 4-6 month old CondKO mice showed a decreased GFR as compared to baseline. 4-6 M, baseline: WT (n = 22), CondKO (n = 16). 4-6 M, Ang II: WT (n = 10), CondKO (n = 11). 9-12 M, baseline: WT (n = 10), CondKO (n = 15). 9-12 M, Ang II: WT (n = 10), CondKO (n = 9). Mixed-effect 2-way ANOVA 4-6 M: genotype < 0.0001, Ang II treatment p = ns, Ang II treatment x genotype p = 0.0080; 9-12 M: Ang II treatment p = ns, genotype p = 0.0002; uncorrected Fisher's LSD, **p < 0.01. ***p < 0.001. Welch's t-test WT vs. CondKO (4-6M, baseline), #<0.05. Abbreviations: Ang II, angiotensin II; CondKO, conditional eNOS knock out or eNOS$^{inv/inv}$; GFR, glomerular filtration rate; M, month old; WT, wild type.*

5. Discussion

The aim of this study was to investigate the cell-specific role of eNOS in the control of kidney function. To this aim, $eNOS^{flox/flox}$ mice and $eNOS^{inv/inv}$ mice were generated and crossed with $DeleterCre^{pos}$ ($DelCre^{pos}$) mice, expressing Cre recombinase in all cells, or with mice expressing Cre recombinase only in ECs or RBCs to generate KO and KI mice and their respective WT and CondKO (global eNOS KO) control littermates. After these crossing procedures, the following lines were generated: global eNOS KO/WT ($eNOS^{flox/flox}$ $DelCre^{pos/neg}$) and global eNOS KI/CondKO ($eNOS^{fl/fl}$ and $eNOS^{inv/inv}$) mice, EC eNOS KO/WT and EC eNOS KI/CondKO mice, as well as RBC eNOS KO/WT and RBC eNOS KI/CondKO mice. While the global and RBC-specific lines are constitutive, the EC-specific lines are inducible, and a treatment with tamoxifen is required to induce the gene-targeted modification.

This study had three main goals: (1) to verify that $eNOS^{inv/inv}$ = CondKO construct was efficient for reactivating eNOS expression in global eNOS KI mice and the effect of eNOS "gene dosage", as proof of concept; (2) to characterize the expression of eNOS in targeted and non-targeted tissues of the mouse lines as compared to the Cre-negative littermates; (3) to investigate the role of eNOS expressed in ECs and RBCs in kidney function.

The main findings were:

1. In the first part of the study, the reactivation of eNOS in global eNOS KI mice was analysed as a proof of concept. The results show that eNOS was successfully reactivated in both alleles ($eNOS^{fl/fl}$ mice) or only in one allele ($eNOS^{fl/inv}$ mice). Reactivation of eNOS in one or both alleles rescued vascular function and blood pressure. Homozygous KI ($eNOS^{fl/fl}$) and heterozygous KI ($eNOS^{fl/inv}$) mice showed similar SBP as WT mice, and a preserved vascular response to ACh, PE, and SNP as WT mice.

2. The expression of eNOS was specific in the targeted cells. EC eNOS KO mice showed a loss of eNOS expression in aorta and a significant decreased eNOS expression in kidney as assessed by real-time RT-PCR, while EC eNOS KI mice expressed eNOS at the same level as WT mice. Western blot analysis showed a lack of eNOS in aorta, heart, and liver of EC eNOS KO and CondKO mice, while a very low expression of eNOS was detected in kidney and lung of EC eNOS KO mice, but not in CondKO mice, due to the presence of eNOS in non-ECs. EC eNOS KI mice showed eNOS in all tissues at the same level as WT mice as assessed by Western blotting as well as by ELISA and published in Leo et al. (Leo et al., 2021). Moreover, tamoxifen induced downregulation of eNOS expression in the kidney. RBC eNOS KO mice showed the lack of eNOS specifically in RBCs as assessed

by Western blot of ghosts, immunoprecipitation of eNOS from RBCs, and immunotransmission electron microscopy analysis in RBCs, while RBC eNOS KI mice showed a preserved eNOS expression. Moreover, eNOS was detected by Western blot in aorta, kidney, heart, lung, and liver lysates of RBC eNOS KO mice at the same level as WT mice, but not in RBC eNOS KI mice, which are phenotypically global eNOS KO. The results show that the deletion/reactivation of eNOS from/in ECs or RBCs was cell-specific and successful.

3. In the third part of this study, the role of eNOS in ECs and RBCs for kidney function was investigated. The results show that EC eNOS modulates sodium excretion and GFR. Specifically, after salt and volume challenge, lack of eNOS in ECs caused a reduction in sodium and urine excretion at baseline, while its reactivation preserved the phenotype in EC eNOS KI mice after Ang II treatment. The reactivation of eNOS specifically in ECs rescued the GFR in EC eNOS KI mice after Ang II infusion.

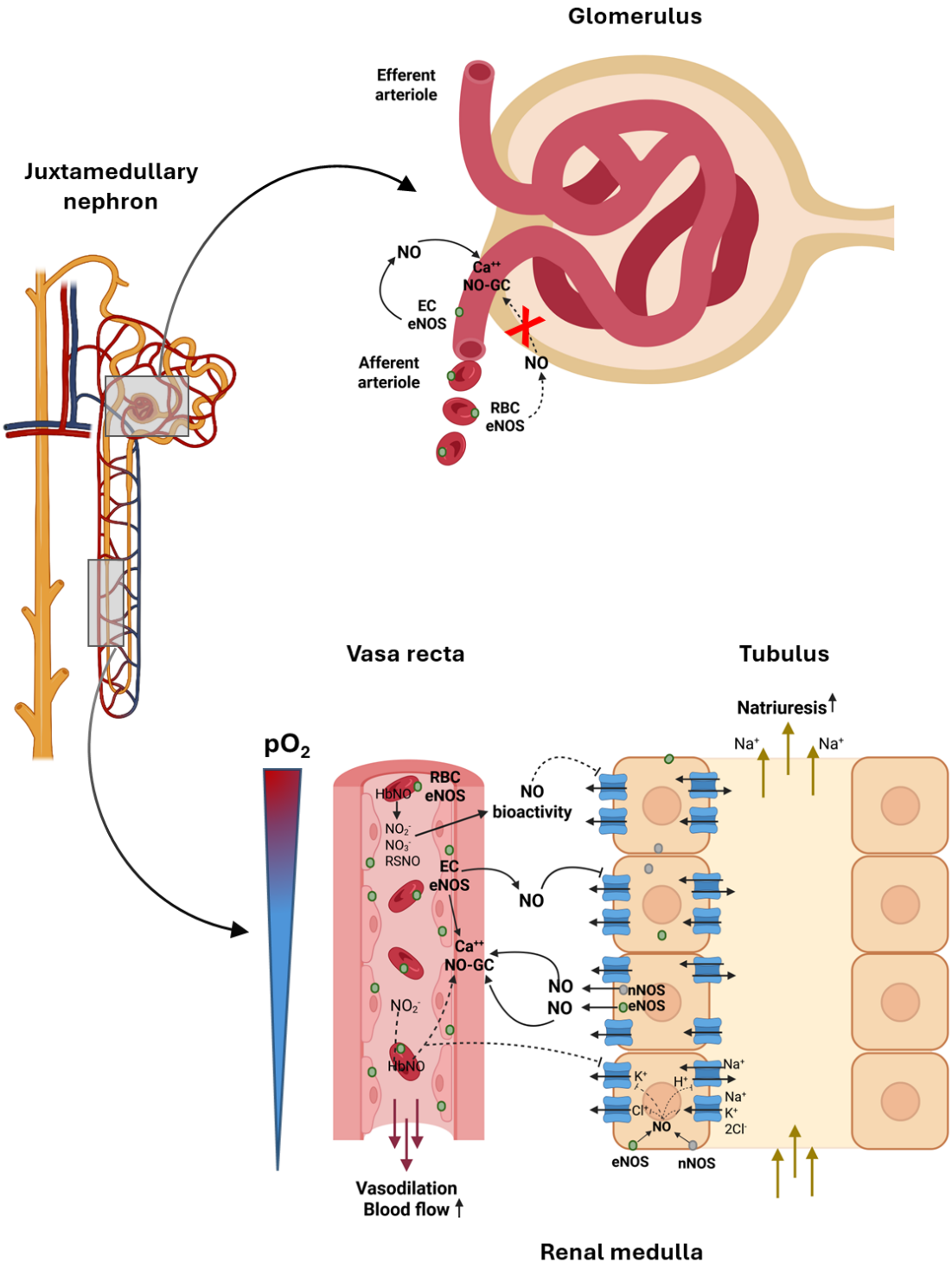

Figure 43 - Role of EC and RBC eNOS in kidney function.

1) After salt and volume challenge, the lack of eNOS in ECs leads to a decrease in sodium and urine excretion at baseline. 2) Reactivation of eNOS specifically in ECs preserves sodium excretion in global eNOS KO mice after Ang II treatment. 3) The reactivation of eNOS specifically in ECs rescued the GFR in global eNOS KO mice after Ang II infusion. 4) RBC eNOS does not regulate GFR, while its role in sodium and urine excretion needs to be further investigated (direct interactions indicated by dashed lines).

5.1. Part 1: Reactivation of eNOS in all cells of CondKO mice rescues vascular function and blood pressure: a proof of concept

The aim of this part of the study was to test the effects of reactivation of eNOS in global eNOS KO mice as proof of concept to verify that $eNOS^{inv/inv}$ = CondKO construct was efficient for reactivating eNOS expression. Moreover, gene dosage was also investigated.

To this aim, $eNOS^{inv/inv}$ mice were crossed with $DelCre^{pos}$ mice, expressing Cre recombinase in all cells. Three different genotypes were generated, depending on how many alleles expressed eNOS: $eNOS^{fl/fl}$ mice, which are homozygous eNOS KI mice; $eNOS^{fl/inv}$ mice, which are heterozygous eNOS KI mice; and $eNOS^{inv/inv}$ mice, which are global eNOS KO mice. These results were published in LoBue et al. (LoBue et al., 2024).

To test the efficiency of the reactivation of eNOS in all cells, the protein levels of eNOS in aorta were investigated by Western blotting. The expression of eNOS in $eNOS^{fl/fl}$ mice was found to be comparable to WT mice. Specifically, the quantification of protein levels of eNOS showed that heterozygous $eNOS^{fl/inv}$ and homozygous $eNOS^{fl/fl}$ mice had comparable levels of eNOS expression as compared to WT ($eNOS^{flox/flox}$) mice. Previously, heterozygous eNOS KI mice generated by Huang showed a 48 ± 13% of eNOS protein levels in lung lysates as compared to WT control mice (n = 3) (Fagan et al., 1999). Accordingly, cardiac tissue homogenates from heterozygous eNOS KI mice generated by Shesley showed a reduction of eNOS protein levels of 50% as compared to WT mice (4-6 mice for each group). These different findings may be due to the different strains and tissues investigated, and the smaller sample size used as compared to this thesis.

Moreover, homozygous $eNOS^{fl/fl}$ and heterozygous $eNOS^{fl/inv}$ mice also showed a fully preserved EDR in response to ACh and endothelium-independent vasorelaxation in response to SNP, as well as a decreased contractile response to PE, while $eNOS^{inv/inv}$ mice showed a lack of vascular function. This was consistent with previous reports showing that eNOS KO mice exhibited no response to ACh-treatment in aortic rings (Huang et al., 1995), as well as no dilatory response to shear stress following occlusion of the iliac artery (Erkens et al., 2015). Moreover, heterozygous eNOS KI mice showed a preserved endothelial-dependent vasodilation and vasoconstriction responses to serotonin and PE (Kojda et al., 1999; Kojda et al., 2001). These results showed that heterozygous eNOS KI compensates for the lack of eNOS, preserving vascular function.

The decreased blood pressure in homozygous $eNOS^{fl/fl}$ mice was consistent with the reactivation of eNOS in the whole body as well as with the preserved vascular function. Indeed, while the founder $eNOS^{inv/inv}$ mice were hypertensive, the $eNOS^{fl/fl}$ mice showed normotension. Moreover, even the reactivation of eNOS in a single allele was sufficient to

completely rescue the hypertensive phenotype, as the blood pressure levels of the heterozygous eNOS$^{fl/inv}$ mice were not different from the homozygous eNOS$^{fl/fl}$ or the WT (eNOS$^{flox/flox}$) mice. These findings are in agreement with the global eNOS KO strains generated in the past, which showed to have high blood pressure (Huang et al., 1995; Shesely et al., 1996; Godecke et al., 1998). Moreover, studies carried out on global eNOS KO mice demonstrated that under basal conditions, heterozygous eNOS KO mice have a blood pressure similar to that of WT mice (Kojda et al., 1999; Kojda et al., 2001). Taken together, the reactivation of eNOS only in one allele rescued the hypertensive phenotype of eNOS KO mice.

Several global eNOS KO mouse strains have been generated in the past, but to the best of my knowledge, this was the first time that exon 2 of the *NOS3* genome was targeted. One of the earliest eNOS KO strains was developed by Huang, in which the HindIII–SalI fragment containing the exons that encode the NADPH ribose and adenine binding sites was replaced (Huang et al., 1995). Another strain was the one generated by Shesely (now available from Jackson Laboratory, JAX stock #002684), where exon 12 of the *eNOS* gene was targeted, disrupting the calmodulin-binding site (Shesely et al., 1996). Gödecke's strain involved deletion of exons 24 and 25, which encode the essential NADPH binding domain (Godecke et al., 1998). Additionally, Morishita generated a strain in which all three NOS isoforms (eNOS, nNOS, and iNOS) were disrupted; this was achieved by crossing the Huang strain with nNOS KO and iNOS KO mice (Morishita et al., 2005).

The eNOS$^{flox/flox}$ and eNOS$^{inv/inv}$ mouse models described in this thesis offer a distinct advantage. By targeting exon 2, neither the eNOS$^{\Delta}$ allele (resulting from Cre-mediated deletion in eNOS^{flox}) nor the eNOS^{inv} allele leads to the production of a coding mRNA or truncated protein. This is particularly important because some eNOS KO strains, such as the commercially available model from Jackson Laboratory, produce a ~70 kDa truncated eNOS protein, which may cause unspecific or misleading phenotypes like the formation of dominant-negative complexes that interfere with proteins targeting the N-terminal region of eNOS.

The first time that the Cre/loxP system was used for gain-of-function studies was in 2002, when point mutations in the CREB-binding domain were introduced in bacteria and stem cells (Z. Zhang et al., 2002). However, not always gene reactivation by the Cre/loxP system led to successful results. As reported in literature, the generation of two CondKO mice for the Impad1 and Clcn7 genes caused a severe lethal phenotype due to the synthesis of non-functional protein (Capulli et al., 2019). Contrary, this study showed that the reactivation of eNOS in all cells was successful.

In summary, the characterization of the CondKO model, as well as the homozygous and heterozygous eNOS KI mice, showed that the reactivation of eNOS in all cells by the use of the Cre/loxP system was successful. Moreover, eNOS expression and function exhibit a clear dosage effect, as the reactivation of eNOS only in one allele is sufficient to compensate for lack of eNOS and to rescue vascular function and blood pressure (data published in (LoBue et al., 2024)).

5.2. Part 2: Characterisation of eNOS expression in gene targeted eNOS KO and KI mice

The results show that the deletion/reactivation of eNOS from/in ECs or RBCs by using the Cre/loxP system was cell-specific and successful.

5.2.1. EC eNOS KO and KI mice

To characterize the changes in eNOS expression in targeted and non-targeted tissues of the Cre-positive mice as compared to the Cre-negative littermates, tissues from EC eNOS KO and their WT control mice were analysed by real-time PCR, real-time RT-PCR, and immunoblotting. Real-time PCR analysis carried out on DNA extracted from aorta showed DNA recombination only in EC eNOS KO mice and not in WT littermates. Real-time RT-PCR showed a lack of mRNA expression of eNOS in EC eNOS KO mice in aorta (see results §4.3) and heart (Cortese-Krott et al., 2022). Accordingly, Western blot analysis of aorta, heart, and liver lysates of EC eNOS KO mice showed a complete lack of eNOS. Previously, other studies suggested the presence of eNOS in human and murine cardiomyocytes and cardiac fibroblasts as assessed by using respectively co-immunoprecipitation (Feron et al., 1996), and immunoblotting and NOS activity assay (R. S. Smith, Jr. et al., 2005; Kazakov et al., 2013). Thus, the lack of eNOS in the heart lysates of EC eNOS KO mice was unexpected.

In the kidney, eNOS mRNA was still partially expressed in EC eNOS KO mice as compared to WT mice, but it was significantly (2.5-fold) downregulated. However, in these models, the use of tamoxifen for gene modification showed non-specific effects as it induced downregulation of eNOS expression in the kidney in WT mice. According to the eNOS mRNA expression in the kidney, Western blot analysis also showed eNOS protein levels in kidney lysates of EC eNOS KO mice, but significantly lower than in WT mice. Contamination derived from non-ECs may confound the characterization of EC eNOS KO mice. In fact, in the kidney, eNOS is not only expressed in the vasculature of the vasa recta and glomerula, but also in the tubular epithelial cells of the proximal tubule, the inner medullary collecting duct (IMCD), and the TAL of the loop of Henle (Wu et al., 1999; Plato et al., 2000; Baines

& Ho, 2002). Similarly, Western blot of lung lysates from EC eNOS KO mice showed a low expression of eNOS. In the lung, eNOS is expressed in ECs of pulmonary arteries and veins the most, but it is also expressed in the airway, specifically in the bronchiolar and alveolar epithelial cells (Shaul et al., 1994; Giaid & Saleh, 1995). Thus, the faint bands indicating the presence of eNOS in the immunoblotting of kidney and lung lysates of EC eNOS KO mice are likely due to the expression of eNOS also in other cell types.

The same kind of characterization was carried out in EC eNOS KI mice and CondKO littermates. Real-time PCR performed on DNA extracted from aorta showed DNA recombination only in EC eNOS KI and not in the CondKO littermates. Real-time RT-PCR showed mRNA eNOS expression in aorta and kidney lysates of EC eNOS KI mice at the same level as WT mice. Accordingly, heart, aorta, lung, liver, and kidney showed preserved protein levels of eNOS in EC eNOS KI mice as assessed by Western blotting as well as by ELISA (published in (Leo et al., 2021)). Contrary, CondKO mice completely lack eNOS in the same tissues as assessed by real-time RT-PCR and Western blotting.

Taken together, these results show that the deletion or reactivation of eNOS in ECs was cell-specific and successful.

5.2.2. RBC eNOS KO and KI mice

RBC eNOS KO mice were also characterized by real-time PCR and Western blotting. Real-time PCR analysis carried out on DNA extracted from bone marrow showed DNA recombination only in RBC eNOS KO mice and not in the WT control mice. Immunoprecipitation of eNOS from RBCs as well as Western blot of ghosts and immunotransmission electron microscopy of RBCs showed a lack of eNOS in RBC eNOS KO mice as compared to WT littermates.

The potential off-target effects of Cre recombinase were also analyzed in these mice. Real-time RT-PCR of kidney lysates, as well as Western blotting of aorta, kidney, heart, liver, and lung lysates, showed a preserved eNOS expression in RBC eNOS KO mice at the same level as WT mice. Off-target effects of gene-targeted recombination are sometimes found in constitutive models generated by the Cre/loxP system. These are caused mainly by recombination at cryptic/pseudo-loxP sites, and overexpression of Cre recombinase (Thyagarajan et al., 2000; Loonstra et al., 2001). This is also the reason why tamoxifen-inducible models were chosen for EC eNOS KO and KI mice. Importantly, in these constitutive mouse models described here, no evidence of such off-target effects was observed, suggesting that Cre recombinase activity was specific and well tolerated.

The same characterization was carried out in RBC eNOS KI mice, which showed DNA recombination in DNA extracted from bone marrow and lack of eNOS expression in aorta, kidney, heart, lung and liver lysates as assessed by Western blotting, while eNOS was present specifically in RBCs as assessed by immunoprecipitation of eNOS from RBCs and immunotransmission electron microscopy.

The characterization of eNOS expression in RBCs of RBC eNOS KO mice is challenged by the expression of eNOS also in other cell types like ECs and WBCs, which may contaminate the RBCs and confound the characterization. To avoid this, RBCs from RBC eNOS KO and KI mice were cleaned from WBC contamination before performing immunoprecipitation of eNOS. Also erythroid cells ($Ter119^+$) used for mRNA expression analysis were isolated from the bone marrow of RBC eNOS KI mice and cleaned from WBC contamination, as published in Leo et al. (Leo et al., 2021). These considerations highlight the importance of the cell-type isolation in order to reliably determine the role of eNOS in the targeted compartment.

All together, these results demonstrate that the generation of EC or RBC-specific eNOS KO and KI models by using the Cre/loxP system was successful.

To conclude, the combined use of KO and KI models allows the precise distinction of the role of eNOS in ECs, RBCs, or in other cell types. Moreover, EC eNOS KO mice clearly revealed the presence of eNOS in non-ECs, allowing the possibility to “unmask” the effect of eNOS in non-ECs. Furthermore, the preserved expression of eNOS in other cell types confirms the specificity and validity of the genetic targeting strategy.

5.2.3. eNOS in ECs and RBCs contribute to blood pressure regulation and to the levels of systemic NO metabolites

EC eNOS KO mice showed a significant increase in blood pressure as compared to their relative WT littermates. Additionally, the reactivation of eNOS specifically in ECs of CondKO mice rescued the phenotype. It is very well known that eNOS is tightly regulated in resistance vessels, which regulate blood pressure through their control of vascular resistance. Previous studies showed the crucial role of eNOS in blood pressure regulation by using only global eNOS KO mice or pharmaceutical inhibitions of eNOS (Rees et al., 1990; Huang et al., 1995; Shesely et al., 1996; Godecke et al., 1998). By knocking out eNOS specifically in ECs, for the first time, it was possible to confirm the specific role of EC eNOS in blood pressure regulation.

Surprisingly, RBC eNOS KO mice also showed a hypertensive phenotype, which was rescued by the reactivation of eNOS specifically in RBCs. It was previously demonstrated

that RBCs also carry an active eNOS, which contributes to the regulation of systemic blood pressure (Cortese-Krott et al., 2012; Wood et al., 2013). With this study, for the first time, it was shown that eNOS in RBCs plays an independent role in the regulation of blood pressure, challenging the traditional view that only EC eNOS is crucial for blood pressure regulation (Leo et al., 2021).

The data presented in this study showed that the total amount of NO metabolites was decreased in plasma, lung, and heart of EC eNOS KO mice, as well as the circulating nitrite and nitrate in plasma. Nitrate was instead increased in liver, confirming the observation that the liver may act as a reservoir of nitrate (Eriksson et al., 2018). A similar phenotype was observed in the CondKO mice, supporting previous observations done using global eNOS KO mice (Erkens et al., 2018). On the other hand, RBC eNOS KO mice showed decreased nitrite and nitrate in plasma, and increased nitrite only in the aorta. NO-heme concentrations were fully preserved in EC eNOS KO mice, while they were significantly lower in RBC eNOS KO mice. Moreover, RBC eNOS KI mice did not show any alteration in NO-Heme levels.

From these observations, it is clear that both ECs and RBCs eNOS contribute to regulating the systemic NO metabolite levels, but in different ways. While EC eNOS is the major contributor to the overall amount of NO metabolites in the tissues, RBC eNOS is a necessary source of NO bound in RBCs (these results were published in (Leo et al., 2021)).

5.3. Part 3: Characterisation of kidney function in gene targeted mice

In this part of the study, the aim was to characterize the kidney function of the mouse lines as compared to the Cre-negative littermates. For this purpose, basal sodium and urine excretion and after salt and volume challenge as well as GFR were investigated before and after Ang II treatment in EC eNOS KO and KI mice and in RBC eNOS KO and KI mice and their respective Cre-negative control littermates.

Ang II plays a key role on blood pressure regulation by multiple mechanisms: direct vasoconstrictor effect on arterioles, renal effects such as stimulating sodium and water retention and aldosterone secretion, activation of the sympathetic nervous system, which leads to an increase in HR and contractility, and promoting structural changes in blood vessels and heart, such as hypertrophy and fibrosis (J. C. Li et al., 2023; Nadasy et al., 2024; Triebel & Castrop, 2024).

The interplay between Ang II and NO in renal function regulation is very complex but necessary to maintain renal hemodynamic stability. In this part of the study, Ang II was used

to challenge the kidney to “unmask” a potential role of eNOS in ECs and/or in RBCs in renal function. Previous studies investigating the role of Ang II in mice lacking eNOS were carried out on global eNOS KO mice, showing an exacerbation of the hypertensive phenotype after low dose (10 ng/min) and high dose (25 ng/min) of Ang II (Whiting et al., 2013). For the first time, this study focused instead on the interaction between Ang II and EC or RBC eNOS-derived NO by using cell-specific eNOS KO mice models, which allowed for a better understanding of the specific role of eNOS in ECs and RBCs.

5.3.1. Analysis of Ang II effect on heart weight index

When the preload (blood volume) and/or afterload (blood pressure) increase, the heart undergoes compensatory hypertrophy in order to maintain the cardiac output stable and reduce the wall stress (Caturano et al., 2022). Ang II plays a significant role in cardiac hypertrophy via the combination of direct effect on cardiomyocytes and the elevation of blood pressure (Geisterfer et al., 1988; Dostal & Baker, 1992; Crowley et al., 2006; Xu et al., 2010). Thus, the effect of Ang II on the heart weight index (a parameter for increased heart size) was investigated here.

EC and RBC eNOS KO mice, as well as tamoxifen-treated and untreated CondKO mice, exhibit hypertension. Additionally, Ang II was used to challenge the kidney and allow for investigation of renal function in all the mouse models. Thus, the heart weight index of all the cell-specific eNOS KO and KI mice was investigated at baseline and after the treatment with Ang II.

WT mice treated with tamoxifen showed a lower heart weight index as compared to untreated WT mice at baseline. Similarly, a previous study showed that subcutaneous treatment with tamoxifen for 12 weeks inhibited cardiac hypertrophy in ovariectomized spontaneously hypertensive rats (Pelzer et al., 2005). Moreover, oral treatment with tamoxifen had a beneficial effect on both isoproterenol and partial abdominal aortic constriction-induced cardiac hypertrophy in Wistar rats (Patel et al., 2014). After treatment with Ang II, the treated and untreated WT mice did not show any difference, as Ang II increased the heart weight index of the tamoxifen-treated WT mice only. Tamoxifen-treated CondKO mice did not show any difference in heart to body weight ratio as compared to the untreated group. However, Ang II led to an increase in heart weight index only in tamoxifen-treated CondKO mice. These data show that Ang II led to an increase in heart weight index only in the presence of tamoxifen, which is not dependent on eNOS. Moreover, CondKO mice treated with tamoxifen had a higher heart weight index as compared to tamoxifen-treated WT mice at baseline, but not after Ang II infusion.

EC eNOS KO mice showed the same heart weight index as compared to WT mice at baseline and after Ang II treatment. Moreover, at baseline, they did not show changes in cardiac output, stroke volume, HR, ejection fraction, and fractional shortening as compared to WT mice, as assessed by echocardiography and published in Cortese-Krott et al. (Cortese-Krott et al., 2022). However, Ang II caused an increase in heart weight index only in WT mice. However, the reactivation of eNOS specifically in ECs did not rescue the phenotype in CondKO mice. Moreover, also in this case, left ventricular function was unchanged in EC eNOS KI mice as compared to CondKO mice (Cortese-Krott et al., 2022).

WT and CondKO mice not treated with tamoxifen showed the same heart to body weight ratio at baseline and after Ang II treatment. Similarly, a previous study showed that 18-23 week old global eNOS KO mice showed the same heart weight index as compared to age-matched WT mice. The difference in the ratio significantly increased with age, as both 27-30 week old and 40 week old global eNOS KO mice showed higher heart weight index as compared to the respective age-matched WT mice (Flaherty et al., 2007). In the present study, 4-6 month old mice were used for comparison, corresponding to the 18-23 week old group examined in the previous study.

RBC eNOS KO mice did not show any difference in heart weight index as compared to WT control mice with/without Ang II. Moreover, both RBC eNOS KO and WT mice showed similar cardiac output, stroke volume, HR, ejection fraction, and fractional shortening as assessed by echocardiography and published in Cortese-Krott et al. (Cortese-Krott et al., 2022). Furthermore, Ang II did not affect the heart to body weight ratio in both groups. Surprisingly, RBC eNOS KI mice showed a lower heart to body weight ratio as compared to CondKO mice at baseline, but the same left ventricular function (Cortese-Krott et al., 2022). However, Ang II did not affect the heart to body weight ration in both RBC eNOS KI and CondKo control.

Taken together, these data show that Ang II leads to an increase in heart weight index in the presence of tamoxifen, which is not dependent on eNOS. However, to define this phenotype as cardiac hypertrophy, further investigations on other key parameters like molecular markers (e.g., atrial natriuretic peptide (ANP), brain natriuretic peptide (BNP), and β-myosin heavy chain (β-MHC)), and functional assessment via echocardiography or pressure-volume loop analysis are needed (Coelho-Filho et al., 2013; Erkens et al., 2015; Sarzani et al., 2022).

5.3.2. Analysis of the off-target effects of tamoxifen on sodium and urine excretion

EC eNOS KO and KI models are transient, and treatment with tamoxifen (75 mg/kg) was necessary to induce the targeted gene modification. However, tamoxifen may have off-target effects. In fact, it was shown that estrogens have effects in regulating water and salt balance, which can vary depending on physiological condition, dosage, and duration (Brunette et al., 2001; X. Zhang et al., 2019). Therefore, the role of tamoxifen per se on sodium and urine excretion was investigated in WT and CondKO mice.

The results showed that tamoxifen does not have an effect on sodium excretion under a regular sodium intake. In fact, tamoxifen-treated WT mice showed the same basal sodium excretion as compared to the untreated WT group, both before and after Ang II treatment. Also CondKO mice showed unchanged basal sodium excretion when treated with tamoxifen before and after Ang II infusion. Similarly, tamoxifen did not have any effect on sodium excretion after salt and volume challenge, both before and after Ang II treatment in WT and CondKO mice. Previous studies showed that treatment with tamoxifen at doses of 25 mg/kg and 50 mg/kg ameliorated the lithium-induced natriuresis in rats with nephrogenic diabetes insipidus, likely due to the attenuation of the decrease in βENaC and γENaC expression in the cortical and outer medullary collecting ducts (Tingskov et al., 2018). The doses of tamoxifen used (25 mg/kg and 50 mg/kg) are both smaller than the one used in the present study (75 mg/kg). However, it is important to note that this happened in a pathological context, not a physiological condition, as tamoxifen was used as a therapeutic approach against lithium-induced natriuresis in rats, while in the present study, tamoxifen was used to induce gene-targeted recombination. Importantly, in the study carried out by Tingskov and colleagues, the tamoxifen effect on sodium excretion was studied during administration, while in this thesis all the experiments, and therefore the investigation of the tamoxifen effects, were performed 21 days after the end of the tamoxifen treatment. The unchanged sodium excretion in basal condition and after sodium challenge both before and after Ang II treatment in WT and CondKO mice shows that tamoxifen does not influence natriuresis.

Tamoxifen did not have any effect on water handling in basal conditions, both before and after Ang II treatment, as there were no differences between treated and untreated WT mice, as well as between treated and untreated CondKO mice in physiological conditions.

Conversely, tamoxifen affected water handling after sodium and volume challenge. In fact, WT mice treated with tamoxifen showed a significantly higher urine excretion before Ang II treatment as compared to the untreated control group. However, CondKO mice did not show any difference in urine excretion as compared to the untreated group, both before and

after Ang II treatment. These results show that the effect of tamoxifen may be eNOS-dependent. These findings are in contrast with previous studies showing that estrogens like estradiol or tamoxifen reduced urine output by decreasing mRNA and protein expression of aquaporin 2 in the collecting duct of ovariectomized female rats or of male rats with lithium-induced nephrogenic diabetes insipidus, respectively (Cheema et al., 2015; Tingskov et al., 2018). However, as discussed above, in this case, the tamoxifen effect on urine excretion was investigated during administration and in a pathological context, which is a condition different from the one investigated here.

Taken together, tamoxifen had no effect on sodium excretion. However, it increased urine excretion in WT mice following salt and volume challenge, but only before Ang II treatment.

5.3.3. EC eNOS modulates sodium and urine excretion

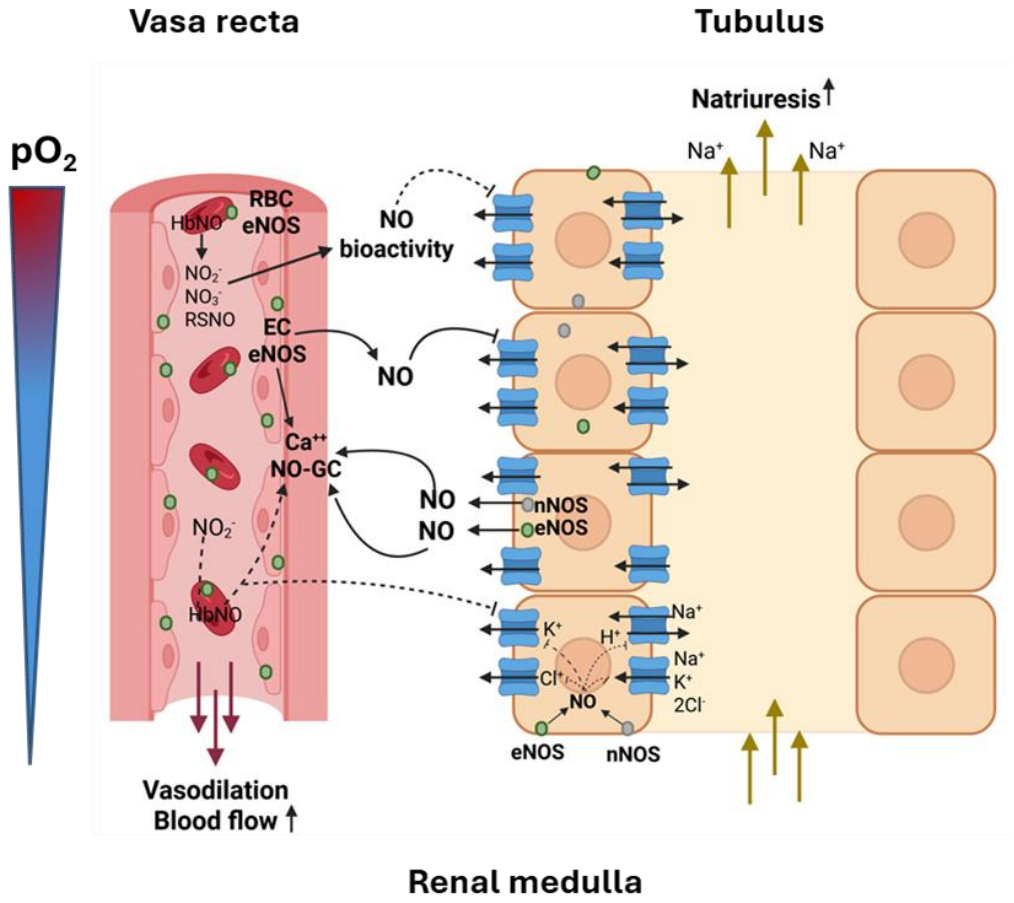

Figure 44 - EC eNOS modulates sodium and urine excretion.

The lack of eNOS in ECs led to decreased sodium and urine excretion after challenging the kidney with high salt and volume load. The reactivation of eNOS specifically in ECs preserved the sodium

excretion in global eNOS KO mice after Ang II treatment. Dashed lines indicate direct interactions that need further investigaions.

In this part of the study, the role of EC eNOS in sodium excretion was investigated at basal conditions and after challenging the kidney with high salt and volume load, before and after Ang II treatment.

In order to first understand the general role of eNOS in sodium excretion, WT and CondKO mice were analysed. For this comparison eNOS$^{flox/flox}$ Cdh5-Cre/ERT2^{neg} + TAM (WT) and eNOS$^{inv/inv}$Cdh5-Cre/ERT2^{neg} + TAM (CondKO) mice were used. CondKO mice showed the same basal sodium excretion as compared to WT mice. Moreover, Ang II treatment did not affect sodium excretion in both WT and CondKO mice as compared to baseline. NO has an important role in sodium and water handling as a result of inhibition of sodium reabsorption along the nephron (Mattson et al., 1994; Schneider et al., 2008; Carlstrom, 2021). It was shown that Ang II has a biphasic effect on the sodium handling *ex vivo*; in fact, at picomolar concentration it stimulates the reabsorption of sodium, while at nanomolar concentration it inhibits its reabsorption (Banday et al., 2011). Specifically, Ang II at a concentration between 10^{-13} M and 10^{-11} M stimulates Na^+-K^+-ATPase activity in isolated rat proximal tubule, while at a concentration above 10^{-10} M, the production of NO by enzymatic activation is triggered, leading to the inhibition of the Na^+-K^+-ATPase activity. (C. Zhang et al., 2001). Previously, it was shown that global eNOS KO mice from Jackson Laboratory (Shesley's strain) had a similar 24-hour urinary sodium excretion as compared to C57BL/6J mice after regular-salt intake (0.4% NaCl) (Kopkan et al., 2010). Additionally, chronic infusion of Ang II (25 ng/min) *in vivo* led to decreased sodium excretion in WT mice, while all the global eNOS KO mice died. On the other hand, a lower dose of Ang II (10 ng/min) did not cause any changes in urinary sodium excretion in WT mice as well as in global eNOS KO mice (Whiting et al., 2013). Considering a body weight of 30 g, these doses correspond to 833 ng/kg/min and 333 ng/kg/min, respectively. In the present study, the dose of Ang II used was of 500 ng/kg/min, which may explain the regular sodium excretion in both CondKO and WT mice after Ang II infusion.

Analysis of overnight excretion of sodium in urine showed that EC eNOS KO mice had the same urinary sodium concentration as WT mice at baseline and after treatment with Ang II. This demonstrates that eNOS in ECs does not regulate sodium excretion under regular sodium intake conditions. Consistent with these results, the reactivation of eNOS specifically in ECs did not affect the urinary sodium concentration before and after Ang II,

as EC eNOS KI and the CondKO littermates showed the same sodium concentration levels in urine after overnight collection.

The role of eNOS on basal urine excretion was also investigated in WT and CondKO mice before and after Ang II treatment. WT and CondKO mice showed the same urine excretion before and after Ang II treatment. Moreover, Ang II did not have any effect on urine excretion in both EC eNOS KO and WT mice as compared to baseline. Conversely, a previous study showed that C57BL/6J mice had increased 24-hour urine output after 7 days of Ang II treatment (1.6 µg/kg/min) by subcutaneous minipumps (C. C. Chen et al., 2010). This can be explained by taking into account that high concentrations of Ang II activate the AT_2 receptors (Angiotensin II receptor type II), which counterbalance the antinatriuresis and pressor effects of Ang II via stimulation of eNOS and activation of the NO/sGC signalling (Siragy et al., 1999; Fatima et al., 2021). Here, the lack of compensatory response to Ang II in WT mice may be due to the lower dose of Ang II used (500 ng/kg/min vs. 1.6 µg/kg/min). Furthermore, Ang II treatment did not affect the urine excretion in either tamoxifen-treated or untreated CondKO mice.

EC eNOS KO mice showed similar urine excretion as WT mice at both baseline and after Ang II. Moreover, EC eNOS KI mice had the same urine excretion as CondKO mice, both with/without Ang II. This suggests that, at low doses of Ang II, eNOS in ECs is not involved in the regulation of water handling.

The role of eNOS in sodium excretion was also investigated after salt and volume challenge. CondKO ($eNOS^{inv/inv}$Cdh5-Cre/$ERT2^{neg}$ + TAM) mice showed the same sodium and urine volume excretion as WT ($eNOS^{flox/flox}$ Cdh5-Cre/$ERT2^{neg}$ + TAM) mice. Previously, eNOS KO mice treated with a high salt diet (4%) for two weeks showed similar sodium excretion as WT mice treated with the same diet (Kopkan et al., 2010). Contrary, previous studies showed that the inhibition of NOS by intravenous infusion of L-NAME at one dose (0.1, 1.0, 10.0 and 50.0 µg/kg/min) in rats as well as 30 minutes infusion of L-NA (0.4 mL/min, pH 6.8) in dogs led to a decrease in sodium excretion and fluid volume (Lahera et al., 1991; Majid et al., 1993). However, this is an acute effect of a pharmaceutical inhibition of NOS, which may have different outcomes than an eNOS KO mouse model.

At baseline, lack of eNOS in ECs led to a significant decreased sodium excretion in urine as compared to WT mice, while Ang II did not have any effect in both groups. Similarly, nephron-specific eNOS KO mice treated with 1.5 mL saline (i.p.) had lower sodium excretion at the fourth hour, as compared to WT mice (Gao et al., 2018). This result might be explained by the evidence that eNOS-derived NO affects the activity of NKCC2 in the TAL of the loop of Henle and the NCC in the distal convoluted tubule (Gao et al., 2018;

Carlstrom, 2021). The results in the present study also show that eNOS in ECs contributes to modulating sodium excretion when the kidney is challenged with high salt intake.

Furthermore, EC eNOS KO mice also showed a decreased urine excretion as compared to WT mice before Ang II treatment. A previous study showed that eNOS KO mice (Shesely's strain) had a significantly lower urine excretion after a high volume load. Moreover, the treatment with the loop diuretic bumetanide abolished the difference between eNOS KO and WT mice, suggesting that eNOS expressed in the TAL of the loop of Henle was primarily involved (Perez-Rojas et al., 2010). In the present study, the lack of eNOS specifically in ECs caused a reduced urine excretion, demonstrating again the important role of eNOS in ECs in modulating urine excretion.

As discussed above, tamoxifen treatment led to an increase in urine excretion in WT mice. Contrary, EC eNOS KO mice showed a significantly decreased urine excretion as compared to WT control mice, indicating that this phenotype is not a tamoxifen artifact, but rather due to the lack of eNOS in ECs.

EC eNOS KI mice showed no difference in basal sodium and urine excretion as compared to the CondKO littermate mice, before and after Ang II. Similarly, also after salt and volume challenge EC eNOS KI mice and CondKO littermates showed the same sodium and urine excretion, both before and after Ang II. However, Ang II had a weak effect only in CondKO mice, as they showed a decreased sodium excretion as compared to baseline (significant only if the Sidak t-test was carried out with correction for multiple comparisons). Instead, urine excretion was unchanged in CondKO mice before and after Ang II. These results show that the reactivation of eNOS specifically in ECs preserved the phenotype of global eNOS KO mice.

Taken together, all the results showed that eNOS in general does not regulate sodium excretion under regular sodium intake conditions. However, when the kidneys are challenged with a high salt and volume load, eNOS in ECs contributes to modulating sodium handling.

5.3.4. Effect of tamoxifen on GFR

The effect of tamoxifen on GFR was investigated in WT and CondKO mice. Tamoxifen did not affect GFR in WT mice at baseline. However, after administration of Ang II, only the tamoxifen-treated WT mice showed a significant increase in GFR as compared to baseline, but there were no differences between treated and untreated groups.

While, to the best of my knowledge, there are no direct studies about the impact of tamoxifen on GFR, there are evidences about its antifibrotic effect, which can ameliorate kidney injury like albuminuria, chronic nephropathy, glomerulosclerosis, and interstitial fibrosis by the activation of estrogen receptors (Delle et al., 2012; H. Y. Ma et al., 2021; Tingskov et al., 2021), which are expressed in the tubular epithelial cells, ECs, mesangial cells and podocytes of the kidney (Irsik et al., 2013; Cheema et al., 2015). However, sex can be an important variable to take into consideration. In fact, a previous study showed that tamoxifen treatment to induce DNA recombination, attenuated fibrosis in female obstructed mouse kidney, but not in males (Falke et al., 2017). Previous studies suggested that treatment of porcine coronary arteries with tamoxifen modulates eNOS activity as shown by an elevated intracellular Ca^{++} in ECs and an increased phosphorylation at Ser-1177 (Leung et al., 2006). Additionally, tamoxifen induced dilation of bovine microvessels via Akt-dependent activation of eNOS (Florian et al., 2004). Whether this also has consequences on volume retention and blood pressure regulation needs to be investigated in future studies.

On the other hand, CondKO mice treated with tamoxifen had similar GFR as the untreated group at baseline. After Ang II treatment, both tamoxifen-treated and untreated CondKO mice showed a significant decrease in GFR as compared to the baseline, but no differences between the two groups. This result showed that tamoxifen did not have any effect on GFR in CondKO mice, suggesting that the increased GFR in WT mice after Ang II may be eNOS-dependent.

5.3.5. Lack of eNOS in ECs affects GFR

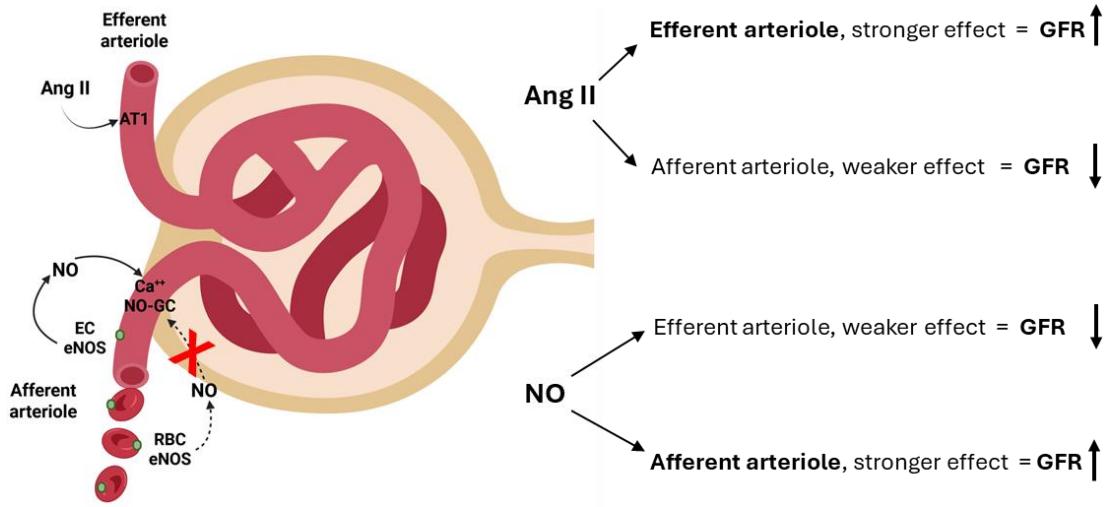

Figure 45 - EC eNOS regulates GFR.

Lack of eNOS in ECs did not affect GFR before and after Ang II treatment. Reactivation of eNOS specifically in ECs rescued the phenotype in global eNOS KO mice after Ang II treatment. RBC eNOS does not play a role in GFR regulation.

To investigate the role of eNOS in GFR regulation, tamoxifen-untreated CondKO ($eNOS^{inv/inv}$ $HbbCre^{neg}$) mice were compared to tamoxifen-untreated WT mice ($eNOS^{flox/flox}$ $HbbCre^{neg}$). CondKO mice showed a decreased baseline GFR as compared to WT mice. This finding is supported by previous studies in which GFR of global eNOS KO mice was significantly lower compared to the WT mice (Schnermann et al., 2001; Kanetsuna et al., 2007; Tao et al., 2023). In contrast, another group showed no changes in GFR of global eNOS KO mice as compared to WT controls (Wang et al., 2004). In this case, global eNOS KO mice from Jackson laboratory (Shesley's) were used, and GFR was measured in anesthetized mice by collecting plasma and urine after infusion with 0.75% FITC-inulin in the infusion solution (2.25% BSA in normal saline), and fluorescence in plasma and urine was detected. No changes in GFR can be explained considering that the method used is different from the one described here. Moreover, Jackson global eNOS KO strain shows an upregulation of nNOS, which may compensate for the lack of eNOS in the regulation of GFR.

Treatment with Ang II led to a decreased GFR in CondKO mice, but not in the WT mice, thus exacerbating the difference between the two groups. These results are consistent with previous studies, which proposed that endogenous Ang II contributes to the decrease in

GFR during an inhibition of NO production in rats (Takenaka et al., 1993). It was later demonstrated that blocking the AT1-receptor (Angiotensin II receptor type I) with Candesartan as well as ACE inhibition in mice led to a reduction of GFR of 80% in global eNOS KO mice, while this did not significantly affect the GFR in WT mice, suggesting that the total lack of eNOS affected the action of Ang II on GFR, possibly due to an enhanced responsiveness of the glomerular arterioles to the available Ang II (Schnermann et al., 2001). Based on these observations, the results in the present study show that eNOS plays a major role in GFR regulation.

To better understand the contribution of EC eNOS in the regulation of GFR, EC eNOS KO and KI mice and their Cre-negative littermate controls were used for measuring GFR at baseline. Moreover, by challenging the kidney with Ang II, the influence of the absence/presence of eNOS in ECs on the Ang II-dependent GFR regulation was investigated as well.

EC eNOS KO mice showed the same GFR as WT control mice at baseline. However, after the administration of Ang II, only the WT mice showed an increase in GFR. As already discussed, the increased GFR after Ang II treatment in WT mice is a tamoxifen artifact. Moreover, the lack of response to Ang II in EC eNOS KO mice confirmed the idea that the effect of tamoxifen on GFR after Ang II treatment is eNOS-dependent.

As already mentioned, CondKO mice showed a decreased GFR as compared to WT mice, but the reactivation of eNOS specifically in ECs did not rescue the phenotype, as EC eNOS KI mice showed the same GFR as compared to the CondKO littermates at baseline. Previously, Gao and colleagues showed that the nephron-specific deletion of eNOS was not associated with a change in GFR (Gao et al., 2018), thus suggesting that the impaired GFR in CondKO mice is due to the lack of eNOS in ECs and not to its lack in epithelial tubular cells. Accordingly, after the treatment with Ang II, only the CondKO mice showed a decreased GFR as compared to baseline, while in EC eNOS KI mice, GFR was preserved, demonstrating that the reactivation of eNOS specifically in ECs rescued the phenotype after challenging the kidney with Ang II. Thus, Ang II appears to “unmask” the role of eNOS specifically in ECs on GFR regulation. Moreover, in this case, tamoxifen had no further effect on GFR.

5.3.6. Lack of eNOS in RBCs does not affect sodium excretion and GFR

As already fully discussed, NO is a key molecule for the regulation of medullary blood flow and natriuresis in the kidney. Moreover, it was demonstrated that NO mediates the tubulovascular crosstalk in the renal medulla. In fact, NO produced in the tubulus by eNOS

and nNOS can diffuse to the vasa recta and activate the NO/sGC signalling in the pericytes to induce vasodilation and increase RBF (Dickhout et al., 2002). The hypothesis of this thesis is that NO produced by eNOS expressed in ECs of the vasa recta or in RBCs may diffuse to the tubule and induce natriuresis.

To better understand the role of RBC eNOS in natriuresis, basal sodium and urine excretion, as well as after salt and volume challenge, were investigated before and after Ang II. RBC eNOS KO mice showed the same basal sodium excretion as compared to WT mice before and after Ang II administration, and Ang II did not have any effect in both groups. Also RBC eNOS KI mice showed similar basal sodium excretion as compared to CondKO littermates, both before and after Ang II treatment. Moreover, Ang II had no effect on sodium excretion as both RBC eNOS KI and CondKO mice showed the same basal sodium excretion as compared to baseline. These results indicate that RBC eNOS is not involved in the regulation of sodium excretion under basal conditions. RBC eNOS KO mice and WT littermates showed the same urine excretion at baseline. Surprisingly, Ang II led to a decrease in urine excretion in RBC eNOS KO, but not in WT littermates. Moreover, RBC eNOS KI showed a lower urine excretion as compared to CondKO mice at baseline, but this difference was abolished after treatment with Ang II. However, Ang II did not affect urine excretion, as both RBC eNOS KI and Cond KO mice had unchanged urine excretion as compared to baseline. These results were unexpected and may depend on the limited sample size, which was due to the low breeding efficiency of this line, resulting in a limited number of offspring available for experimentation. Thus, this phenotype needs further investigation.

Similarly, after salt and volume challenge, RBC eNOS KO mice showed the same sodium and urine volume excretion as the WT control mice before and after Ang II treatment. Accordingly, RBC eNOS KI mice did not show any difference as compared to CondKO littermate mice.

Based on the data available, RBC eNOS is not involved in the regulation of sodium and urine excretion in basal conditions and after salt and volume challenge.

The role of RBC eNOS in GFR regulation was also investigated. Since the gene modification in these mouse models is constitutive, the investigation of the effect of age on GFR was also possible. For this purpose, the Cre-negative controls mice ($eNOS^{flox/flox}HbbCre^{neg}$ and $eNOS^{inv/inv}HbbCre^{neg}$) were first used. The results showed that age did not worsen GFR in both WT and CondKO mice. Moreover, age did not exacerbate the difference between CondKO and WT mice. Previously, the effect of NOS-inhibition was studied in spontaneously hypertensive rats, which were generated in the 1960s by breeding selected

hypertensive rats for six generations (Okamoto et al., 1963). This model had a further decline with aging when treated with a continuous infusion of L-NAME (500 µg/kg/min) (Kvam et al., 2000). To determine GFR, the rats were infused with ^{125}I-Na-iothalamate (0.5 µCi/ml) for clearance determination. However, another study showed that GFR, measured as clearance of ^{51}Cr- EDTA after a single injection, was decreased in C57BL/6J and in CBA/HT6J mice, but not in their B6CBAF hybrids with age, underlying the importance of the background/strain in the change of renal function during aging (Hackbarth et al., 1982).

To better understand whether RBC eNOS has a role in GFR and whether age may affect the GFR when eNOS is specifically lacking in RBCs, three different sets of RBC eNOS KO mice grouped by age (4-6 month old, 9-12 month old mice, and 21-31 month old) were investigated. Both RBC eNOS KO groups showed the same GFR as compared to age-matched WT littermate mice at baseline. Moreover, Ang II treatment in both 4-6 month old and 9-12 month old mice did not affect the GFR.

Accordingly, RBC eNOS KI mice did not show any difference as compared to CondKO mice at baseline. With Ang II treatment, 4-6 month old RBC eNOS KI and age-matched CondKO mice showed a significant decreased GFR as compared to baseline. However, only 9-12 month old RBC eNOS KI mice showed a significant decrease in GFR after Ang II treatment, while it was unchanged in age-matched CondKO mice.

Taken together, these results show that RBC eNOS is not involved in the regulation of GFR, as the lack of eNOS in RBCs did not impair GFR, and the reactivation of eNOS specifically in RBCs did not rescue the phenotype of CondKO mice. Furthermore, age does not play a role in the regulation of GFR in these mouse models.

6. Summary & Perspective

Overall, this study aimed to investigate the cell-specific role of eNOS in kidney function. The first goal was to verify that $eNOS^{inv/inv}$ = CondKO construct was efficient for reactivating eNOS expression in global eNOS KI mice as proof of concept and rescued the hypertensive phenotype of global eNOS KO mice. The analysis showed that the reactivation of eNOS can occur in only one allele ($eNOS^{fl/inv}$ mice) or in both alleles ($eNOS^{fl/fl}$ mice), but the expression of eNOS in both genotypes was at a similar level as WT mice. Moreover, $eNOS^{fl/fl}$ and $eNOS^{fl/inv}$ mice showed a fully preserved vascular function, which was instead impaired in $eNOS^{inv/inv}$ mice. Additionally, the reactivation of eNOS only in one allele was sufficient to rescue the blood pressure in CondKO mice, as both $eNOS^{fl/fl}$ and $eNOS^{fl/inv}$ mice were normotensive. These data were published in LoBue et al. (LoBue et al., 2024).

The second goal of this study was to characterize the expression of eNOS in targeted and non-targeted tissues of the mouse lines as compared to the Cre-negative littermates. The investigation of EC eNOS KO/KI mice and RBC eNOS KO/KI mice, as well as of the Cre-negative littermates, showed that eNOS was specifically deleted in ECs and RBCs of EC eNOS KO mice and RBC eNOS KO mice, respectively. Moreover, EC eNOS KI and RBC eNOS KI mice showed expression of eNOS only in ECs and RBCs, respectively. Furthermore, specific deletion or reactivation of eNOS in ECs or RBCs was specific and did not show any off-target effects.

EC eNOS KO and RBC eNOS KO mice were hypertensive, while the reactivation of eNOS specifically in ECs or RBCs rescued the hypertensive phenotype, as both EC eNOS KI and RBC eNOS KI mice were normotensive. These data demonstrate that EC eNOS and RBC eNOS independently regulate blood pressure. Additionally, this study showed that EC eNOS contributes to the level of systemic NO metabolites, but not of NO-Heme, which instead depends on the presence of eNOS in RBCs. These data were published in Leo et al. (Leo et al., 2021).

The third goal of this study was to investigate the role of eNOS expressed in ECs and RBCs in kidney function. To this aim, all the mouse lines were treated with Ang II (500 ng/kg/min), and all parameters were investigated before and after the treatment. Lack of eNOS in ECs did not worsen the hypertrophic effect of Ang II. Surprisingly, Ang II infusion led to an increase in heart weight index in RBC eNOS KI mice, but not in the CondKO controls.

Sodium and urine excretion at basal conditions and after salt challenge, as well as GFR, were investigated before and after Ang II treatment in all the mouse lines. The results showed that in basal conditions, eNOS is not involved in sodium and water handling, before

and after Ang II treatment. When the kidney is challenged with high salt and volume intake, EC eNOS, but not RBC eNOS, is involved in the modulation of sodium and urine excretion. In fact, EC eNOS KO mice showed decreased sodium and urine excretion before Ang II treatment. Moreover, CondKO mice showed a weak decrease in sodium excretion after Ang II treatment, which was instead preserved in EC eNOS KI mice. Furthermore, EC eNOS is involved in the regulation of GFR as EC eNOS KI mice rescued the phenotype of CondKO mice after Ang II treatment. Thus, eNOS in ECs plays a role in the modulation of sodium and urine excretion after high salt and volume load, and in the regulation of GFR. On the other hand, RBC eNOS does not play any role on sodium and water handling, as RBC eNOS KO and KI mice did not show any difference as compared to the respective WT and CondKO littermates. Moreover, the reactivation of eNOS specifically in RBCs did not rescue the GFR in CondKO mice.

A limitation of this study is the limited sample size in the basal sodium and urine excretion experiments. Thus, further investigations are required to better understand the role of eNOS in basal sodium and urine excretion.

The use of tamoxifen to induce gene targeting modifications increased urine excretion and GFR after Ang II treatment in WT mice. Thus, these effects were taken into account for the results interpretation. Moreover, tamoxifen downregulated eNOS expression in the whole kidney. The use of constitutive EC eNOS KO and KI models could simplify the understanding of the role of eNOS in kidney function. However, this approach can also have disadvantages like defects in angiogenesis/vasculogenesis during development and off-target effects mainly due to recombination at cryptic/pseudo loxP sites, and overexpression of Cre recombinase (Thyagarajan et al., 2000; Loonstra et al., 2001).

A further experiment that may help to better identify the role of eNOS in kidney function regulation is the analysis of sodium and urine excretion, and GFR in WT mice after treating them with a non-selective NOS inhibitor (e.g., L-NAME) to verify any compensatory response by nNOS or iNOS. Also measurement of blood pressure after Ang II by telemetry in all the lines would give further information about the blood pressure response after Ang II administration in the presence or absence of eNOS only in ECs or RBCs.

The lack of eNOS in ECs or RBCs in worsening the hypertrophic effect of the Ang II was investigated by only comparing the heart to body weight ratios of all mouse lines before and after Ang II infusion. In the future, further investigations regarding morphological parameters (e.g. cardiomyocytes cross-sectional area and fibrosis assessment), molecular markers (e.g. ANP, BNP, and β-MHC), and functional assessment via echocardiography or

pressure-volume loop analysis are needed (Coelho-Filho et al., 2013; Erkens et al., 2015; Sarzani et al., 2022).

One of the key roles of NO in the kidney is to maintain the RBF stable during fluctuations in blood pressure as well as to maintain a constant renal perfusion (Thieme et al., 2017; Mergia et al., 2018). Thus, measurement of RBF in preglomerular arterioles, as well as kidney perfusion analysis in all the mouse lines, would give further information about the role of eNOS specifically in ECs and RBCs on regulating RBF and renal perfusion. Additionally, the isolated perfused kidney system would be optimal to investigate *ex vivo* the role of eNOS in regulating the reactivity of the vessels to vasoactive compounds, in an environment isolated from systemic variables (Hering et al., 2020).

In the future, the molecular mechanism of decreased GFR in KO mice needs to be investigated. Parameters like albuminuria (Verma et al., 2024), which is correlated to glomerular damage, in combination with kidney histology, and ADMA and SDMA concentration in plasma (Vallance et al., 1992; Fliser et al., 2005) need to be determined. By investigating all the lines, this would reveal whether the lack of eNOS only in ECs or in RBCs is sufficient to cause kidney disease.

Overall, these mouse models are a valid tool to investigate the role of eNOS specifically in ECs and RBCs in kidney function. The study of EC eNOS and RBC eNOS in kidney function may lead to the identification of new pharmacological targets for the treatment of kidney diseases.

7. References

Abremski, K., & Hoess, R. (1984). Bacteriophage P1 site-specific recombination. Purification and properties of the Cre recombinase protein. *J Biol Chem, 259*(3), 1509-1514. Retrieved from https://www.ncbi.nlm.nih.gov/pubmed/6319400

Abremski, K., Hoess, R., & Sternberg, N. (1983). Studies on the properties of P1 site-specific recombination: evidence for topologically unlinked products following recombination. *Cell, 32*(4), 1301-1311. doi:10.1016/0092-8674(83)90311-2

Alheid, U., Frolich, J. C., & Forstermann, U. (1987). Endothelium-derived relaxing factor from cultured human endothelial cells inhibits aggregation of human platelets. *Thromb Res, 47*(5), 561-571. doi:10.1016/0049-3848(87)90361-6

Ambrosino, P., Bachetti, T., D'Anna, S. E., Galloway, B., Bianco, A., D'Agnano, V., Papa, A., Motta, A., Perrotta, F., & Maniscalco, M. (2022). Mechanisms and Clinical Implications of Endothelial Dysfunction in Arterial Hypertension. *J Cardiovasc Dev Dis, 9*(5)doi:10.3390/jcdd9050136

Bachmann, S., Bosse, H. M., & Mundel, P. (1995). Topography of nitric oxide synthesis by localizing constitutive NO synthases in mammalian kidney. *Am J Physiol, 268*(5 Pt 2), F885-898. doi:10.1152/ajprenal.1995.268.5.F885

Baines, A., & Ho, P. (2002). Glucose stimulates O2 consumption, NOS, and Na/H exchange in diabetic rat proximal tubules. *Am J Physiol Renal Physiol, 283*(2), F286-293. doi:10.1152/ajprenal.00330.2001

Banday, A. A., & Lokhandwala, M. F. (2011). Angiotensin II-mediated biphasic regulation of proximal tubular Na+/H+ exchanger 3 is impaired during oxidative stress. *Am J Physiol Renal Physiol, 301*(2), F364-370. doi:10.1152/ajprenal.00121.2011

Brandes, R. P. (2014). Endothelial dysfunction and hypertension. *Hypertension, 64*(5), 924-928. doi:10.1161/HYPERTENSIONAHA.114.03575

Brunette, M. G., & Leclerc, M. (2001). Effect of estrogen on calcium and sodium transport by the nephron luminal membranes. *J Endocrinol, 170*(2), 441-450. doi:10.1677/joe.0.1700441

Bryan, N. S., Rassaf, T., Maloney, R. E., Rodriguez, C. M., Saijo, F., Rodriguez, J. R., & Feelisch, M. (2004). Cellular targets and mechanisms of nitros(yl)ation: an insight into their nature and kinetics in vivo. *Proc Natl Acad Sci U S A, 101*(12), 4308-4313. doi:10.1073/pnas.0306706101

Capulli, M., Costantini, R., Sonntag, S., Maurizi, A., Paganini, C., Monti, L., Forlino, A., Shmerling, D., Teti, A., & Rossi, A. (2019). Testing the Cre-mediated genetic switch for the generation of conditional knock-in mice. *PLoS One, 14*(3), e0213660. doi:10.1371/journal.pone.0213660

Carlstrom, M. (2021). Nitric oxide signalling in kidney regulation and cardiometabolic health. *Nat Rev Nephrol, 17*(9), 575-590. doi:10.1038/s41581-021-00429-z

Caturano, A., Vetrano, E., Galiero, R., Salvatore, T., Docimo, G., Epifani, R., Alfano, M., Sardu, C., Marfella, R., Rinaldi, L., & Sasso, F. C. (2022). Cardiac Hypertrophy: From Pathophysiological Mechanisms to Heart Failure Development. *Rev Cardiovasc Med, 23*(5), 165. doi:10.31083/j.rcm2305165

Cheema, M. U., Irsik, D. L., Wang, Y., Miller-Little, W., Hyndman, K. A., Marks, E. S., Frokiaer, J., Boesen, E. I., & Norregaard, R. (2015). Estradiol regulates AQP2 expression in the collecting duct: a novel inhibitory role for estrogen receptor alpha. *Am J Physiol Renal Physiol, 309*(4), F305-317. doi:10.1152/ajprenal.00685.2014

Chen, C. C., Pedraza, P. L., Hao, S., Stier, C. T., & Ferreri, N. R. (2010). TNFR1-deficient mice display altered blood pressure and renal responses to ANG II infusion. *Am J Physiol Renal Physiol, 299*(5), F1141-1150. doi:10.1152/ajprenal.00344.2010

Chen, S., Cao, L., Intengan, H. D., Humphreys, M., & Gardner, D. G. (2002). Osmoregulation of endothelial nitric-oxide synthase gene expression in inner medullary collecting duct cells. Role in activation of the type A natriuretic peptide receptor. *J Biol Chem, 277*(36), 32498-32504. doi:10.1074/jbc.M202321200

Coelho-Filho, O. R., Shah, R. V., Mitchell, R., Neilan, T. G., Moreno, H., Jr., Simonson, B., Kwong, R., Rosenzweig, A., Das, S., & Jerosch-Herold, M. (2013). Quantification of cardiomyocyte hypertrophy by cardiac magnetic resonance: implications for early cardiac remodeling. *Circulation, 128*(11), 1225-1233. doi:10.1161/CIRCULATIONAHA.112.000438

Cortese-Krott, M. M., Rodriguez-Mateos, A., Sansone, R., Kuhnle, G. G., Thasian-Sivarajah, S., Krenz, T., Horn, P., Krisp, C., Wolters, D., Heiss, C., Kroncke, K. D., Hogg, N., Feelisch, M., & Kelm, M. (2012). Human red blood cells at work: identification and visualization of erythrocytic eNOS activity in health and disease. *Blood, 120*(20), 4229-4237. doi:10.1182/blood-2012-07-442277

Cortese-Krott, M. M., Suvorava, T., Leo, F., Heuser, S. K., LoBue, A., Li, J., Becher, S., Schneckmann, R., Srivrastava, T., Erkens, R., Wolff, G., Schmitt, J. P., Grandoch, M., Lundberg, J. O., Pernow, J., Isakson, B. E., Weitzberg, E., & Kelm, M. (2022). Red blood cell eNOS is cardioprotective in acute myocardial infarction. *Redox Biol, 54*, 102370. doi:10.1016/j.redox.2022.102370

Crowley, S. D., Gurley, S. B., Herrera, M. J., Ruiz, P., Griffiths, R., Kumar, A. P., Kim, H. S., Smithies, O., Le, T. H., & Coffman, T. M. (2006). Angiotensin II causes hypertension and cardiac hypertrophy through its receptors in the kidney. *Proc Natl Acad Sci U S A, 103*(47), 17985-17990. doi:10.1073/pnas.0605545103

Cyr, A. R., Huckaby, L. V., Shiva, S. S., & Zuckerbraun, B. S. (2020). Nitric Oxide and Endothelial Dysfunction. *Crit Care Clin, 36*(2), 307-321. doi:10.1016/j.ccc.2019.12.009

Davignon, J., & Ganz, P. (2004). Role of endothelial dysfunction in atherosclerosis. *Circulation, 109*(23 Suppl 1), III27-32. doi:10.1161/01.CIR.0000131515.03336.f8

Delle, H., Rocha, J. R., Cavaglieri, R. C., Vieira, J. M., Jr., Malheiros, D. M., & Noronha, I. L. (2012). Antifibrotic effect of tamoxifen in a model of progressive renal disease. *J Am Soc Nephrol, 23*(1), 37-48. doi:10.1681/ASN.2011010046

Denton, K. M., Anderson, W. P., & Sinniah, R. (2000). Effects of angiotensin II on regional afferent and efferent arteriole dimensions and the glomerular pole. *Am J Physiol Regul Integr Comp Physiol, 279*(2), R629-638. doi:10.1152/ajpregu.2000.279.2.R629

Dickhout, J. G., Mori, T., & Cowley Jr, A. W. (2002). Tubulovascular nitric oxide crosstalk: buffering of angiotensin II–induced medullary vasoconstriction. *Circulation research, 91*(6), 487-493.

Dostal, D. E., & Baker, K. M. (1992). Angiotensin II stimulation of left ventricular hypertrophy in adult rat heart. Mediation by the AT1 receptor. *Am J Hypertens, 5*(5 Pt 1), 276-280. doi:10.1093/ajh/5.5.276

Edwards, A., & Kurtcuoglu, V. (2022). Renal blood flow and oxygenation. *Pflugers Arch, 474*(8), 759-770. doi:10.1007/s00424-022-02690-y

Eriksson, K. E., Yang, T., Carlstrom, M., & Weitzberg, E. (2018). Organ uptake and release of inorganic nitrate and nitrite in the pig. *Nitric Oxide, 75*, 16-26. doi:10.1016/j.niox.2018.02.001

Erkens, R., Kramer, C. M., Luckstadt, W., Panknin, C., Krause, L., Weidenbach, M., Dirzka, J., Krenz, T., Mergia, E., Suvorava, T., Kelm, M., & Cortese-Krott, M. M. (2015). Left ventricular diastolic dysfunction in Nrf2 knock out mice is associated with cardiac hypertrophy, decreased expression of SERCA2a, and preserved endothelial function. *Free Radic Biol Med, 89*, 906-917. doi:10.1016/j.freeradbiomed.2015.10.409

Erkens, R., Suvorava, T., Sutton, T. R., Fernandez, B. O., Mikus-Lelinska, M., Barbarino, F., Flogel, U., Kelm, M., Feelisch, M., & Cortese-Krott, M. M. (2018). Nrf2 Deficiency Unmasks the Significance of Nitric Oxide Synthase Activity for Cardioprotection. *Oxid Med Cell Longev, 2018*, 8309698. doi:10.1155/2018/8309698

Fagan, K. A., Fouty, B. W., Tyler, R. C., Morris, K. G., Jr., Hepler, L. K., Sato, K., LeCras, T. D., Abman, S. H., Weinberger, H. D., Huang, P. L., McMurtry, I. F., & Rodman, D. M. (1999). The pulmonary circulation of homozygous or heterozygous eNOS-null mice is hyperresponsive to mild hypoxia. *J Clin Invest, 103*(2), 291-299. doi:10.1172/JCI3862

Falke, L. L., Broekhuizen, R., Huitema, A., Maarseveen, E., Nguyen, T. Q., & Goldschmeding, R. (2017). Tamoxifen for induction of Cre-recombination may confound fibrosis studies in female mice. *J Cell Commun Signal, 11*(2), 205-211. doi:10.1007/s12079-017-0390-x

Fatima, N., Patel, S. N., & Hussain, T. (2021). Angiotensin II Type 2 Receptor: A Target for Protection Against Hypertension, Metabolic Dysfunction, and Organ Remodeling. *Hypertension, 77*(6), 1845-1856. doi:10.1161/HYPERTENSIONAHA.120.11941

Feil, R., Wagner, J., Metzger, D., & Chambon, P. (1997). Regulation of Cre recombinase activity by mutated estrogen receptor ligand-binding domains. *Biochem Biophys Res Commun, 237*(3), 752-757. doi:10.1006/bbrc.1997.7124

Feron, O., Belhassen, L., Kobzik, L., Smith, T. W., Kelly, R. A., & Michel, T. (1996). Endothelial nitric oxide synthase targeting to caveolae. Specific interactions with caveolin isoforms in cardiac myocytes and endothelial cells. *J Biol Chem, 271*(37), 22810-22814. doi:10.1074/jbc.271.37.22810

Flaherty, M. P., Brown, M., Grupp, I. L., Schultz, J. E., Murphree, S. S., & Jones, W. K. (2007). eNOS deficient mice develop progressive cardiac hypertrophy with altered cytokine and calcium handling protein expression. *Cardiovasc Toxicol, 7*(3), 165-177. doi:10.1007/s12012-007-0028-y

Fliser, D., Kronenberg, F., Kielstein, J. T., Morath, C., Bode-Boger, S. M., Haller, H., & Ritz, E. (2005). Asymmetric dimethylarginine and progression of chronic kidney disease: the mild to moderate kidney disease study. *J Am Soc Nephrol, 16*(8), 2456-2461. doi:10.1681/ASN.2005020179

Florian, M., Lu, Y., Angle, M., & Magder, S. (2004). Estrogen induced changes in Akt-dependent activation of endothelial nitric oxide synthase and vasodilation. *Steroids, 69*(10), 637-645. doi:10.1016/j.steroids.2004.05.016

Fox, S. W., & Chow, J. W. (1998). Nitric oxide synthase expression in bone cells. *Bone, 23*(1), 1-6. doi:10.1016/s8756-3282(98)00070-2

Gallo, G., Volpe, M., & Savoia, C. (2021). Endothelial Dysfunction in Hypertension: Current Concepts and Clinical Implications. *Front Med (Lausanne), 8*, 798958. doi:10.3389/fmed.2021.798958

Gao, Y., Stuart, D., Takahishi, T., & Kohan, D. E. (2018). Nephron-Specific Disruption of Nitric Oxide Synthase 3 Causes Hypertension and Impaired Salt Excretion. *J Am Heart Assoc, 7*(14)doi:10.1161/JAHA.118.009236

Garcia, N. H., Pomposiello, S. I., & Garvin, J. L. (1996). Nitric oxide inhibits ADH-stimulated osmotic water permeability in cortical collecting ducts. *Am J Physiol, 270*(1 Pt 2), F206-210. doi:10.1152/ajprenal.1996.270.1.F206

Geisterfer, A. A., Peach, M. J., & Owens, G. K. (1988). Angiotensin II induces hypertrophy, not hyperplasia, of cultured rat aortic smooth muscle cells. *Circ Res, 62*(4), 749-756. doi:10.1161/01.res.62.4.749

Giaid, A., & Saleh, D. (1995). Reduced expression of endothelial nitric oxide synthase in the lungs of patients with pulmonary hypertension. *N Engl J Med, 333*(4), 214-221. doi:10.1056/NEJM199507273330403

Godecke, A., Decking, U. K., Ding, Z., Hirchenhain, J., Bidmon, H. J., Godecke, S., & Schrader, J. (1998). Coronary hemodynamics in endothelial NO synthase knockout mice. *Circ Res, 82*(2), 186-194. doi:10.1161/01.res.82.2.186

Gu, H., Marth, J. D., Orban, P. C., Mossmann, H., & Rajewsky, K. (1994). Deletion of a DNA polymerase beta gene segment in T cells using cell type-specific gene targeting. *Science, 265*(5168), 103-106. doi:10.1126/science.8016642

Guyton, A. C., Coleman, T. G., Cowley, A. V., Jr., Scheel, K. W., Manning, R. D., Jr., & Norman, R. A., Jr. (1972). Arterial pressure regulation. Overriding dominance of the kidneys in long-term regulation and in hypertension. *Am J Med, 52*(5), 584-594. doi:10.1016/0002-9343(72)90050-2

Hackbarth, H., & Harrison, D. E. (1982). Changes with age in renal function and morphology in C57BL/6, CBA/HT6, and B6CBAF1 mice. *J Gerontol, 37*(5), 540-547. doi:10.1093/geronj/37.5.540

Hall, J. E., & Hall, M. E. (2020). *Guyton and Hall Textbook of Medical Physiology E-Book: Guyton and Hall Textbook of Medical Physiology E-Book*: Elsevier Health Sciences.

Hambrecht, R., Wolf, A., Gielen, S., Linke, A., Hofer, J., Erbs, S., Schoene, N., & Schuler, G. (2000). Effect of exercise on coronary endothelial function in patients with coronary artery disease. *N Engl J Med, 342*(7), 454-460. doi:10.1056/NEJM200002173420702

Hanna, F. S., Alkhouri, S., Rajagopalan, C., Ji, K., Mattingly, R. R., & Yingst, D. R. (2022). Ang II acutely stimulates Na,K-pump in cells from proximal tubules by increasing its phosphorylation at S938 via a PI3K/AKT pathway. *Physiol Rep, 10*(21), e15508. doi:10.14814/phy2.15508

He, P., Klein, J., & Yun, C. C. (2010). Activation of Na+/H+ exchanger NHE3 by angiotensin II is mediated by inositol 1, 4, 5-triphosphate (IP3) receptor-binding protein released with IP3 (IRBIT) and Ca2+/calmodulin-dependent protein kinase II. *Journal of Biological Chemistry, 285*(36), 27869-27878.

Helfrich, M. H., Evans, D. E., Grabowski, P. S., Pollock, J. S., Ohshima, H., & Ralston, S. H. (1997). Expression of nitric oxide synthase isoforms in bone and bone cell cultures. *J Bone Miner Res, 12*(7), 1108-1115. doi:10.1359/jbmr.1997.12.7.1108

Hering, L., Rahman, M., Hoch, H., Marko, L., Yang, G., Reil, A., Yakoub, M., Gupta, V., Potthoff, S. A., Vonend, O., Ralph, D. L., Gurley, S. B., McDonough, A. A., Rump, L. C., & Stegbauer, J. (2020). alpha2A-Adrenoceptors Modulate Renal Sympathetic Neurotransmission and Protect against Hypertensive Kidney Disease. *J Am Soc Nephrol, 31*(4), 783-798. doi:10.1681/ASN.2019060599

Herrera, M., & Garvin, J. L. (2005). A high-salt diet stimulates thick ascending limb eNOS expression by raising medullary osmolality and increasing release of endothelin-1. *Am J Physiol Renal Physiol, 288*(1), F58-64. doi:10.1152/ajprenal.00209.2004

Heymes, C., Vanderheyden, M., Bronzwaer, J. G., Shah, A. M., & Paulus, W. J. (1999). Endomyocardial nitric oxide synthase and left ventricular preload reserve in dilated cardiomyopathy. *Circulation, 99*(23), 3009-3016. doi:10.1161/01.cir.99.23.3009

Huang, P. L., Huang, Z., Mashimo, H., Bloch, K. D., Moskowitz, M. A., Bevan, J. A., & Fishman, M. C. (1995). Hypertension in mice lacking the gene for endothelial nitric oxide synthase. *Nature, 377*(6546), 239-242. doi:10.1038/377239a0

Ichihara, A., Imig, J. D., Inscho, E. W., & Navar, L. G. (1998). Interactive nitric oxide-angiotensin II influences on renal microcirculation in angiotensin II-induced hypertension. *Hypertension, 31*(6), 1255-1260. doi:10.1161/01.hyp.31.6.1255

Irsik, D. L., Carmines, P. K., & Lane, P. H. (2013). Classical estrogen receptors and ERalpha splice variants in the mouse. *PLoS One, 8*(8), e70926. doi:10.1371/journal.pone.0070926

Kanetsuna, Y., Takahashi, K., Nagata, M., Gannon, M. A., Breyer, M. D., Harris, R. C., & Takahashi, T. (2007). Deficiency of endothelial nitric-oxide synthase confers susceptibility to diabetic nephropathy in nephropathy-resistant inbred mice. *Am J Pathol, 170*(5), 1473-1484. doi:10.2353/ajpath.2007.060481

Kazakov, A., Hall, R., Jagoda, P., Bachelier, K., Muller-Best, P., Semenov, A., Lammert, F., Bohm, M., & Laufs, U. (2013). Inhibition of endothelial nitric oxide synthase induces and enhances myocardial fibrosis. *Cardiovasc Res, 100*(2), 211-221. doi:10.1093/cvr/cvt181

Kilkenny, C., Browne, W. J., Cuthill, I. C., Emerson, M., & Altman, D. G. (2010). Improving bioscience research reporting: the ARRIVE guidelines for reporting animal research. *PLoS Biol, 8*(6), e1000412. doi:10.1371/journal.pbio.1000412

Kojda, G., Cheng, Y. C., Burchfield, J., & Harrison, D. G. (2001). Dysfunctional regulation of endothelial nitric oxide synthase (eNOS) expression in response to exercise in mice lacking one eNOS gene. *Circulation, 103*(23), 2839-2844. doi:10.1161/01.cir.103.23.2839

Kojda, G., Laursen, J. B., Ramasamy, S., Kent, J. D., Kurz, S., Burchfield, J., Shesely, E. G., & Harrison, D. G. (1999). Protein expression, vascular reactivity and soluble guanylate cyclase activity

in mice lacking the endothelial cell nitric oxide synthase: contributions of NOS isoforms to blood pressure and heart rate control. *Cardiovasc Res, 42*(1), 206-213. doi:10.1016/s0008-6363(98)00315-0

Kopkan, L., Hess, A., Huskova, Z., Cervenka, L., Navar, L. G., & Majid, D. S. (2010). High-salt intake enhances superoxide activity in eNOS knockout mice leading to the development of salt sensitivity. *Am J Physiol Renal Physiol, 299*(3), F656-663. doi:10.1152/ajprenal.00047.2010

Kubes, P., Suzuki, M., & Granger, D. N. (1991). Nitric oxide: an endogenous modulator of leukocyte adhesion. *Proc Natl Acad Sci U S A, 88*(11), 4651-4655. doi:10.1073/pnas.88.11.4651

Kvam, F. I., Ofstad, J., & Iversen, B. M. (2000). Role of nitric oxide in the autoregulation of renal blood flow and glomerular filtration rate in aging spontaneously hypertensive rats. *Kidney Blood Press Res, 23*(6), 376-384. doi:10.1159/000025986

Lahera, V., Salom, M. G., Miranda-Guardiola, F., Moncada, S., & Romero, J. C. (1991). Effects of NG-nitro-L-arginine methyl ester on renal function and blood pressure. *Am J Physiol, 261*(6 Pt 2), F1033-1037. doi:10.1152/ajprenal.1991.261.6.F1033

Landmesser, U., Hornig, B., & Drexler, H. (2004). Endothelial function: a critical determinant in atherosclerosis? *Circulation, 109*(21 Suppl 1), II27-33. doi:10.1161/01.CIR.0000129501.88485.1f

Leo, F., Suvorava, T., Heuser, S. K., Li, J., LoBue, A., Barbarino, F., Piragine, E., Schneckmann, R., Hutzler, B., Good, M. E., Fernandez, B. O., Vornholz, L., Rogers, S., Doctor, A., Grandoch, M., Stegbauer, J., Weitzberg, E., Feelisch, M., Lundberg, J. O., Isakson, B. E., Kelm, M., & Cortese-Krott, M. M. (2021). Red Blood Cell and Endothelial eNOS Independently Regulate Circulating Nitric Oxide Metabolites and Blood Pressure. *Circulation, 144*(11), 870-889. doi:10.1161/CIRCULATIONAHA.120.049606

Leung, H. S., Yung, L. M., Leung, F. P., Yao, X., Chen, Z. Y., Ko, W. H., Laher, I., & Huang, Y. (2006). Tamoxifen dilates porcine coronary arteries: roles for nitric oxide and ouabain-sensitive mechanisms. *Br J Pharmacol, 149*(6), 703-711. doi:10.1038/sj.bjp.0706921

Li, J., LoBue, A., Heuser, S. K., & Cortese-Krott, M. M. (2024). Determination of Nitric Oxide and Its Metabolites in Biological Tissues Using Ozone-Based Chemiluminescence Detection: A State-of-the-Art Review. *Antioxidants (Basel), 13*(2)doi:10.3390/antiox13020179

Li, J., White, J., Guo, L., Zhao, X., Wang, J., Smart, E. J., & Li, X. A. (2009). Salt inactivates endothelial nitric oxide synthase in endothelial cells. *J Nutr, 139*(3), 447-451. doi:10.3945/jn.108.097451

Li, J. C., Jia, J., Dong, L., Hu, Z. J., Huang, X. R., Wang, H. L., Wang, L., Yang, S. J., & Lan, H. Y. (2023). Angiotensin II mediates hypertensive cardiac fibrosis via an Erbb4-IR-dependent mechanism. *Mol Ther Nucleic Acids, 33*, 180-190. doi:10.1016/j.omtn.2023.06.017

Liang, M., & Knox, F. G. (1999). Nitric oxide reduces the molecular activity of Na+,K+-ATPase in opossum kidney cells. *Kidney Int, 56*(2), 627-634. doi:10.1046/j.1523-1755.1999.00583.x

Liu, F. Y., & Cogan, M. G. (1988). Angiotensin II stimulation of hydrogen ion secretion in the rat early proximal tubule. Modes of action, mechanism, and kinetics. *J Clin Invest, 82*(2), 601-607. doi:10.1172/JCI113638

Liu, F. Y., & Cogan, M. G. (1989). Angiotensin II stimulates early proximal bicarbonate absorption in the rat by decreasing cyclic adenosine monophosphate. *J Clin Invest, 84*(1), 83-91. doi:10.1172/JCI114174

LoBue, A., Heuser, S. K., Lindemann, M., Li, J., Rahman, M., Kelm, M., Stegbauer, J., & Cortese-Krott, M. M. (2023). Red blood cell endothelial nitric oxide synthase: A major player in regulating cardiovascular health. *Br J Pharmacol*doi:10.1111/bph.16230

LoBue, A., Li, Z., Heuser, S. K., Li, J., Leo, F., Vornholz, L., Dunaway, L. S., Suvorava, T., Isakson, B. E., & Cortese-Krott, M. M. (2024). Generation and characterization of a conditional eNOS knock out mouse model for cell-specific reactivation of eNOS in gain-of-function studies. *Nitric Oxide, 153*, 106-113. doi:10.1016/j.niox.2024.10.009

Loonstra, A., Vooijs, M., Beverloo, H. B., Allak, B. A., van Drunen, E., Kanaar, R., Berns, A., & Jonkers, J. (2001). Growth inhibition and DNA damage induced by Cre recombinase in mammalian cells. *Proc Natl Acad Sci U S A, 98*(16), 9209-9214. doi:10.1073/pnas.161269798

Lundberg, J. O., & Weitzberg, E. (2022). Nitric oxide signaling in health and disease. *Cell, 185*(16), 2853-2878. doi:10.1016/j.cell.2022.06.010

Ma, H. Y., Chen, S., & Du, Y. (2021). Estrogen and estrogen receptors in kidney diseases. *Ren Fail, 43*(1), 619-642. doi:10.1080/0886022X.2021.1901739

Ma, J., Li, Y., Yang, X., Liu, K., Zhang, X., Zuo, X., Ye, R., Wang, Z., Shi, R., Meng, Q., & Chen, X. (2023). Signaling pathways in vascular function and hypertension: molecular mechanisms and therapeutic interventions. *Signal Transduct Target Ther, 8*(1), 168. doi:10.1038/s41392-023-01430-7

Majid, D. S., & Navar, L. G. (1994). Blockade of distal nephron sodium transport attenuates pressure natriuresis in dogs. *Hypertension, 23*(6 Pt 2), 1040-1045. doi:10.1161/01.hyp.23.6.1040

Majid, D. S., Williams, A., & Navar, L. G. (1993). Inhibition of nitric oxide synthesis attenuates pressure-induced natriuretic responses in anesthetized dogs. *Am J Physiol, 264*(1 Pt 2), F79-87. doi:10.1152/ajprenal.1993.264.1.F79

Massion, P. B., Dessy, C., Desjardins, F., Pelat, M., Havaux, X., Belge, C., Moulin, P., Guiot, Y., Feron, O., Janssens, S., & Balligand, J. L. (2004). Cardiomyocyte-restricted overexpression of endothelial nitric oxide synthase (NOS3) attenuates beta-adrenergic stimulation and reinforces vagal inhibition of cardiac contraction. *Circulation, 110*(17), 2666-2672. doi:10.1161/01.CIR.0000145608.80855.BC

Mattson, D. L., Lu, S., Nakanishi, K., Papanek, P. E., & Cowley, A. W., Jr. (1994). Effect of chronic renal medullary nitric oxide inhibition on blood pressure. *Am J Physiol, 266*(5 Pt 2), H1918-1926. doi:10.1152/ajpheart.1994.266.5.H1918

Mergia, E., Thieme, M., Hoch, H., Daniil, G., Hering, L., Yakoub, M., Scherbaum, C. R., Rump, L. C., Koesling, D., & Stegbauer, J. (2018). Impact of the NO-Sensitive Guanylyl Cyclase 1 and 2 on Renal Blood Flow and Systemic Blood Pressure in Mice. *Int J Mol Sci, 19*(4)doi:10.3390/ijms19040967

Metzger, D., Clifford, J., Chiba, H., & Chambon, P. (1995). Conditional site-specific recombination in mammalian cells using a ligand-dependent chimeric Cre recombinase. *Proc Natl Acad Sci U S A, 92*(15), 6991-6995. doi:10.1073/pnas.92.15.6991

Morishita, T., Tsutsui, M., Shimokawa, H., Sabanai, K., Tasaki, H., Suda, O., Nakata, S., Tanimoto, A., Wang, K. Y., Ueta, Y., Sasaguri, Y., Nakashima, Y., & Yanagihara, N. (2005). Nephrogenic diabetes insipidus in mice lacking all nitric oxide synthase isoforms. *Proc Natl Acad Sci U S A, 102*(30), 10616-10621. doi:10.1073/pnas.0502236102

Nadasy, G. L., Balla, A., Dornyei, G., Hunyady, L., & Szekeres, M. (2024). Direct Vascular Effects of Angiotensin II (A Systematic Short Review). *Int J Mol Sci, 26*(1)doi:10.3390/ijms26010113

Nakanishi, K., Mattson, D. L., & Cowley, A. W., Jr. (1995). Role of renal medullary blood flow in the development of L-NAME hypertension in rats. *Am J Physiol, 268*(2 Pt 2), R317-323. doi:10.1152/ajpregu.1995.268.2.R317

O'Gallagher, K., Shabeeh, H., Munir, S., Roomi, A., Jiang, B., Guilcher, A., Brett, S., & Chowienczyk, P. (2020). Effects of Inhibition of Nitric Oxide Synthase on Muscular Arteries During Exercise: Nitric Oxide Does Not Contribute to Vasodilation During Exercise or in Recovery. *J Am Heart Assoc, 9*(16), e013849. doi:10.1161/JAHA.119.013849

Okamoto, K., & Aoki, K. (1963). Development of a strain of spontaneously hypertensive rats. *Jpn Circ J, 27*, 282-293. doi:10.1253/jcj.27.282

Patel, B. M., & Desai, V. J. (2014). Beneficial role of tamoxifen in experimentally induced cardiac hypertrophy. *Pharmacol Rep, 66*(2), 264-272. doi:10.1016/j.pharep.2014.02.004

Pawloski, J. R., Hess, D. T., & Stamler, J. S. (2001). Export by red blood cells of nitric oxide bioactivity. *Nature, 409*(6820), 622-626. doi:10.1038/35054560

Pelzer, T., Jazbutyte, V., Hu, K., Segerer, S., Nahrendorf, M., Nordbeck, P., Bonz, A. W., Muck, J., Fritzemeier, K. H., Hegele-Hartung, C., Ertl, G., & Neyses, L. (2005). The estrogen receptor-

alpha agonist 16alpha-LE2 inhibits cardiac hypertrophy and improves hemodynamic function in estrogen-deficient spontaneously hypertensive rats. *Cardiovasc Res, 67*(4), 604-612. doi:10.1016/j.cardiores.2005.04.035

Perez-Rojas, J. M., Kassem, K. M., Beierwaltes, W. H., Garvin, J. L., & Herrera, M. (2010). Nitric oxide produced by endothelial nitric oxide synthase promotes diuresis. *Am J Physiol Regul Integr Comp Physiol, 298*(4), R1050-1055. doi:10.1152/ajpregu.00181.2009

Peterson, K. R., Fedosyuk, H., Zelenchuk, L., Nakamoto, B., Yannaki, E., Stamatoyannopoulos, G., Ciciotte, S., Peters, L. L., Scott, L. M., & Papayannopoulou, T. (2004). Transgenic Cre expression mice for generation of erythroid-specific gene alterations. *Genesis, 39*(1), 1-9. doi:10.1002/gene.20020

Pitulescu, M. E., Schmidt, I., Benedito, R., & Adams, R. H. (2010). Inducible gene targeting in the neonatal vasculature and analysis of retinal angiogenesis in mice. *Nat Protoc, 5*(9), 1518-1534. doi:10.1038/nprot.2010.113

Plato, C. F., Shesely, E. G., & Garvin, J. L. (2000). eNOS mediates L-arginine-induced inhibition of thick ascending limb chloride flux. *Hypertension, 35*(1 Pt 2), 319-323. doi:10.1161/01.hyp.35.1.319

Plato, C. F., Stoos, B. A., Wang, D., & Garvin, J. L. (1999). Endogenous nitric oxide inhibits chloride transport in the thick ascending limb. *Am J Physiol, 276*(1), F159-163. doi:10.1152/ajprenal.1999.276.1.F159

Rassaf, T., Preik, M., Kleinbongard, P., Lauer, T., Heiss, C., Strauer, B. E., Feelisch, M., & Kelm, M. (2002). Evidence for in vivo transport of bioactive nitric oxide in human plasma. *J Clin Invest, 109*(9), 1241-1248. doi:10.1172/JCI14995

Rees, D. D., Palmer, R. M., Schulz, R., Hodson, H. F., & Moncada, S. (1990). Characterization of three inhibitors of endothelial nitric oxide synthase in vitro and in vivo. *Br J Pharmacol, 101*(3), 746-752. doi:10.1111/j.1476-5381.1990.tb14151.x

Sandner, P., Kornfeld, M., Ruan, X., Arendshorst, W. J., & Kurtz, A. (1999). Nitric oxide/cAMP interactions in the control of rat renal vascular resistance. *Circ Res, 84*(2), 186-192. doi:10.1161/01.res.84.2.186

Sarzani, R., Allevi, M., Di Pentima, C., Schiavi, P., Spannella, F., & Giulietti, F. (2022). Role of Cardiac Natriuretic Peptides in Heart Structure and Function. *Int J Mol Sci, 23*(22)doi:10.3390/ijms232214415

Sato, K., Kihara, M., Hashimoto, T., Matsushita, K., Koide, Y., Tamura, K., Hirawa, N., Toya, Y., Fukamizu, A., & Umemura, S. (2004). Alterations in renal endothelial nitric oxide synthase expression by salt diet in angiotensin type-1a receptor gene knockout mice. *J Am Soc Nephrol, 15*(7), 1756-1763. doi:10.1097/01.asn.0000130922.75125.b8

Schneider, M. P., Ge, Y., Pollock, D. M., Pollock, J. S., & Kohan, D. E. (2008). Collecting duct-derived endothelin regulates arterial pressure and Na excretion via nitric oxide. *Hypertension, 51*(6), 1605-1610. doi:10.1161/HYPERTENSIONAHA.107.108126

Schnermann, J., Huang, Y. G., & Briggs, J. P. (2001). Angiotensin II blockade causes acute renal failure in eNOS-deficient mice. *J Renin Angiotensin Aldosterone Syst, 2*(1_suppl), S199-S203. doi:10.1177/14703203010020013501

Schreiber, A., Shulhevich, Y., Geraci, S., Hesser, J., Stsepankou, D., Neudecker, S., Koenig, S., Heinrich, R., Hoecklin, F., Pill, J., Friedemann, J., Schweda, F., Gretz, N., & Schock-Kusch, D. (2012). Transcutaneous measurement of renal function in conscious mice. *Am J Physiol Renal Physiol, 303*(5), F783-788. doi:10.1152/ajprenal.00279.2012

Schwenk, F., Baron, U., & Rajewsky, K. (1995). A cre-transgenic mouse strain for the ubiquitous deletion of loxP-flanked gene segments including deletion in germ cells. *Nucleic Acids Res, 23*(24), 5080-5081. doi:10.1093/nar/23.24.5080

Seliger, S. L., Salimi, S., Pierre, V., Giffuni, J., Katzel, L., & Parsa, A. (2016). Microvascular endothelial dysfunction is associated with albuminuria and CKD in older adults. *BMC Nephrol, 17*(1), 82. doi:10.1186/s12882-016-0303-x

Shaul, P. W., North, A. J., Wu, L. C., Wells, L. B., Brannon, T. S., Lau, K. S., Michel, T., Margraf, L. R., & Star, R. A. (1994). Endothelial nitric oxide synthase is expressed in cultured human bronchiolar epithelium. *J Clin Invest, 94*(6), 2231-2236. doi:10.1172/JCI117585

Shesely, E. G., Maeda, N., Kim, H. S., Desai, K. M., Krege, J. H., Laubach, V. E., Sherman, P. A., Sessa, W. C., & Smithies, O. (1996). Elevated blood pressures in mice lacking endothelial nitric oxide synthase. *Proc Natl Acad Sci U S A, 93*(23), 13176-13181. doi:10.1073/pnas.93.23.13176

Silva, F. C. d., Araújo, B. J. d., Cordeiro, C. S., Arruda, V. M., Faria, B. Q., Guerra, J. F. D. C., Araújo, T. G. D., & Fürstenau, C. R. (2022). Endothelial dysfunction due to the inhibition of the synthesis of nitric oxide: Proposal and characterization of an in vitro cellular model. *Frontiers in Physiology, 13*, 978378.

Silva, I. V. G., de Figueiredo, R. C., & Rios, D. R. A. (2019). Effect of Different Classes of Antihypertensive Drugs on Endothelial Function and Inflammation. *Int J Mol Sci, 20*(14)doi:10.3390/ijms20143458

Siragy, H. M., Inagami, T., Ichiki, T., & Carey, R. M. (1999). Sustained hypersensitivity to angiotensin II and its mechanism in mice lacking the subtype-2 (AT2) angiotensin receptor. *Proc Natl Acad Sci U S A, 96*(11), 6506-6510. doi:10.1073/pnas.96.11.6506

Smith, A. J., De Sousa, M. A., Kwabi-Addo, B., Heppell-Parton, A., Impey, H., & Rabbitts, P. (1995). A site-directed chromosomal translocation induced in embryonic stem cells by Cre-loxP recombination. *Nat Genet, 9*(4), 376-385. doi:10.1038/ng0495-376

Smith, R. S., Jr., Agata, J., Xia, C. F., Chao, L., & Chao, J. (2005). Human endothelial nitric oxide synthase gene delivery protects against cardiac remodeling and reduces oxidative stress after myocardial infarction. *Life Sci, 76*(21), 2457-2471. doi:10.1016/j.lfs.2004.11.028

Sorensen, I., Adams, R. H., & Gossler, A. (2009). DLL1-mediated Notch activation regulates endothelial identity in mouse fetal arteries. *Blood, 113*(22), 5680-5688. doi:10.1182/blood-2008-08-174508

Stamler, J. S., Loh, E., Roddy, M. A., Currie, K. E., & Creager, M. A. (1994). Nitric oxide regulates basal systemic and pulmonary vascular resistance in healthy humans. *Circulation, 89*(5), 2035-2040. doi:10.1161/01.cir.89.5.2035

Sternberg, N., & Hamilton, D. (1981). Bacteriophage P1 site-specific recombination. I. Recombination between loxP sites. *J Mol Biol, 150*(4), 467-486. doi:10.1016/0022-2836(81)90375-2

Sternberg, N., Sauer, B., Hoess, R., & Abremski, K. (1986). Bacteriophage P1 cre gene and its regulatory region. Evidence for multiple promoters and for regulation by DNA methylation. *J Mol Biol, 187*(2), 197-212. doi:10.1016/0022-2836(86)90228-7

Steudel, W., Watanabe, M., Dikranian, K., Jacobson, M., & Jones, R. C. (1999). Expression of nitric oxide synthase isoforms (NOS II and NOS III) in adult rat lung in hyperoxic pulmonary hypertension. *Cell Tissue Res, 295*(2), 317-329. doi:10.1007/s004410051238

Stoos, B. A., Garcia, N. H., & Garvin, J. L. (1995). Nitric oxide inhibits sodium reabsorption in the isolated perfused cortical collecting duct. *J Am Soc Nephrol, 6*(1), 89-94. doi:10.1681/ASN.V6189

Sudharsanan, N., Theilmann, M., Kirschbaum, T. K., Manne-Goehler, J., Azadnajafabad, S., Bovet, P., Chen, S., Damasceno, A., De Neve, J. W., Dorobantu, M., Ebert, C., Farzadfar, F., Gathecha, G., Gurung, M. S., Jamshidi, K., Jorgensen, J. M. A., Labadarios, D., Lemp, J., Lunet, N., Mwangi, J. K., Moghaddam, S. S., Bahendeka, S. K., Zhumadilov, Z., Barnighausen, T., Vollmer, S., Atun, R., Davies, J. I., & Geldsetzer, P. (2021). Variation in the Proportion of Adults in Need of Blood Pressure-Lowering Medications by Hypertension Care Guideline in Low- and Middle-Income Countries: A Cross-Sectional Study of 1 037 215 Individuals From 50 Nationally Representative Surveys. *Circulation, 143*(10), 991-1001. doi:10.1161/CIRCULATIONAHA.120.051620

Suvorava, T., Lauer, N., Kumpf, S., Jacob, R., Meyer, W., & Kojda, G. (2005). Endogenous vascular hydrogen peroxide regulates arteriolar tension in vivo. *Circulation, 112*(16), 2487-2495. doi:10.1161/CIRCULATIONAHA.105.543157

Takenaka, T., Mitchell, K. D., & Navar, L. G. (1993). Contribution of angiotensin II to renal hemodynamic and excretory responses to nitric oxide synthesis inhibition in the rat. *J Am Soc Nephrol, 4*(4), 1046-1053. doi:10.1681/ASN.V441046

Tao, Y., Young-Stubbs, C., Yazdizadeh Shotorbani, P., Su, D. M., Mathis, K. W., & Ma, R. (2023). Sex and strain differences in renal hemodynamics in mice. *Physiol Rep, 11*(6), e15644. doi:10.14814/phy2.15644

Thieme, M., Sivritas, S. H., Mergia, E., Potthoff, S. A., Yang, G., Hering, L., Grave, K., Hoch, H., Rump, L. C., & Stegbauer, J. (2017). Phosphodiesterase 5 inhibition ameliorates angiotensin II-dependent hypertension and renal vascular dysfunction. *Am J Physiol Renal Physiol, 312*(3), F474-F481. doi:10.1152/ajprenal.00376.2016

Thyagarajan, B., Guimaraes, M. J., Groth, A. C., & Calos, M. P. (2000). Mammalian genomes contain active recombinase recognition sites. *Gene, 244*(1-2), 47-54. doi:10.1016/s0378-1119(00)00008-1

Tingskov, S. J., Jensen, M. S., Pedersen, C. T., de Araujo, I., Mutsaers, H. A. M., & Norregaard, R. (2021). Tamoxifen attenuates renal fibrosis in human kidney slices and rats subjected to unilateral ureteral obstruction. *Biomed Pharmacother, 133*, 111003. doi:10.1016/j.biopha.2020.111003

Tingskov, S. J., Kwon, T. H., Frokiaer, J., & Norregaard, R. (2018). Tamoxifen Decreases Lithium-Induced Natriuresis in Rats With Nephrogenic Diabetes Insipidus. *Front Physiol, 9*, 903. doi:10.3389/fphys.2018.00903

Tojo, A., Kimoto, M., & Wilcox, C. S. (2000). Renal expression of constitutive NOS and DDAH: separate effects of salt intake and angiotensin. *Kidney Int, 58*(5), 2075-2083. doi:10.1111/j.1523-1755.2000.00380.x

Triebel, H., & Castrop, H. (2024). The renin angiotensin aldosterone system. *Pflugers Arch, 476*(5), 705-713. doi:10.1007/s00424-024-02908-1

Vallance, P., Leone, A., Calver, A., Collier, J., & Moncada, S. (1992). Accumulation of an endogenous inhibitor of nitric oxide synthesis in chronic renal failure. *Lancet, 339*(8793), 572-575. doi:10.1016/0140-6736(92)90865-z

Verma, A., Schmidt, I. M., Claudel, S., Palsson, R., Waikar, S. S., & Srivastava, A. (2024). Association of Albuminuria With Chronic Kidney Disease Progression in Persons With Chronic Kidney Disease and Normoalbuminuria : A Cohort Study. *Ann Intern Med, 177*(4), 467-475. doi:10.7326/M23-2814

Wang, W., Mitra, A., Poole, B., Falk, S., Lucia, M. S., Tayal, S., & Schrier, R. (2004). Endothelial nitric oxide synthase-deficient mice exhibit increased susceptibility to endotoxin-induced acute renal failure. *Am J Physiol Renal Physiol, 287*(5), F1044-1048. doi:10.1152/ajprenal.00136.2004

Whiting, C., Castillo, A., Haque, M. Z., & Majid, D. S. (2013). Protective role of the endothelial isoform of nitric oxide synthase in ANG II-induced inflammatory responses in the kidney. *Am J Physiol Renal Physiol, 305*(7), F1031-1041. doi:10.1152/ajprenal.00024.2013

Wood, K. C., Cortese-Krott, M. M., Kovacic, J. C., Noguchi, A., Liu, V. B., Wang, X., Raghavachari, N., Boehm, M., Kato, G. J., Kelm, M., & Gladwin, M. T. (2013). Circulating blood endothelial nitric oxide synthase contributes to the regulation of systemic blood pressure and nitrite homeostasis. *Arterioscler Thromb Vasc Biol, 33*(8), 1861-1871. doi:10.1161/ATVBAHA.112.301068

World Health Organization (2023). Hypertentsion. Available from https://www.who.int/news-room/fact-sheets/detail/hypertension (accessed 14 April 2025

Wu, F., Park, F., Cowley, A. W., Jr., & Mattson, D. L. (1999). Quantification of nitric oxide synthase activity in microdissected segments of the rat kidney. *Am J Physiol, 276*(6), F874-881. doi:10.1152/ajprenal.1999.276.6.F874

Xu, J., Carretero, O. A., Liao, T. D., Peng, H., Shesely, E. G., Xu, J., Liu, T. S., Yang, J. J., Reudelhuber, T. L., & Yang, X. P. (2010). Local angiotensin II aggravates cardiac remodeling in hypertension. *Am J Physiol Heart Circ Physiol, 299*(5), H1328-1338. doi:10.1152/ajpheart.00538.2010

Zhang, C., & Mayeux, P. R. (2001). NO/cGMP signaling modulates regulation of Na+-K+-ATPase activity by angiotensin II in rat proximal tubules. *Am J Physiol Renal Physiol, 280*(3), F474-479. doi:10.1152/ajprenal.2001.280.3.F474

Zhang, X., Ge, Y., Bukhari, A. A., Zhu, Q., Shen, Y., Li, M., Sun, H., Su, D., & Liang, X. (2019). Estrogen negatively regulates the renal epithelial sodium channel (ENaC) by promoting Derlin-1 expression and AMPK activation. *Exp Mol Med, 51*(5), 1-12. doi:10.1038/s12276-019-0253-z

Zhang, Z., & Lutz, B. (2002). Cre recombinase-mediated inversion using lox66 and lox71: method to introduce conditional point mutations into the CREB-binding protein. *Nucleic acids research, 30*(17), e90-e90.

Zou, A. P., & Cowley, A. W., Jr. (1997). Nitric oxide in renal cortex and medulla. An in vivo microdialysis study. *Hypertension, 29*(1 Pt 2), 194-198. doi:10.1161/01.hyp.29.1.194

8. Acknowledgment

The first and greatest thank you goes to Prof. Dr. Miriam Cortese-Krott, who gave me this incredible opportunity. Like only a true mentor can, she guided me through this challenging and intense journey, inspiring in me a profound curiosity and passion for research. She was always present and available for every question, every doubt, and open to any scientific discussion. Her support was essential not only for my academic growth and the successful completion of this project but also on a personal level. Perhaps the biggest thank you is for always believing in me, even more than I believed in myself.

I would like to thank Prof. Dr. Holger Gohlke for his mentorship and for reviewing my doctoral thesis.

I want to thank Prof. Dr. med. Johannes Stegbauer for being open to scientific discussions and for sharing ideas and insights. His deep expertise in the field was indispensable for interpreting the results and bringing this project to completion.

I would like to thank Dr. Tatsiana Suvorava for performing the vascular function assessments, Prof. Dr. Brant Isakson for the TEM imaging, Stefanie Becher for providing part of the Millar-based blood pressure measurements, Dr. med. Carmen Barthuber for the analysis of urine samples, Alicia Carvalho and Marla Lindemann for their support with mRNA expression analysis and the salt challenge experiments, respectively.

I am thankful to Dr. Lydia Hering, who taught me how to measure GFR, and to Prof. Dr. Dr. med. André Heinen for training me in Millar-based blood pressure measurement technique.

A big thank you goes to Dr. Francesca Leo, not only for performing part of the Millar-based blood pressure measurements, but above all for the invaluable support she offered to me when I first moved here.

A special thanks goes to my colleagues Dr. Sophia Heuser and Dr. Junjie Li for the DNA recombination analysis and part of the mRNA expression experiments, and the NO metabolites measurements, respectively. But the biggest thank you goes to you both for making this journey truly special and unforgettable. Moving to a new country, far from my loved ones, and with no knowledge of the languages, was not easy. From the first day, you welcomed me, supported me, and understood me. You became my family away from home, and I could not have made it this far without you.

I would also like to thank Zhixin Li, MSc, Diana Costanzo, MSc, and Malwin Barthen. Your presence added even more joy and positivity to the lab. Thank you for your support and for being there whenever I needed help.

Acknowledgment

I would like to thank Prof. Dr. Axel Gödecke and Dr. Sandra Berger as indispensable members of the IRTG 1902, which gave me the opportunity to meet and collaborate with other PhD students and participate in valuable training courses.

To my friends, both near and far:

Gloria, thank you for always being there for me, even from thousands of kilometers away. Your empathy, care, and understanding have been a steady emotional anchor throughout this journey.

Simona, for being the lifelong friend I can always count on. Thank you for every laugh, every advice, and every evening spent together.

Claudia and Katia, the kind of friends who remind you that not seeing or hearing from each other constantly will never change the bounds of true friendship. Thank you for always supporting me and believing in me.

Giorgia, the friend who was always ready to listen and encourage me. Destiny, unfortunately, took you away too early, but I know that right now, you are here with me, celebrating this success.

Raffaele, one of those people who believes in me without limits. Your presence, your honesty, and at the same time your understanding, helped me face the hardest and most emotional moments with more clarity and strength.

Emre, Antonella, and Sheetal, my companions from the German course: I may not have learned German, but I found something much more valuable: your friendship. Thank you for the lightness you brought into my life when work felt overwhelming.

Omar, who supported me in all my decisions, always gave me the freedom to choose for my future. Your support was essential in helping me overcome all my fears and in giving me the courage to start this new journey.

Finally, my most heartfelt thanks go to my parents and my brother. You are the people who have always believed in me the most. You supported every decision I made, even when it meant moving to another country far from you. I can never thank you enough for all you have done. Without your love, strength, and constant encouragement, I would not be who I am today.

9. Publications & Manuscripts

Parts of this dissertation were already published in peer-reviewed scientific journals and presented at scientific conferences.

Original publications:

1. **LoBue A.,** Li Z., Heuser S. K., Li J., Leo F., Vornholz L., Dunaway L. S., Suvorava T., Isakson B. E., et al. (2024). Generation and characterization of a conditional eNOS knock out mouse model for cell-specific reactivation of eNOS in gain-of-function studies. Nitric Oxide., 153: 106-113. doi.org/10.1016/j.niox.2024.10.009.

   Contribution: Writing – original draft, Writing – review & editing, Visualization, Investigation, Formal analysis, Conceptualization, Data curation, Project administration.

2. Dunaway L. S., Saii K., **LoBue A**., Nyshadham S., Abib N., Heuser S. K., Loeb S. A., Simonsen U., Cortese-Krott M. M., et al. (2024). The hemodynamic response to nitrite is acute and dependent upon tissue perfusion. Nitric oxide: biology and chemistry, 150, 47–52. https://doi.org/10.1016/j.niox.2024.07.005.

   Contribution: Visualization, Investigation (blood pressure measurements), Formal analysis, Data curation, Project administration.

3. Heuser S. K., **LoBue A.**, Li J., Zhuge Z., Leo F., Suvorava T., Olsson A., Schneckmann R., Guimaraes Braga D. D., et al. (2022). Downregulation of eNOS and preserved endothelial function in endothelial-specific arginase 1-deficient mice. Nitric Oxide.;125-126:69-77. doi: 10.1016/j.niox.2022.06.004.

   Contribution: Writing – review & editing, Visualization, Investigation (Western blots and protein quantification analysis), Formal analysis, Data curation, Project administration.

4. Cortese-Krott M. M., Suvorava T., Leo F., Heuser S. K., **LoBue A.**, Li J., Becher S., Schneckmann R., Srivrastava T., Erkens R., et al. (2022). Red blood cell eNOS is cardioprotective in acute myocardial infarction. Redox biology, 54, 102370. https://doi.org/10.1016/j.redox.2022.102370.

   Contribution: Writing – review & editing, Visualization, Investigation (Western blots), Formal analysis, Data curation, Project administration.

5. Leo F.*, Suvorava T.*, Heuser S. K., Li J., **LoBue A.**, Barbarino F., Piragine E., Schneckmann R., Hutzler Beate, et al. (2021). Red Blood Cell and Endothelial eNOS

Independently Regulate Circulating Nitric Oxide Metabolites and Blood Pressure. Circulation, 144(11), 870-889. doi:10.1161/CIRCULATIONAHA.120.049606

Contribution: Writing – review & editing, Visualization, Investigation (Western blots, immunoprecipitation, NO metabolites detection), Formal analysis, Data curation, Project administration.

Reviews:

1. Li Z., **LoBue A.**, Heuser S. K., Li J., Engelhardt E., Papapetropoulos A., Patel H. H, Lolley L., et al. (2025). Best practices for blood collection and anaesthesia in mice: Selection, application and reporting. Br J Pharmacoldoi:10.1111/bph.70029. doi.org/10.1111/bph.70029.

   Contribution: Writing – review & editing

2. Heuser S. K.*, Li J.*, Pudewell S., **LoBue A.**, Li Z., & Cortese-Krott M. M. (2025). Biochemistry, pharmacology, and in vivo function of arginases. Pharmacological reviews, 77(1), 100015. https://doi.org/10.1124/pharmrev.124.001271.

   Contribution: Writing – original draft, Writing – review & editing, Visualization.

3. Li J., **LoBue A.**, Heuser S. K., & Cortese-Krott M. M. (2024). Determination of Nitric Oxide and Its Metabolites in Biological Tissues Using Ozone-Based Chemiluminescence Detection: A State-of-the-Art Review. Antioxidants (Basel, Switzerland), 13(2), 179. https://doi.org/10.3390/antiox13020179.

   Contribution: Writing – original draft, Writing – review & editing.

4. **LoBue A.**, Heuser S. K., Lindemann M., Li J., Rahman M., Kelm M., Stegbauer J., & Cortese-Krott M. M. (2023). Red blood cell endothelial nitric oxide synthase: A major player in regulating cardiovascular health. British journal of pharmacology, 10.1111/bph.16230. Advance online publication. https://doi.org/10.1111/bph.16230

   Contribution: Writing – original draft, Writing – review & editing, Visualization, Conceptualization.

5. Li J.*, **LoBue A.***, Heuser S. K., Leo F., & Cortese-Krott M. M. (2021). Using diaminofluoresceins (DAFs) in nitric oxide research. Nitric Oxide, 115, 44-54. doi:10.1016/j.niox.2021.07.002.

   Contribution: Writing – original draft, Writing – review & editing, Visualization, Conceptualization.

Manuscripts in preparation:

1. Heuser S. K.*, Li J.*, Li Z., **LoBue A.**, Heard K., Cadeddu R. P., Strupp C., Suvorava T., et al. Contrasting role of red blood cell arginase in human and mouse: RBC Arg1 KO mice show preserved systemic L-arginine bioavailability and infarct size in vivo.

   To be submitted in July 2025

   Contribution: Writing – review & editing, Investigation (NO metabolites and blood pressure measurements, blood count), Formal analysis, Data curation.

2. Heuser S. K., **LoBue A.**, Li J., Li Z., Cadeddu R. P., Dunaway L., Koesling D., Strupp C., et al. Erythroid specific knock out of soluble guanylate cyclase leads to disrupted erythropoiesis in bone marrow and splenomegaly in mice.

   To be submitted in 2025

   Contribution: Writing – review & editing, Investigation (blood pressure measurements), Formal analysis, Data curation.

3. **LoBue A.**, Arifaj D., Lindemann M., Heuser S. K., Li J., Lundberg J. O., Carlström M., Stegbauer J., et al. Endothelial cell eNOS regulates sodium excretion and glomerular filtration rate in the kidney as determined in endothelial cell-specific eNOS KO and KI mice.

   To be submitted in 2025-2026

   Contribution: Writing – original draft, Writing – review & editing, Visualization, Investigation (mRNA expression analysis, measurement of basal sodium and urine excretion and after salt challenge, GFR measurements), Formal analysis, Conceptualization, Data curation, Project administration.

*Contributed equally

10. Curriculum Vitae

Personal Information

First Name	Anthea
Family Name	Lo Bue
Date of Birth	March 11th, 1993
Place of Birth	Palermo (Italy)
Nationality	Italian

Education

11.2020	PhD candidate at Myocardial Infarction Research Laboratory, Medical Faculty, Heinrich Heine University, Düsseldorf, Germany Title of PhD thesis: Endothelial cell eNOS regulates sodium excretion and glomerular filtration rate in the kidney as determined in endothelial cell-specific eNOS KO and KI mice
2012 - 2019	MSc in Pharmaceutical Chemistry and Technology, Department of Pharmacy, University of Pisa, Italy
2007 - 2012	High School, Liceo Scientifico Antonino Sciascia, Canicattì, Italy

Supervision of graduate students and teaching responsibilities

15.05.2025	Lecture “Nitric oxide in regulation of vascular function and blood pressure” in Master Module M1100 24/25 of the Master in Molecular Biomedicine, Medical Faculty, Heinrich Heine University
May - July 2023	Supervision of an undergraduate student from the University of Michigan (US), founded by the DAAD-RISE program
Since 2021	Lecture “Nitric oxide and its detection” in Master Module M3550 “Pharmaceutical Biotechnology” and “Molecular Oncology” of

	the Master in Molecular Biomedicine, Medical Faculty, Heinrich Heine University

Working experiences

05.2020 – 09.2020	Pharmacist at Alliance Farmacie Comunali, Pontedera, Italy
2017 - 2018	Trainee at Farmacia Mannerucci, Pisa, Italy

Certificates and Licences

06.2021	FELASA Accredited Course F048/16, Heinrich Heine University, Düsseldorf, Germany
12.2019	License to practise as a pharmacist, Pisa, Italy

Participation in international conferences

9-14.02.2025	Gordon Research Conference: Nitric Oxide and Sulfide in Redox Signaling and Medicine, Ventura, US
	Oral presentation: Endothelial cell eNOS specific regulation of renal function in vivo: lessons from loss-of-function and gain-of-function cell-specific mouse models
	Poster Presentation: Endothelial cell eNOS regulates sodium excretion and glomerular filtration rate in the kidney as determined in cell-specific eNOS KO mice
8-9.02.2025	Gordon Research Seminar: Nitric Oxide and Sulfide in Redox Signaling and Medicine, Ventura, US
	Poster Presentation: Endothelial cell eNOS regulates sodium excretion and glomerular filtration rate in the kidney as determined in cell-specific eNOS KO mice
21-23.08.2024	The 13th international conference on the biology, chemistry, and therapeutic applications of nitric oxide 2024, Stockholm, Sweden
	Poster presentation: Endothelial cell eNOS regulates sodium excretion but not glomerular filtration rate in the kidney as determined in cell-specific eNOS KO mice

12-17.02.2023	Gordon Research Conference Nitric Oxide, Ventura, US
	Poster Presentation: The role of red cell eNOS in the regulation of renal function and systemic hemodynamics
11-12.02.2023	Gordon Research Seminar Nitric Oxide, Ventura, US
	Poster Presentation: The role of red cell eNOS in the regulation of renal function and systemic hemodynamics
	Discussion Leader at the session “Endogenous Nitric Oxide and Signaling Pathways”
15-17.06.2022	IRTG 1902 Summer school, Düsseldorf, Germany
	Poster Presentation: The role of red cell eNOS in the regulation of renal blood flow and systemic hemodynamics
01-02.06.2021	Cardiovascular Disease (CaVaD) Symposium 2021, Düsseldorf, Germany
	Poster Presentation: The role of red cell eNOS in the regulation of renal blood flow and systemic hemodynamics

Awards and Grants

9-14.02.2025	Poster Award at the Gordon Research Conference: Nitric Oxide and Sulfide in Redox Signaling and Medicine, Ventura, US
22.05.2023 - 31.07.2023	DAAD Rise Germany: selected as host supervisor for an undergraduate student from the University of Michigan, USA, founded by the DAAD Rise program
16.12.2022	Award for HeRa Travel Grants: grant of 1000 euros for the active participation in the Conference “Nitric Oxide Research Conference” in Ventura, US